The role of Sonic Hedgehog in regulating proliferation, cell survival, and cell-cycle exit in the zebrafish fin buds and neural-plate derived tissues

Dissertation

submitted to the
Combined Faculties for the Natural Sciences and Mathematics
of the Ruperto-Carola University of Heidelberg, Germany
for the degree of
Doctor of Natural Sciences

Sergey Prykhozhij,
BSc Honours (Molecular Biology)

Dissertation

submitted to the
Combined Faculties for the Natural Sciences and for Mathematics
of the Ruperto-Carola University of Heidelberg, Germany
for the degree of
Doctor of Natural Sciences

Presented by
Sergey Prykhozhij
from Pinsk, Belarus
2009

The role of Sonic Hedgehog in regulating proliferation, cell survival, and cell-cycle exit in the zebrafish fin buds and neural-plate derived tissues

Referees: Dr. Detlev Arendt
Prof. Dr. Herbert Steinbeisser

Thesis defense: 23.07.2009

Table of Contents

ZUSAMMENFASSUNG

Die Entwicklung von multizellulären Organismen hängt von der Integration zwischen Musterbildung und der Regulation der Zellenanzahl ab. Das sekretierte Signalprotein Sonic Hedgehog (Shh) ist in die Regulation beider Prozesse einbezogen worden, was darauf hindeutet, dass es am Erreichen dieser Integration teilnehmen könnte. Die Rolle von Shh beim Regeln der Musterbildung in vertebraten Modellsystemen, einschliesslich dem Zebrafisch, ist während der letzten Jahrzehnten gut beschrieben worden. Unter den Organen, in denen die Musterbildungsfunktion von Shh am besten untersucht worden ist, sind die Gliedanlagen, die Retina, und die Neuraltube. Daher habe ich gewählt die Rolle von Shh in der Regulation von Zellteilung und Zelltod in diesen Organen von Zebrafisch zu untersuchen. Zudem habe ich die Interaktion zwischen Shh und einigen anderen Faktoren untersucht, die Zellteilung und Zelltod regeln, einschliesslich des sekretierten Signalproteins Fgf und des Transkriptionsfaktors p53.

Im Kontext der gepaarten Brustflossenanlagen des Zebrafisches habe ich den Akzent auf das Zusammenspiel zwischen Shh und Fgf gesetzt. Shh gestaltet die Musterbildung entlang der vorder/hinteren Achse vom vertebraten Glied, während mehrere Fgfs die Musterbildung entlang der proximal/distalen Gliedachse gestalten. Zudem sind Shh und Fgf Signalwege in der Gliedanlage aufeinander angewiesen. Daher war ich bestrebt den relativen Einfluss eines jeden Signalwegs auf die Zellproliferation in diesem Organ zu bestimmen. In *shh* Mutanten sind Zellproliferation sowie der Fgf-signalweg in den Brustflossenanlagen anfangs normal, später aber verringern sie sich stark. Darüber hinaus hat eine kurzfristige pharmakologische Inhibition des Hedgehogsignalweges wenig Wirkung, weder auf den Fgf Signalweg, noch auf die Expression von Genen die am Zellzyklus beteiligt sind, während längere Inhibition zur Verminderung von beiden Prozessen führt. Im Gegensatz dazu führt eine kurzfristige pharmakologische Inhibition des Fgfsignalweges zür Störung der zellzyklischen Genexpression und der Zellproliferation in den Brustflossenanlagen, ohne den Shhsignalweg zu beeinflussen. Aktivierung des Fgfsignalwegs durch Implantation von FGF4-getränkten Heparinkügelchen in die Brustflossenanlagen der *shh* Mutanten führt zur Wiederherstellung der zellzyklischen Genexpression und Zellproliferation in diesen Organanlagen. Diese Ergebnisse zeigen, dass die Rolle von Shh in diesem Prozessen nicht direkt ist, und durch den

Effekt auf den Fgfsignalweg vermittelt wird. Im Kontrast dazu wirkt der Fgfsignalweg auf die Zellteilung direkt und unabhängig von seinem Effekt auf Shh.

In den aus der Neuralplatte entstehenden Geweben wie die Retina und die Neuraltube ist Shh erforderlich für das Überleben von Zellen während der Entwicklung. In diesem Projekt fand ich heraus, dass p53 ein erforderlicher Vermittler vom Zelltod in der Zebrafisch *shh* Mutante ist, da p53 Zielgene in der Abwesenheit von Shh Aktivität aktiviert werden, und der Verlust von *p53* zur Unterdrückung der Apoptose in den *shh* Mutanten führt. p53 induziert Apoptose in der Abwesenheit von Shh durch Aktivierung der Expression von proapoptotischen Genen, zum Beispiel *puma* und *bax1*, die den intrinsischen Weg der Apoptose induzieren und deren Expressionsniveaus mit dem Schweregrad von apoptotischen Phenotypen korrelieren. Die Hypothese, dass p53 Aktivierung aus dem Verlust von Shh Signaling resultiert, wird des weiteren dadurch unterstützt, dass p53 Zielgenexpression und die Apoptose durch Überexpression von dominant-negativer PKA in den *shh* Mutanten unterdrückt wird. Um die Aktivierung von p53 in lebenden Zebrafischembryonen zu beobachten habe ich eine transgene Linie konstruiert, die das fluoreszierende Protein GFP unter Kontrolle vom p53-getriebenen Promoter exprimiert. In der Tat korreliert die Expression von diesem p53 Reporter sehr gut mit dem Apoptoseniveua in Zebrafischembryonen, außer in der frühen Retina. Darüber hinaus kann die Expression vom p53 Reporter durch genotoxische Drogen induziert werden und kolokalisiert mit der aktiven Caspase3. Zudem waren p53 Reporter-positive Zellen defektiv in ihrem Zellzyklus, und dem Verlauf durch die G2/M-Phase. Die Untersuchungen von Zellteilung in Doppelmutanten von *shh* und *p53* zeigen, dass der Verlust des *p53* Gens in der *shh* Mutante den normalen Zellzyklusausstieg wieder herstellt, und die mitotische Frequenz während der Neurogenese in der Retina anhebt. Zudem wird Differenzierung von Amakrinzellen und Photorezeptoren in der *shh p53* doppelmutanten Retina wiederherstellt. Diese Ergebnisse zeigen, dass p53 in der Abwesenheit von Shh im Zebrafisch für die Induzierung von Apoptose erforderlich ist, und des weiteren Zellproliferation, Zellzyklusausstieg und Differenzierung in der Retina reguliert.

Insgesamt zeigen meine Ergebnisse, dass Shh eine wichtige Rolle in der Regulation von Zellteilung und Zelltod während der Wirbeltierentwicklung spielt, und es beeinflusst diese Prozesse unterschiedlich in verschiedenen Geweben. Im Kontext der gepaarten Brustflossenanlagen reguliert Shh die Musterbildung und fördert die Zellproliferation durch

Aktivierung des Fgfsignalweges. In den Geweben die aus der Neuralplatte entstehen spielt Shh nicht nur eine Musterbildende Rolle, sondern fördert auch Zellüberleben und Zellteilung dadurch, dass es der Aktivierung des p53Transkriptionsfaktors entgegenwirkt.

SUMMARY

The development of multicellular organisms depends on the integration between pattern formation and the regulation of cell number. The secreted signaling protein Sonic Hedgehog (Shh) has been implicated in directing both of these processes, suggesting it may participate in achieving this integration. The role of Shh in directing pattern formation in vertebrate model systems, including the zebrafish, has been well characterized during the last decades. Among the organs in which the patterning function of Shh has been best studied are the limb buds, the retina, and the neural tube. I therefore chose to study the role of Shh in regulating cell proliferation, cell death, and cell survival in these organs of the zebrafish. In addition, I also examined the interaction between Shh and several other factors directing cell proliferation and cell death, including the secreted signaling protein Fgf, and the transcription factor p53.

In the context of the zebrafish paired fin buds, I focused on the interplay between Shh and the Fgf signaling pathways. Shh directs pattern formation along the anterior/posterior axis of the vertebrate limb, whereas several Fgfs in combination direct pattern formation along the proximal/distal axis of the limb. In addition, Shh and Fgf signaling pathways in the limb bud are mutually interdependent. Therefore, I aimed to determine the relative importance of each pathway for proliferation in this organ. In zebrafish *shh* mutants, both proliferation and Fgf signaling in the pectoral fin buds are initially normal, but later are strongly reduced. Furthermore, pharmacological inhibition of Hh signaling for short periods has little effect on either Fgf signaling, or on cell-cycle gene expression, whereas long periods of inhibition lead to the downregulation of both. By contrast, even short periods of pharmacological inhibition of Fgf signaling lead to strong disruption of proliferation in the fin buds, without affecting Shh signaling. Activation of Fgf signaling by implantation of FGF4-soaked beads into *shh* mutant pectoral fin buds leads to the rescue of cell-cycle gene expression and proliferation in these organs. These results show that the role of Shh in this process is indirect, and is mediated by its effect on Fgf signaling. By contrast, the activity of the Fgf pathway affects proliferation directly and independently of its effect on Shh.

In neural-plate derived tissues such as the retina and the neural tube, Shh is essential for survival of cells during development. Here I identify p53 as the mediator of cell death in *shh* mutant since in the absence of Shh activity, p53 target genes are induced, and *p53* loss leads to suppression of apoptosis in *shh* mutants. p53 induces apoptosis in the absence of Shh signaling by activating expression of the pro-apoptotic target genes *puma* and *bax1*, which induce the intrinsic pathway of apoptosis and whose level of expression correlates with the severity of apoptotic phenotypes. In support of the hypothesis that p53 activation results from loss of Shh signaling, p53 target gene expression and apoptosis are both suppressed by over-expression of dominant-negative PKA in *shh* mutants. To monitor p53 activation in living zebrafish embryos, I constructed a transgenic line expressing fluorescent protein under the control of the p53-driven promoter. Indeed, p53 reporter expression correlates very well with apoptosis levels *in vivo*, except in the early retina. Furthermore, p53 reporter can be induced by genotoxic drugs and colocalises with active-Caspase3. p53 reporter-positive cells were also found defective in their cell cycle progression at 48 hpf. Consistent with this result, proliferation assays on the double *shh p53* mutant revealed that loss of p53 rescues normal cell-cycle exit and increases the rate of mitosis in the *shh* mutant retina. Moreover, differentiation of amacrine cells and photoreceptors was rescued in the double *shh p53* mutant retina. These results show that in the absence of *shh*, p53 is required for the induction of apoptosis, and also regulates proliferation, cell-cycle exit and differentiation in the retina.

Taken together, my results show that Shh plays an important role in regulating both proliferation and cell survival during vertebrate development, and that it affects these processes distinctly in different tissues. In the context of the paired fin buds Shh directs pattern formation and in addition promotes cell proliferation, via activation of the Fgf signaling pathway. In neural-plate derived tissues Shh not only plays a patterning role, but also promotes cell survival and proliferation by antagonizing activation of the transcription factor p53.

Acknowledgements

In this section, I would like to thank a number of people who made this thesis possible and helped me along the way either by tackling practical matters, by creating a good working atmosphere or by providing moral support. In particular my thanks go to:

Carl Neumann, for taking me as a PhD student in his laboratory, for good advice and encouragement, for his optimistic views on the progress of my work, and for fostering my independence in research.

Francesca Peri, for letting me finish my thesis work as a member of her lab, for teaching me live microscopy, for an opportunity to start a new exciting project on imaging microglia and macrophages, and for critical reading of thesis drafts.

The members of my thesis advisory committee, Detlev Arendt, Darren Gilmour and Herbert Steinbeisser, for their helpful evaluations of my progress, advice on experiments and directing me to formulate more specific experimental questions. I would also like to thank Soojin Ryu for agreeing to take part in my Thesis Defense committee.

Past members of Neumann lab and present members of the Peri lab for making both of these labs great places to work, for many interesting and valuable discussions and for their practical help. I want to thank Sabine Fischer, Gill Brunt and Sandra Gandre for providing excellent technical support and for creating a great working climate in the lab. Additionally, I would like to thank William Norton and Marlene Rau for helping me with the fin bud project and for being really fun people to work with.

I would also like to thank Alexis Perez-Gonzalez and Andy Riddell for help with FACS analyses.

Моих родителей и брата за их поддержку и веру в меня во время моей учебы и понимание важности работы в науке для меня, хотя это заставляет меня редко их видеть. Еще я бы хотел поблагодарить мою жену Ирину за ее поддержку, терпение и любовь.

Index of Figures

1 INTRODUCTION

1.1 Signaling pathways in regulation of proliferation and cell death

During development, organ growth is tightly regulated by controlling cell numbers. While cell number regulation remains one of the most complex problems in developmental and cell biology, work from many labs has shown that this is achieved by balancing proliferation and cell death within tissues. Localised regulation of cell numbers also contributes to organ shapes. Division and survival decisions inside the cell often require specific external signals. Several families of diffusible signaling molecules have been shown to affect both proliferation and cell death. In this thesis, I will focus on the Hedgehog signalling pathway and in particular on its role in regulating proliferation and cell death. In recent years, it has become clear that a true picture of signalling pathway function can be obtained from considering them a part of a network. This way of thinking influenced my work on Shh functions in proliferation and cell survival regulation by leading me to focus on interactions of Fgf signalling and p53 pathways with Shh signalling.

1.2 Hedgehog signaling

1.2.1 Hedgehog family of proteins

The curious name “Hedgehog” for this class of signaling molecules comes from the spiky phenotype of the *Hedgehog (Hh)* mutant *Drosophila* larvae identified in the forward genetic screen finished in 1980 (Nüsslein-Volhard and Wieschaus, 1980). Subsequently, similar genes were found in many other animals and in recent years our understanding of this class of signaling molecules has progressed dramatically. Undoubtedly, the Hh family of proteins is a key regulator of animal development, as it is involved in patterning and differentiation, regulation of proliferation and survival, may act as chemotactic cues and regulate morphogenesis via a combination of these functions.

Structural phylogenetics studies show that Hedgehog proteins contain two domains: Hedge and Hog domains, which have signaling function and protein splicing functions, respectively, and can be found independently in other proteins (Bürglin, 2008). Hh proteins appeared in early metazoan evolution, since sponges have some proteins containing the Hedge domain, and Cnidaria such as *Nematostella vectensis* have full Hh proteins. Most other Eumetazoa carry *Hh* genes except for some nematode species that lost these genes secondarily.

Regarding the main model systems, *Drosophila* carries a single *Hh* gene and vertebrates have three *Hh* genes: *Sonic Hedgehog* (*Shh*), *Indian Hedgehog* (*Ihh*) and *Desert Hedgehog* (*Dhh*). In zebrafish (*Danio rerio*), which underwent additional genome duplication, there are two *Shh* homologs (*Shha* and *tiggy-winkle hedgehog*), two *Ihh* homologs (*Ihha* and *Echidna Hedgehog*) and one *Dhh* homolog (Varjosalo and Taipale, 2008).

1.2.2 Hedgehog biosynthesis, secretion and spreading in tissues

Hedgehog is initially produced as a 45 kDa precursor protein, which is then processed to a 19 kDa active signaling peptide HhNp (Fig. 1). First, the signal peptide is cleaved during precursor transport into the endoplasmic reticulum, then the C-terminal domain catalyzes intramolecular protein cleavage of N-terminal domain via a thioester intermediate. This intermediate then reacts with cholesterol through the hydroxyl group to form HhN molecule. The final HhNp molecule is formed when Skinny Hedgehog enzyme (or HHAT in vertebrates) attaches palmitate to HhN (Chamoun et al., 2001; Lee et al. 2001; Buglino and Resh, 2008) (Fig. 1). This lipid-modified form of Hedgehog can tightly attach to cell membranes of the producing cells. In both *Drosophila* and vertebrates, the secretion of Hh depends on Dispatched, a 12-span transmembrane protein homologous to Hh receptor Patched (Burke et al., 1999; Ma et al., 2002; Kawakami et al., 2002). Loss of *Dispatched* in all cases produces a phenotype similar to a complete loss of Hh signaling and results in accumulation of Hh proteins inside the secreting cells (Burke et al., 1999; Ma et al., 2002; Kawakami et al., 2002).

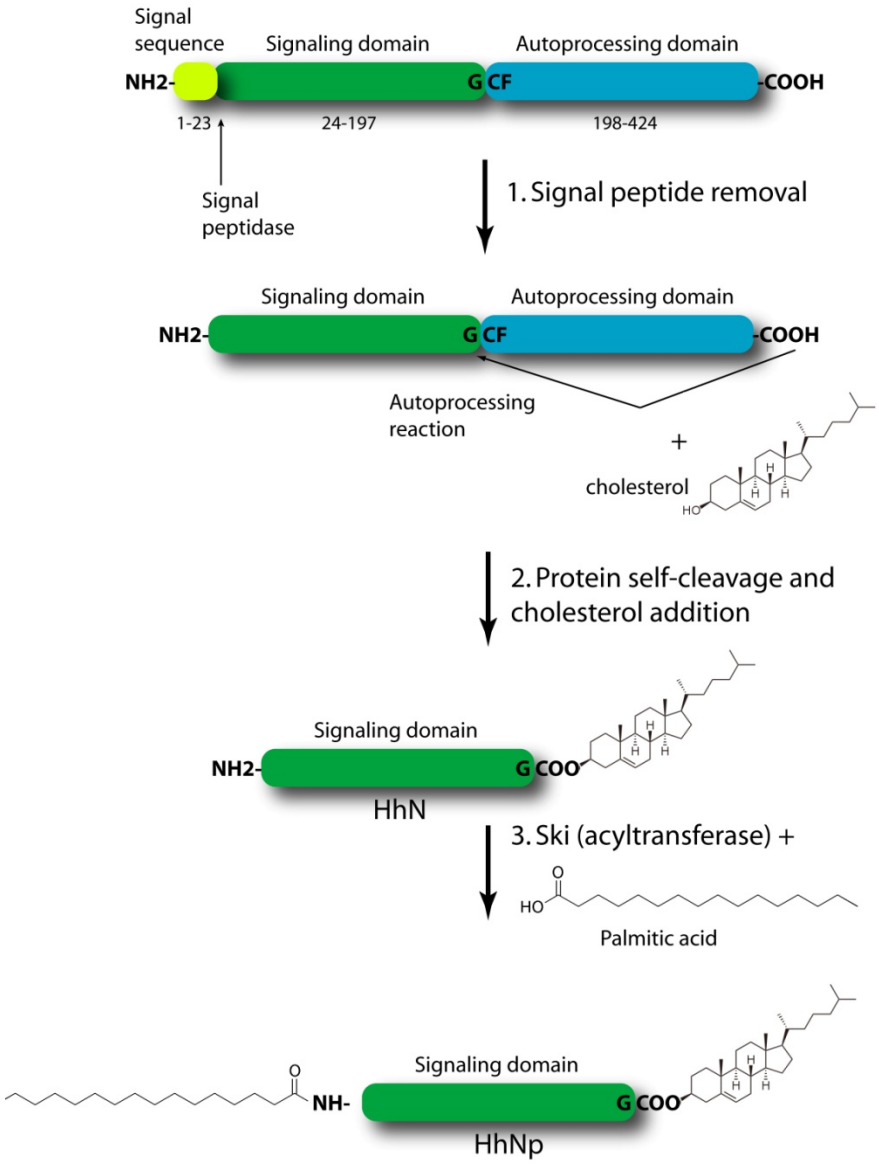

Figure 1. Hedgehog protein cleavage and lipid modification pathway.
After its synthesis, the signal sequence of Hedgehog precursor protein is removed by the signal peptidase in the endoplasmic reticulum (1). The C-terminal part of Hedgehog then catalyzes coordinated intramolecular proteolytic cleavage and cholesterol moiety addition (2). The next step is addition of palmitic acid by Skinny Hedgehog (Ski) acyl-transferase (3). N-terminal part of Hedgehog (HhN) (24-197 aa) modified with cholesteroyl- and palmitate moieties (HhNp) is highly lipophilic and is the final active signaling molecule. The figure was redrawn with modifications from Varjosalo and Taipale, 2008.

Whereas Hh processing and secretion are well understood, it is not clear, how Hh proteins spread in gradients across 50-300 μm depending on the organism and tissue (Zhu and Scott, 2004). Several studies propose that Hh spreads over long distances in the form of multimere complexes containing lipids (Zeng et al., 2001) or lipoproteins (Panakova et al., 2005; Calejo et al., 2006). However, a recent study in *Drosophila* (Katanaev et al., 2008) proposed two secretion pathways for Hh protein: a short range and a long-range pathway, whose function depends on a membrane microdomain protein Reggie-1, which suggests that additional mechanisms may be involved in Hh spreading. Since Hh spreads in tissues in lipoprotein complexes, what is the role of Hh lipid modifications in this process? Indeed, lipid modifications are required for Hh protein distribution *in vivo* (Guerrero and Chiang, 2007; Varjosalo and Taipale, 2008). Palmitoylation is necessary for Hh activity and long-range signaling in both *Drosophila* and vertebrates (Chamoun et al., 2001; Chen et al., 2004), and the effect of palmitoylation loss on long-range Hh signaling in vertebrates is due to defects in Hh lipoprotein complex formation. It is unclear whether cholesterol enhances or hinders Hh transport *in vivo* since different studies produced conflicting results, and the associated caveats include unequal protein expression, Dispatched-independent secretion and potential lack of palmitoylation (Varjosalo and Taipale, 2008).

Hh tissue spreading is controlled not only by lipid modifications but also by cell-surface Hh-binding molecules and proteoglycans in the extracellular space. Genetic studies on exostosin (EXT)/*tout velu* family of heparan sulfate proteoglycan (HSPG)-synthesizing enzymes in *Drosophila* have first suggested that HSPGs are involved in Hh spreading (Lin, 2004) by synthesizing Dally and Dally-like (Dlp) glypicans, glycosylphosphatidylinositol (GPI) – linked heparan sulfate proteoglycans, which are attached to the cell surface and whose polysaccharide chains protrude into the extracellular space. Overall, glypicans have two main functions in *Drosophila*: contributing to Hh spreading and cell-autonomously enhancing signaling pathway activation (Jiang and Hui, 2008). Loss of these proteins inhibits Hh signaling in *Drosophila* similarly to the loss of HSPG-synthesizing enzymes. In particular, in wing discs Hh fails to move into cell clones mutant for HSPG synthesizing enzymes leading to abnormal accumulation of the protein in more posterior regions. This requirement of HSPGs for Hh spreading is limited to lipidated HhNp, present in lipoprotein particles. By contrast, the non-lipidated form of Hh can move farther than HhNp and does not require HSPGs for its

movement. In addition, it has been shown, that HSPGs are involved in maintaining Hh protein stability. How Hh interacts with glypicans is not completely understood, but there is evidence in *Drosophila* that Shifted is crucial for this interaction (Glise et al., 2005; Gorfinkiel et al., 2005). Shifted is a secreted protein necessary for Hh spreading and signaling activation in developing wing blade, notum and eye tissues in the fly. In these tissues Shifted can bind both Hh and glypicans thus mediating their interactions. However, Shifted-mediated binding is not the only mechanism of Hh interaction with proteoglycans, which may also be direct. Moreover, Hh-glypican interaction may not even depend completely on polysaccharide chains of glypicans (Filmus et al., 2008). In contrast to *Drosophila*, where glypicans activate Hh signaling, mouse Glypican3 (GPC3) is a negative regulator of the Hh pathway (Capurro et al., 2008). Mice and humans lacking GPC3 exhibit an overgrowth phenotype. Mechanistically, GPC3 binds Hh proteins and the resulting complex becomes endocytosed and degraded, thereby reducing Hedgehog level in the tissues. Consistently, in the absence of GPC3, the level of Shh protein and expression of Hh target genes are significantly higher. Similarly to GPC3, *Drosophila* glypicans also induce endocytosis of Hh in a complex with Ptc releasing inhibition of Smo thus activating Hh signaling (Beckett et al., 2008).

There are two additional ways to regulate the Hh gradient (Varjosalo and Taipale, 2008). On the one hand, high levels of Hh signaling can induce secondary production of Hh proteins in cells responding to it (Tabata et al., 1992; Roelink et al., 1995). On the other hand, Hh signaling leads to its own down-regulation by inducing expression of Patched (Ptc), Hh receptor, and the complex is degraded in the lysosomes (Chen and Struhl, 1996; Incardona et al. 2000). Similarly, in vertebrates Hh induces expression of Hip1 binding Hh to the cell surface and thus preventing its spreading (Chuang and McMahon, 1999).

1.2.3 Hedgehog signaling pathway

Hedgehog signalling is a signal transduction pathway regulating proteolytic processing of its downstream effector transcription factors Cubitus interruptus (Ci) in *Drosophila* and Gli in vertebrates (Fig. 2; Lum and Beachy, 2004; Jiang and Hui, 2008; Varjosalo and Taipale, 2008). In the absence of Hh signals, proteolysis leads to formation of repressive forms of Ci

and Gli factors, whereas when Hh ligands are present this proteolysis is inhibited and the full-length Ci and Gli can activate their target genes.

The most upstream signal transducer Smoothened (Smo) is inhibited by Hh receptor Ptc in the absence of Hh signal via a catalytic mechanism possibly involving oxysterols or vitamin D3 metabolites. Hh ligand binding to Ptc relieves Smo inhibition that Ptc mediates thus activating the signal transduction pathway. Hh ligands are aided in their binding to Ptc by proteoglycans, as well as membrane-spanning co-receptors Ihog and Boi (Cdo and Boc in vertebrates, respectively), stimulating Hh signaling (Allen et al., 2007; Tenzen et al., 2006; Yao et al., 2006; Zhang et al., 2006). Negative regulation of expression of these co-receptors by Hh signaling, transcriptional activation of negative Hh signaling regulators *patched, hip1* and Gli degradation-promoting HIB/SPOP genes, negative regulators of Hh signaling, ensures robust negative feedback regulation of Hh signaling (Varjosalo and Taipale, 2008).

Upon Hh stimulation, *Drosophila* Smo (dSmo) accumulates at the membrane, is phosphorylated by Protein Kinase A (PKA), Casein Kinase I (CKI) and changes its conformation (Zhao et al., 2007). In vertebrates, GRK2 induces similar activatory phosphorylation of Smo thereby activating downstream signaling (Chen et al., 2004b; Meloni et al., 2006). The C-terminus of dSmo is a binding platform for multiple factors: Costal2 (Cos2), Ci, Fused kinase (Fu), PKA and several other kinases. Cos2 belongs to the kinesin superfamily and serves as a molecular scaffold protein for Ci phosphorylation by PKA, CKI and GSK3β. Without Hh, Cos2-mediated phosphorylation of Ci leads to Slimb-dependent ubiquitination and proteolytic processing of Ci into a repressive form CiR, while upon Hh stimulation, Cos2 is recruited by dSmo and cannot promote degradation of Ci. Inhibition of Ci degradation leads to accumulation of full-length activatory form CiA, for whose complete activation Suppressor-of-Fused (Sufu) must be removed from CiA by Fu-mediated phosphorylation. This phosphorylation occurs upon Cos2 binding to dSmo since Cos2 brings Fu close to Sufu bound to Ci. The Fu requirement for Sufu inactivation was confirmed by dispensability of Fu for Hh signaling upon Sufu loss (Ohlmeyer and Kalderon, 1998; Lefers et al., 2001).

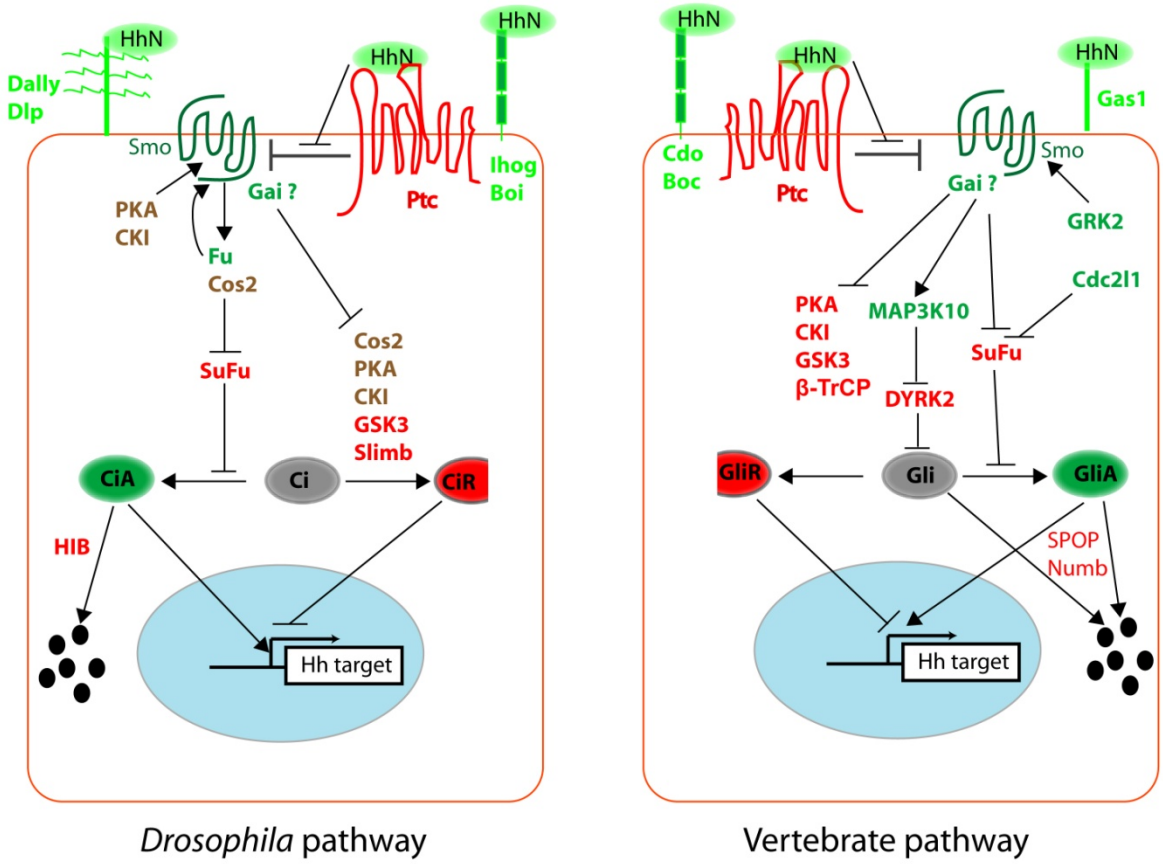

Figure 2. The Hedgehog signaling pathway in *Drosophila* and vertebrates.
Hh reception is enhanced by its binding to coreceptors Ihog/Boi in *Drosophila* and Cdo/Boc/Gas1 in mammals. *Drosophila* Dally and Dlp1 HSPGs bind and concentrate Hh molecules on the surface of the cell. Patched controls Hh signaling by inhibition of Smo. Lack of Smo activity allows phosphorylation of Ci/Gli (Gli2 and Gli3) by PKA, CKI, GSK3 and possibly other kinases, which leads to ubiquitination by Slimb/β-TrCP SCF subunits and proteasome-mediated proteolysis. This proteolysis generates truncated repressor forms CiR/GliR of full-length Ci/Gli. In *Drosophila*, Cos2 promotes phosphorylation of Ci acting as a molecular scaffold to bring Ci and its kinases in close proximity. Hh binding to Ptc blocks its inhibition of Smo. dSmo is then phosphorylated on the C-terminal domain by PKA and CKI, which leads to its activation and cell surface accumulation. In vertebrates, GRK2 can activate Smo by phosphorylation. Recruitment of Cos2-Fu by Smo leads to dissociation of Cos2-Ci complexes and reduction in Ci phosphorylation and abundance of repressor form of Ci. Hedgehog signaling also stimulates CiA activity by promoting Fu-mediated inhibition of Sufu. Hh-promoted expression of HIB targeting CiA for degradation is another negative-feedback loop in Hh signaling. In vertebrates, Sufu is the main Gli inhibitor and is inhibited by Cdc2l1 kinase. DYRK2 kinase targets Gli2 for degradation, while MAP3K10 activates Gli2 by inhibiting DYRK2. Additionally there is evidence for $G_{\alpha i}$ (Gai) function in signaling downstream of Smo in both *Drosophila* and vertebrates. In brown are indicated *Drosophila* proteins playing both positive and negative roles in Hedgehog signaling regulation, negative regulators are in red and positive regulators are in green. The figure was modified from Jiang and Hui (2007).

The mechanism of Hh signaling in vertebrates differs from the one in *Drosophila* (Fig. 2; Varjosalo and Taipale, 2008). For its signal transduction the vertebrate Hh pathway unlike the one in *Drosophila* requires the primary cilium, a small microtubule-based structure with a sensory function in most vertebrate cells (Wong and Reiter, 2008). Mutations in intra-flagellar transport (IFT) components affecting primary cilium structure and function lead to Hh signaling inhibition in the neural tube, but to its apparent activation in the limbs. Consistent with the role of IFT in Hh signaling, Smo, Ptc, Sufu and Gli factors localize to the primary cilium, and there is evidence that the main role of the primary cilia is to promote processing of Gli proteins to both activatory and repressive forms. Hh signal transduction prior to Gli processing also occurs in the primary cilia, where Hh signaling is initiated when Smo is released from its Ptc-mediated inhibition. Ptc inhibition of Smo ciliary localization is removed by Shh stimulation leading to Smo recruitment to the primary cilium, where it co-localises with other Hh signaling components (Rohatgi and Scott, 2007). In contrast to Smo, Ptc leaves the primary cilium after binding Shh and cannot inhibit ciliary recruitment of Smo.

Functions of vertebrate homologs of Hh signaling mediators downstream of Smo are still unclear. The zebrafish Cos2 homolog has been suggested to negatively regulate Hh signaling and interact with Gli1 (Tay et al., 2004). However, mouse Cos2 homologs, Kif7 and Kif27, cannot bind either Smo or Gli factors and are functional kinesin motors in contrast to Cos2 (Varjosalo et al., 2006). Like in the case of Cos2, the zebrafish Fused homolog has been implicated in Hh signaling in the context of muscle pioneer generation (Wolff et al., 2003), whereas mouse Fused homologue is highly divergent and non-essential for Hh signaling (Jiang and Hui, 2008). Another difference of Hh signaling in vertebrates and in *Drosophila* is signal transduction downstream of Smo, and only recently kinases involved in this process were identified. Evangelista and colleagues (2008) identified Cdc2l1 kinase as necessary and sufficient for Hh signaling activation. Mechanistically, Cdc2l1 binds and inactivates Sufu, a potent Gli inhibitor. Another systematic kinase screen identified DYRK2 and MAP3K10 kinases involved in Hh signal transduction (Varjosalo et al., 2008). DYRK2 negatively regulates Hh signaling by phosphorylating and promoting degradation of Gli2, whereas MAP3K10 is a positive regulator of Hh signaling inhibiting DYRK2 and possibly other kinases. Identification of these kinases is important for understanding Hh signaling, because, like Ci, GLI2 and GLI3 can be phosphorylated and targeted to degradation in the absence of

Hh signals. When Hh signal is present, both proteins remain full-length and can activate target genes. Several kinases and protein degradation machinery are crucial for controlling Gli activity. PKA phosphorylation of Gli3 primes it for further phosphorylation by CKI, GSK3β and other kinases and subsequent ubiquitination by SCF ubiquitin ligase complex (Wang et al., 2000; Jiang, 2006). Moreover, Gli2 processing is also regulated by PKA, and Gli2 without PKA sites is much more active (Pan et al., 2009). How the newly identified kinases fit into the current models of Gli regulation is currently unclear.

1.3 The role of Sonic Hedgehog in regulating proliferation in development and tumourigenesis

There is now abundant evidence that Hh signaling is involved in regulation of proliferation. In most instances, Hh ligands stimulate proliferation by direct regulation of cell-cycle promoting genes, through activation of secondary signaling pathways inducing cell cycle progression or via other mechanisms that are still unknown. Several early studies found clear evidence that Hh signaling regulates proliferation. Fan and Khavari (1999) artificially expressed Shh in the mouse skin and showed that it can increase cell numbers and override p21 CDK inhibitor-mediated cell cycle arrest. This result suggested a potent proliferative activity of Shh and could potentially explain the origin of basal cell carcinoma. Similarly, Shh produced by Purkinje cells has been shown to promote granular cell precursor (GCP) proliferation in the developing cerebellum (Wechsler-Reya and Scott, 1999; Dahmane and Ruiz i Altaba, 1999). Increase in GCP proliferation by Shh was abolished by Hh signaling inhibition, and this effect could be observed both in cultured cell lines and *in vivo*. Tectum and neocortex are two other dorsal brain parts which require Shh for cell proliferation (Dahmane et al., 2001). These observations provided important clues to why Hh signaling is activated in tumours of the neural origin. Later studies also showed that Hh signaling is required for cell proliferation in several stem cell niches in the postnatal and adult brain (Machold et al., 2003; Palma et al., 2005). Cayuso and colleagues (2006) showed that Shh requirement for proliferation in the developing spinal cord is mediated by Gli factors. Subsequent studies on the mechanisms of Hh signaling-mediated proliferation found that Hh signaling is required for expression of cell cycle regulators. Direct effects of Hh signaling on expression of cell cycle regulators were identified in both *Drosophila* and vertebrates in several different tissues.

During *Drosophila* eye development Hh signaling is required for normal expression of cyclins and proliferation, and its activation suppresses the phenotype due to negative cell cycle regulator RBF (Retinoblastoma) overexpression. In this case, Hh signaling promoted cell cycle progression by transcriptional upregulation of D-type and E-type cyclins in target cells (Duman-Scheel et al., 2002). This transcriptional up-regulation of cell-cycle genes has been shown to occur as a direct response to promoter binding of Gli factors (Duman-Scheel et al., 2002; Yoon et al., 2002). In the mouse cerebellum, Kenney and Rowitch (2000) found that Shh signaling maintains GCP proliferation by regulating *cyclinD* gene expression. Expression profiling of genes in the GCP cells showed that Shh regulates cell cycle progression by inducing N-Myc, which activates its downstream transcription program (Oliver et al., 2003).

Also during retinal development, Shh plays a major role in regulating proliferation. Early studies showed that Shh stimulates proliferation of retinal progenitors in tissue culture (Jensen and Wallace, 1997; Levine et al., 1997) and in the ciliary marginal zone (CMZ) of newly born mice and chickens (Moshiri and Reh, 2004; Moshiri et al., 2005). During mouse retina development, Shh positively regulates cell cycle progression probably by regulating *cyclinD1* expression, and without Shh cells cannot continue proliferating and exit the cell cycle becoming retinal ganglion cells (Wang et al., 2005). Consistently, in the zebrafish *shh* mutant retina, proliferation was reduced during neurogenesis (Stenkamp et al., 2002). Explaining positive effects of Shh on retinal proliferation, Locker and co-workers (2007) found that in *Xenopus* Shh signaling promotes retinal progenitor proliferation by shortening G1- and G2-phases of the cell cycle. This effect may be caused by Shh-mediated positive regulation of *cyclinD1*, *cyclinA2*, *cyclinB1* and *cdc25C* gene expression, which would lead retinal cells to faster cell cycle progression towards the final mitosis and cell-cycle exit.

Despite its widespread role in promoting proliferation, Shh does not function as the classical mitogen since it cannot make terminally differentiated cells enter the cell cycle from a quiescent phase and does not induce mitogen-activated protein kinase (MAPK) pathway (Roy and Ingham, 2002).

On the other hand, Hh signaling has also been shown to have a negative role on cell cycle progression. In the mouse gut, Ihh is required for cell cycle exit and differentiation of colonocytes both *in vivo* and in a colonocyte cell line through activation of *p21* CDK inhibitor expression (van den Brink et al., 2004). Although there is strong evidence for a positive role of

Shh in retinal proliferation, studies in the zebrafish retina show that this signaling pathway is required for retinal cell-cycle exit. In zebrafish *shh* mutant retina and under conditions of Hh signaling inhibition by forskolin, most retinal cells fail to express *p57Kip2* CDK inhibitor and do not exit the cell cycle (Shkumatava and Neumann, 2005; Masai et al., 2005). Consistent with these studies in vertebrates, in *Drosophila* retina development, Hh signaling is involved in promoting cell-cycle exit but only in a strict combination with Dpp signaling (Firth and Baker, 2005).

Regulation of other signaling pathways which in turn promote cell cycle progression may be another strategy for Hh signaling to regulate proliferation during development. One clear case of such a mechanism is regulation of proliferation during *Drosophila* wing disc development. In this context, Hh promotes proliferation by regulating Dpp expression, a morphogen of the TGF-β family. Wing disc cells lacking receptors for Dpp have proliferation defects suggesting a cell-autonomous role for Dpp signaling in regulating proliferation (Burke and Basler, 1996). Furthermore, Martín-Castellanos and Edgar (2002) provided complementary evidence showing that activated Dpp receptor activates cell cycle progression in wing disc cells.

Consistent with its role in regulating proliferation, Hh signaling activation was implicated in brain cancers such as glioma and medulloblastoma, skin cancer basal cell carcinoma (BCC), adenosarcomas of oesophagus, stomach, liver, colon and pancreas, rhabdomyosarcoma in the muscle, small-cell lung carcinoma, some cancers of breast, prostate (Rubin and Sauvage, 2006; Beachy et al., 2004). In addition to mentioned solid tumours, stroma-derived Hh ligands facilitate growth of B-cell lymphomas by providing survival signals (Lindemann, 2008). Inactivation of *PATCHED* and *SUFU* releases negative regulation of Hh signaling and is a frequent way to initiate tumour formation. Alternatively overexpression of Gli factors and activating mutations in *SMO* gene represent Hh signaling activation mechanisms leading to tumour formation. Therefore, cancers resulting from Hh signaling activation do not depend on Hh ligand stimulation but can be inhibited with Smo antagonists such as cyclopamine (Jiang and Hui, 2008). Hh signaling alterations and some signaling inputs ultimately result in a certain activity level of Gli factors, a Gli code. Gli codes change during tumourigenesis progression translating into different cancer cell behaviours, such as enhanced proliferation and eventually metastasis (Ruiz i Altaba et al., 2007). There are several potential

mechanisms by which Hh signaling can promote tumourigenesis: activation of proliferation, suppression of apoptosis, induction of epithelial-to-mesenchymal transition and promoting angiogenesis. These possibilities should be important considerations guiding the search for cancer therapies (Rubin and Sauvage, 2006).

1.4 Sonic Hedgehog and Fibroblast Growth Factors in vertebrate limb bud patterning and as potential limb bud mitogens

Limb development is highly amenable to experimental and genetic manipulation in several model organisms, and the main signaling pathways that direct limb development are well characterized (Fig. 3; reviewed in Capdevila and Izpisúa Belmonte, 2001; Niswander 2002; Tickle 2002). The zone of polarizing activity (ZPA), a small group of cells in the posterior mesenchyme, controls polarity along the anterior/posterior axis (Saunders and Gasseling, 1963). The secreted signaling protein Shh is expressed in the ZPA, and has been shown to mediate the effect of the ZPA during limb development (Fig. 3; Riddle et al., 1993; Chang et al., 1994; López-Martínez et al., 1995; Neumann et al., 1999). The apical ectodermal ridge (AER) is another major signaling center of the limb bud. It runs along the distal margin of the limb bud, and is the site of expression of several Fgf genes (Fig. 3; reviewed in Martin 1998). The AER is required for outgrowth and patterning of the limb along its proximal/distal axis, and can be functionally replaced by FGF-soaked beads in chicken embryos, indicating that Fgf signaling can mediate AER function (Fallon et al., 1994; Niswander et al., 1993). Furthermore, conditional inactivation of both Fgf4 and Fgf8 in the mouse AER leads to failure of proximal/distal outgrowth (Sun et al., 2002). Factors from the AER and ZPA form a mutual feedback loop that allows growth and patterning of the different axes to be coordinated. Thus *fgf-4*, which is expressed in the posterior AER, can be induced in the anterior AER of the chicken limb bud by ectopic Shh protein (Niswander et al., 1994; Laufer et al., 1994). Furthermore, removal of Shh activity from the zebrafish fin buds leads to loss of *fgf4* and *fgf8* expression in the AER (Neumann et al., 1999), and, conversely, removal of Fgf4 and Fgf8 activity from the mouse AER leads to loss of *shh* expression in the ZPA (Sun et al., 2002), indicating that each signaling pathway is required for the maintenance of the other pathway.

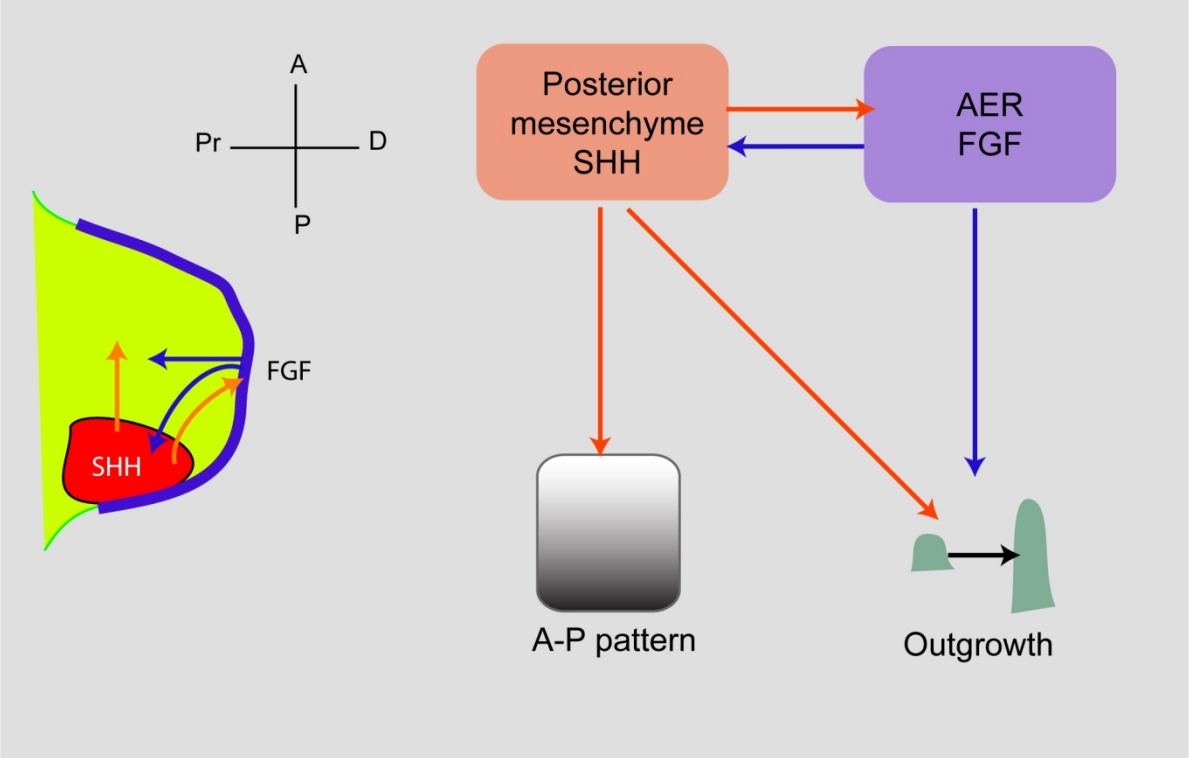

Figure 3. Shh and Fgf signaling pathways in limb patterning and outgrowth.
Shh and Fgf signaling pathways are interdependent due to mutual regulation of expression and both pathways affect limb bud mesenchyme. Shh signaling can affect both anterior-posterior patterning and limb bud outgrowth. Fgf is mainly required for outgrowth and proximo-distal patterning.

Despite all the advances in defining how limb patterning occurs, our understanding of how proliferation during limb development is regulated is still fragmentary. More specifically, since cells in many different contexts proliferate in response to mitogens, it has been important to define the proliferation-stimulating molecules in the context of the vertebrate limb bud. The two best mitogen candidates in limb buds are Shh and Fgf proteins. Similar to Hh signaling, Fgf signaling positively regulates proliferation in a number of contexts. Indeed, Fgf1 and Fgf2 were initially identified as mitogenic factors in fibroblast tissue culture, and subsequently, other members of the FGF protein family were found to have a similar activity (Powers et al., 2000). Furthermore, Fgf signaling has also been shown to have a mitogenic activity *in vivo* during embryonic development. Thus FGF-4 is necessary for proliferation of the inner cell mass during early post-implantation development in the mouse (Feldman et al., 1995), and FGF-8 and FGF-17 are required for proliferation in the mouse dorsal midbrain (Partanen,

2007). In addition, Fgf signaling promotes proliferation of osteoblasts (Ohbayashi et al., 2002), of lens cells (Robinson, 2006), and during hematopoiesis (Moroni et al., 2006).

In zebrafish there is genetic evidence that Shh is required for fin bud outgrowth and cell proliferation (Neumann et al., 1999) and defects in digit formation in mice lacking *shh* gene may be due to the role of Shh in proliferation (Towers et al., 2008; Zhu et al., 2008). As the manuscript containing some of the data in this thesis was under review (Prykhozhij and Neumann, 2008), a paper was published proposing a direct role of Shh in regulating proliferation in developing chick limb buds (Towers et al., 2008). Following observations that inhibition of Hh signaling for long periods leads to loss of posterior digits, the authors investigated whether this result is due to the morphogen or proliferation-promoting property of Shh. Although cyclopamine inhibition only led to a reduction of *cyclinD2* without affecting *cyclinD1* and *N-Myc*, implantation of Shh-soaked beads led to an increase of *cyclinD1* and *N-Myc* expression. This induction of G1- and S-phase genes by Shh-soaked bead implantation was apparently independent of the AER region. Moreover, derepression of Hh signaling by loss of *Gli3* led to a strong induction of *cyclinD1, cyclinD2* and *N-Myc*.

In contrast to direct proliferation regulation by Shh during limb bud development, several studies suggest that Fgf signaling may be fulfilling this function. Dudley et al. (2002) surgically removed AER on the chick limb buds and analysed proliferation several hours after the cut. They found a clear decrease in proliferation in the underlying mesenchyme suggesting that proliferation during limb bud development is regulated by Fgf molecules released by AER. However, another interpretation of such experiments is that loss of AER also leads to defects of Shh signaling. In contrast to the AER removal studies, genetic inactivation *Fgf4* and *Fgf8* genes in the mouse limb buds leads to reductions in limb bud size most likely due to an increase in cell death since the proliferation rate is normal (Sun et al., 2002). Still, there may be other Fgf ligands besides Fgf4 and Fgf8, which may be sufficient to maintain proliferation (Niswander 2003). Thus, to date the relative contributions of Shh and Fgf signaling pathways in maintaining limb bud proliferation remain uncleal.

1.5 Sonic Hedgehog in zebrafish retinal development

From a developmental and functional point of view, the retina is a part of the nervous system. Its function is to perceive light and transduce the resulting information to the brain.

The retina has a highly ordered structure consisting of three cell layers interconnected by synapses localized in two layers (Fig. 4B; Bilotta and Saszik, 2001). There are seven main cell types in the retina: retinal ganglion cells (RGCs), amacrine cells, bipolar cells, horizontal cells, cone photorecetors, rod photoreceptors and Müller glia (Fig. 4A). A recent study of *Xenopus* retina found that retinal cell types are born in the following order: RGCs, horizontal cells, cone photoreceptors, rod photoreceptors, amacrine cells, bipolar cells and Müller glia (Wong and Rapaport, 2009). RGCs are all located in a single layer and their axons transmit visual information to the optic tectum. Inner plexiform layer (IPL) is located between the RGC layer and the inner nuclear layer (INL) and contains synapses of RGCs with amacrine and bipolar cells. The INL follows the RGC layer and contains amacrine, bipolar, horizontal and Müller glia cells. Finally, the outer-most part of the retina is outer nuclear layer (ONL) containing cone and rod photoreceptors. Synaptic connections between INL and ONL are located in the outer plexiform layer, where bipolar and horizontal cells make synapses with photoreceptors. Outside of the neural retina lies retinal pigmented epithelium absorbing stray light and thereby protecting retinal cells from light-induced damage.

Conversion of multipotent retinal progenitors to differentiated retinal cell types occurs during the complex process of differentiation, which is influenced both by intrinsic and extrinsic factors with unclear relative contributions. In particular, the competence model suggests that retinal progenitors go through a number of intrinsically defined states and have different propensities to become specific cell types (Livesey and Cepko, 2001). Intrinsic factors are mainly transcription factors belonging to basic helix-loop-helix or homeobox families (Stenkamp, 2007), which alone or in combinations determine the fates of the progenitor cells. According to the competence model, extrinsic factors can influence the ratios of different cell types, but they cannot induce cell types of a different progenitor competence state. Despite some progress, it is still unclear to what extent the extrinsic factors control retinal cell fates.

The role of Shh during retina development is especially well-inderstood in zebrafish. Shh influences zebrafish retina throughout its development and its known functions consist of early proximo-distal patterning of the optic vesicle, promoting retinal neurogenesis and cell type differentiation and retinotectal projection of RGC axons (Stadler et al., 2004). After optic vesicle formation, Shh and Twhh are required for patterning this structure into optic stalk and

neural retina. In this context, Hh signaling is promoting optic stalk cell fate by activating Pax2 (Ekker et al., 1995; Macdonald et al., 1995) and Vax1 and Vax2 homeobox genes (Stadler et al., 2004). Indeed, the activation of Hh signaling leads to expansion of optic stalk tissue at the expense of neural retina (Macdonald et al., 1995; Masai et al., 2000), as in the neural retina, Hh signaling leads to inhibition of Pax6 expression and activation of Pax2 thereby converting the neural retina into the optic stalk. By contrast, inhibition of Hh signaling leads to expansion of the neural retina and reduction of the optic stalk.

During retinal neurogenesis, progenitors undergo final mitoses and differentiate into retinal cell types. Initiation of zebrafish retinal neurogenesis is induced by Fgf signaling from the optic stalk (Martinez-Morales et al., 2005). Neurogenesis is first induced in the ventro-nasal patch of the zebrafish eye at 28 hpf, and after RGCs are born, neurons are born in the INL and ONL in distinct waves (Hu and Easter, 1999). Shh expression in the retina is first initiated in newly-born RGCs and then spreads in a wave as new RGCs are born (Neumann and Nüsslein-Volhard, 2000). The requirement of Hh signaling for RGC development is mediated through positive regulation of the *ath5* gene (Stenkamp and Frey, 2003; Neumann and Nüsslein-Volhard, 2000). Subsequent spreading of Shh expression in amacrine cells also occurs in a wave independent of Shh expression in RGCs (Shkumatava et al., 2004). In that study it has also been shown that Shh is required for differentiation of all retinal cell types except for some RGCs. Although it was previously proposed that Shh expressed by pigmented retinal epithelium is required for photoreceptor differentiation (Stenkamp et al., 2000), Shkumatava and colleagues (2004) conclusively show that short-range Shh signaling from neural retina is necessary and sufficient to induce photoreceptor and Müller glia differentiation. Another possibility suggested by Stenkamp (2007) is that Shh is required for amacrine and photoreceptor survival rather than differentiation. The role of Shh in Müller glia differentiation seems to be conserved since in the mouse retina Müller glia express Hh signaling target genes and require Shh for their normal organization (Wang et al., 2002). In the context of retinal differentiation, Shh also promotes cell-cycle exit of differentiating cells (Masai et al., 2005; Shkumatava and Neumann, 2005). Indeed, *shh* mutant embryos had a pronounced delay in *p57kip2* expression and blocking *p57kip2* function with morpholino oligonucleotides leads to a *shh* mutant phenocopy, that is lack of differentiation in the retina, cell-cycle exit defects and a high level of apoptosis in the retina.

Up to date, it is unclear how to reconcile the results concerning the functions of Shh in the retina. Since Shh signaling in the retina regulates neurogenesis, proliferation, cell-cycle exit and cell survival, an obvious question is how a single signaling pathway can control these distinct cell behaviors.

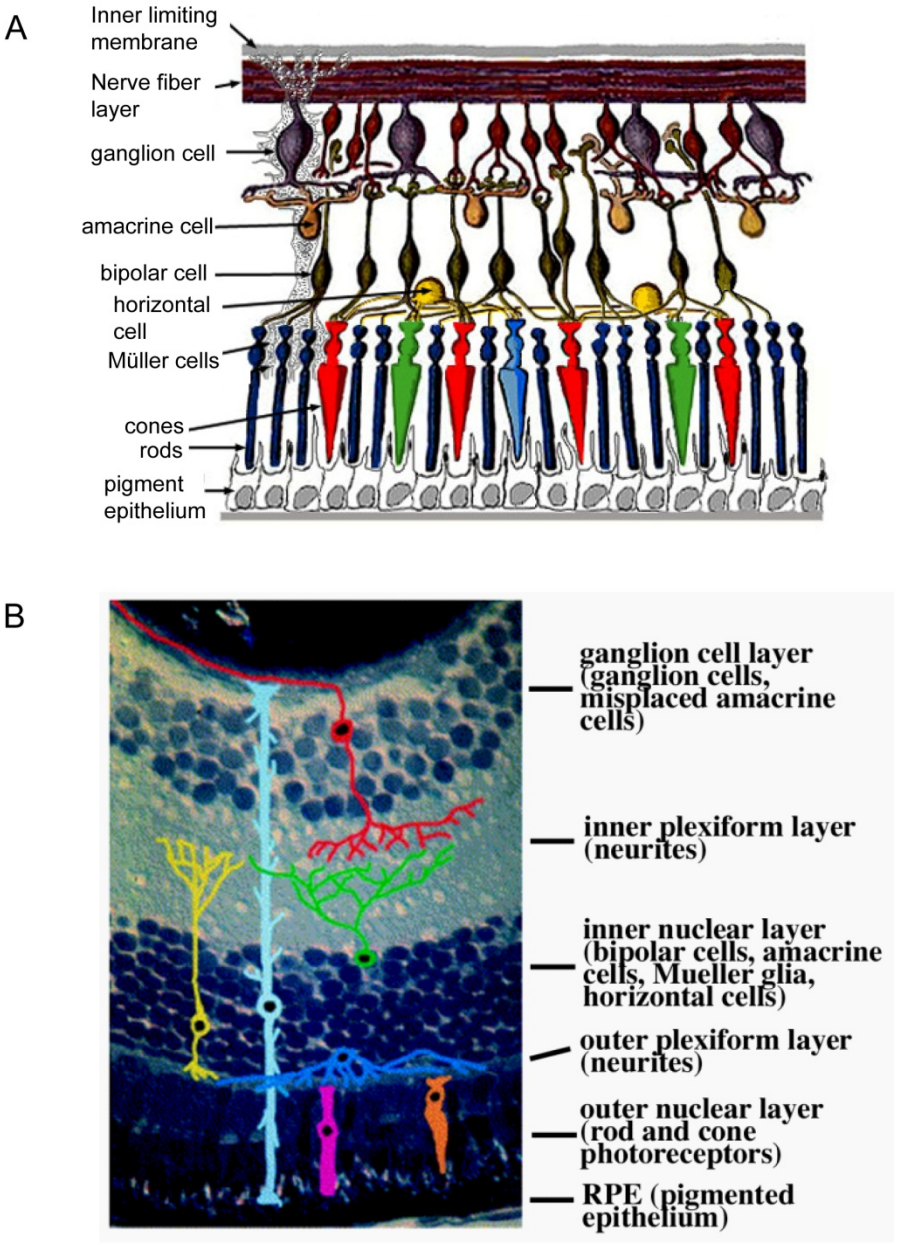

Figure4. Retinal cell types and layer structure.
A. Illustration of the spatial relationships between different cell types in the neural retina.
B. Retinal layers and main cell types. Red – ganglion cell, green – amacrine cell, light-blue – Müller glia, yellow – bipolar cell, blue- horizontal cell, pink – rod photoreceptor and orange – cone photoreceptor.
Reproduced with modifications from http://webvision.med.utah.edu/

1.6 The survival function of Sonic Hedgehog signaling

Hh signaling pathway regulates cell survival during development in addition to its pattern formation, proliferation and differentiation functions in a variety of contexts (reviewed in Ingham and McMahon, 2001; Ulloa and Briscoe, 2007; Ruiz i Altaba et al., 2003). There are several examples for the survival role of Shh. In the mouse *shh*$^{-/-}$ mutant, neural tube and ventral sclerotome showed high level of apoptotic cells (Borycki et al., 1999; Litingtung and Chiang, 2000). Similarly, surgical manipulations to prevent formation of the notochord in chick embryos lead to extensive apoptosis in the neural tube implicating Shh as a survival factor in the neural tube (Charrier et al., 2001). These findings are confirmed by the fact that restoration of Hh signaling by provision of Shh sources or de-repression of Hh signaling by deletion of *gli3* gene, repressor of Hedgehog target genes,could suppress apoptosis (Charrier et al., 2001; Litingtung and Chiang, 2000). However, it is possible that cell survival depends on the patterning role of Shh in the neural tube (Briscoe and Ericson, 1999; Patten and Placzek, 2000). This seems not to be the case, as, for example, Cayuso and colleagues (2006) showed that the effect of Hh signaling on cell survival occurs much earlier than patterning or differentiation. Also, lack of Shh in chick embryos leads to striking apoptosis in the neural crest (Ahlgren and Bronner-Fraser, 1999), which is similar to the phenotype the mouse *Smo* gene knockout embryos with decreased proliferation and increased apoptosis in the branchial arches (Jeong et al., 2004). By contrast, studies of Shh in neural crest development in zebrafish confirmed an important role of Shh in cartilage differentiation, but did not identify the cell survival function of Shh signaling likely due to using cyclopamine treatments and a hypomorphic *shh* mutant (Wada et al., 2005; Eberhart et al., 2006). These results also suggest that the levels of Hh signaling required for cell survival may be lower than those required for differentiation. Zebrafish retina is another tissue requiring Shh for survival of most cell types as shown by *shh*$^{-/-}$ mutant analysis (Shkumatava and Neumann, 2005).

However, there is still some controversy about the underlying mechanism of the survival role of Shh. Activation of pro-survival genes by Shh signaling represents the simplest scenario, and indeed, Gli1 can activate BCL2 gene in human cell lines by binding to several near-consensus sites in the BCL2 promoter, one of which plays a crucial role in Gli1-mediated induction. Likewise, Gli1 over-expression in the mouse keratinocytes (Bigelow et al., 2004)

and over-expression of the Gli3 dominant-active form in developing chick embryos leads to induction of *Bcl2* (Cayuso et al., 2006). In contrast to this transcriptional mechanism, another study proposed that in the absence of Shh Patched1 mediates neural tube apoptosis, in a way that is independent of the canonical Shh signaling pathway and to function through more direct caspase activation (Thibert et al., 2003). Patched1 could function in this context as a dependency receptor, i.e. a receptor inducing cell death in the absence of cognate ligand binding (Chao, 2003; Guerrero and Ruiz i Altaba, 2003). However, another study (Cayuso et al., 2006) concluded that Hh survival function is mediated entirely by Gli transcription factors. Consistent with and complementary to the results in this thesis, Abe et al (2008) showed that activation of Hh signaling can suppress p53 pathway in tissue culture systems. To activate Hh signaling, the authors employed dominant-active Smo mutants and Gli transcription factor overexpression. They found that Hh signaling activation leads to phosphorylation of Hdm2 (human Mdm2) on serines 166 and 186. The phosphorylated Hdm2 becomes activated and catalyses ubiquitination of p53, which leads to suppression of p53-mediated tumour suppression in conditions of DNA damage and oncogenic stress. The authors concluded that Hh signaling induces expression of an unknown factor activating Mdm2. The results by Abe et al. (2008) raise the question whether p53 induces apoptosis *in vivo* in the absence of Shh signaling. Taken together, the studies suggest that we still know very little about the role of Shh in cell survival and the signal transduction mechanisms activating cell death machinery in the absence of Shh. Another important topic is the fate of surviving cells when apoptosis due to *shh* loss is suppressed.

1.7 p53 pathway in apoptosis induction and cell cycle regulation

Because of its tumour-suppressive role, p53 is one of the best-investigated proteins. The most fundamental function of p53 is to allow cells to respond to a variety of stresses as DNA damage, hypoxia, nucleotide depletion, and aberrant growth signals by oncogenes. Activation of p53 by DNA damage and oncogenes are considered of highest relevance for tumour suppression. The signal transduction from DNA damage to p53 is accomplished by ATM/ATR, Chk1 and Chk2 kinases (Fig. 5). Oncogenic signaling in mammalian systems leads to elevation of *p14ARF (ARF)* gene expression, which activates p53 through Mdm2 inhibition (Fig. 5; Efeyan and Serrano, 2007). Both oncogenic signaling to ARF (Efeyan and

Serrano, 2007) and DNA damage response signaling (Vousden and Lane, 2007) may play important roles in p53-mediated tumour suppression. The best investigated functions of p53 are apoptosis induction, cell cycle arrest and senescence. However, recent studies (reviewed in Vousden and Lane, 2007) show that p53 regulates glycolysis and oxidative stress regulation, cell death by autophagy, repair of genotoxic damage and cell differentiation. p53 activation by AMP kinase due to a low glucose level helps cell survive starvation conditions (Jones et al., 2005). p53 also regulates metabolism under normal conditions by activating expression of SCO2, cytochrome c oxidase assembly factor, and thus promotes oxidative phosphorylation in mitochondria (Matoba et al., 2006) and this could be the reason why p53 mutant mice have low endurance. Additionally, p53 regulates expression of many proteins with anti-oxidant functions such as sestrins, ALDH4 and TIGAR (Vousden and Lane, 2007; Bensaad et al., 2007). Another novel function of p53 is to induce autophagy, digestion of cellular contents by vesicular organelles autophagosomes, by *DRAM* gene activation (Crighton et al., 2006).

Regulation of p53 activity and abundance depends on two factors: Mdm2 and Mdm4. While Mdm2 is required for degradation of p53, Mdm4 inhibits its activity (Marine and Jochemsen, 2004). For p53 to become activated and more abundant, the negative regulation by Mdm2 must be prevented. The precise mechanism is still unknown, however, the currently favored model is that in unstressed cells, Mdm2 controls p53 stability by ubiquitination, which targets p53 to proteasomal degradation, and Mdm4 blocks the transcription activation domain of p53 (Toledo and Wahl, 2006). Upon DNA damage and other stresses, Mdm2 becomes modified and promotes degradation of itself and Mdm4 (Stommel and Wahl, 2004). This eventually leads to higher p53 activity, resulting in an increase in Mdm2 expression further increasing p53 activity. Upon stress relief, Mdm2 starts targeting p53 and stops promoting Mdm4 degradation, which brings the system back to the unstressed condition. Due to importance of Mdm2 and Mdm4, factors regulating these proteins may be involved in p53 activation.

Cell cycle regulation is another important function of p53. Cell cycle consists of several phases dividing the time from one cell division to the next. G1-phase is the period when cells growth and preparation to DNA replication occur. During S-phase DNA is replicated and in the second growth G2-phase, cells prepare to divide through mitosis (M-phase). To prevent inappropriate cell cycle progression upon damage, cells employ cell-cycle checkpoints, in

which p53 plays a key role. One of the p53-mediated cell responses is cell-cycle arrest, a transient block of cells in G1 or G2/M phase (reviewed Brown et al., 2007). Induction of *CDKN1A* gene encoding p21 cyclin-dependent kinase (CDK) inhibitor by p53 leads to cell cycle arrest before G1/S transition. p21 inhibits Cdk4/6-mediated phosphorylation and inactivation of Retinoblastoma (Rb) protein. Indeed, loss of *CDKN1A* strongly impairs p53-mediated cell cycle arrest in fibroblasts after irradiation (Brugarolas et al., 1995). Unphosphorylated Rb represses E2F-regulated cell cycle genes involved in S-phase progression. Expression of p21 leads to accumulation of unphosphorylated Rb and maintenance of S-phase cell cycle gene repression. Thus, a model emerged that p53 regulates cell cycle directly through p21-mediated CDK inhibition and indirectly, through Rb, inhibits expression of S-phase cell cycle genes (Liebermann et al., 2007). More recently, several studies established that members of the miR-34 family are p53 targets with important roles in p53-mediated G1/S transition regulation (reviewed in He et al., 2007). More specifically, miR-34 can inhibit translation of CDK4, CDK6, cyclinE2 and E2F3 thereby blocking G1- to S-phase cell cycle progression. Another mechanism of cell cycle regulation by p53 is repression of *C-MYC,* a gene involved in G1/S cell cycle progression. Induction of G2/M arrest was found to be a much more complex process with many potential effectors induced by p53 (Brown et al., 2007). p53 regulates CyclinB-Cdk1 complex expression by inhibiting NF-Y transcription factor which regulates expression of *CyclinB* and *Cdk1*. Moreover, expression of p53 targets p21 and GADD45*α* inhibits Cdk1 kinase activity. Cdc25C is required for activatory dephosphorylation of Cdk1, and p53 prevents this Cdk1 dephosphorylation by repressing expression of *Cdc25C* gene. p53 also influences localisation of CyclinB-Cdk1 complexes by activating *14-3-3σ* gene. 14-3-3σ prevents nuclear localization of CyclinB-Cdk1 complex and Cdc25C. *GADD45α* is another p53 target involved in G2/M cell-cycle arrest, which disrupts CyclinB-Cdk1 complex. The list of other p53-regulated genes with less well-characterized functions in G2/M cell-cycle arrest includes *Reprimo*, *MCG10* and *Gtse-1*.

The essential tumour-suppressive role of p53 is induction of apoptosis. Most studies suggest that p53 mediates apoptosis via the intrinsic mitochondrial apoptotic pathway. Transcriptional and transcription-independent activities (TIA) of p53 were proposed to be involved in the process. As mutations in p53 affect both its transcription activity and its localization and activity in mitochondria, it has not been possible to unambiguously separate

the two activities (Schuler and Green, 2005). It has been shown that p53 rapidly localizes to mitochondria after stress induction. Interestingly, proline-rich domain of p53 is not required for p53-mediated transactivation but is necessary for induction of apoptosis. P72R mutation in this domain enhanced p53 apoptotic activity through more efficient mitochondrial localization due to enhanced nuclear export. In addition, p53 physically interacts with Bcl-2 and Bcl-xL anti-apoptotic proteins suggesting a functional similarity of p53 to BH3-only pro-apoptotic Bcl-2 proteins (Yee and Vousden, 2003). *In vitro* models of p53 TIA showed that purified p53 from DNA-damaged cells combined with Bax could permeabilise mitochondrial and liposomal membranes.

The transactivation function of p53 is clearly required for apoptosis induction by p53. Some of p53 targets regulate generation of reactive oxygen species (ROS) with a strong damaging potential for DNA, membrane lipids and proteins. ROS excess may lead to apoptosis probably through disruption of mitochondrial membranes. Importantly, ROS generation can be both suppressed and induced by p53 (Michalak et al., 2005). Suppression of ROS generation can be achieved by p53-responsive sestrin genes PA26 and Hi95. Sestrin proteins PA26 and Hi95 are enzymes producing peroxiredoxins maintaining cellular redox balance. p53 also induces expression of ALDH4 proline degradation enzyme protecting cells from increased levels of ROS. TIGAR is a p53 target which negatively regulates glycolisis by enzymatically reducing the level of Fructose-2,6-bisphosphate (Bensaad et al., 2007). Thus, glucose becomes diverted into the pentose pathway generating NADPH, a potent anti-oxidant, which neutralizes reactive oxygene species (ROS) and contributes to cell survival. By contrast, induction of ROS may also be induced by p53. For instance, PIG8 and PIG3 p53 target genes were implicated into generation of ROS and induction of apoptosis.

Intrinsic pathway of apoptosis is activated by disruption of the outer mitochondrial membrane and subsequent release of cytochrome C. Cytochrome C binds Apaf1 to form the apoptosome complex which serves to activate Caspase9 and downstream effector caspases (Fig. 6). Apaf-1, the integral component of the apoptosome (Fig. 6), was shown to be a transcriptional p53 target (Fortin et al., 2001). However, loss of APAF-1 does not completely protect cells from death and in p53-deficient mice its expression is not affected. Intrinsic apoptotic pathway is activated by BH3-only Bcl2 family proteins, which interact with downstream pro-apoptotic Bcl2 family proteins Bax and Bak. Pro-apoptotic Bcl2 family

proteins are antagonized by anti-apoptotic Bcl2 family members. There is now abundant evidence that p53-mediated apoptosis can be inhibited by Bcl2 overexpression, removal of BAX and BAK genes and by loss of BH3-only Bcl2 family member PUMA (Michalak et al., 2005). Consistent with these findings, p53 regulates expression of Bcl2 family genes. BAX was the first identified p53 target involved in intrinsic pathway of apoptosis (Selvakumaran et al., 1994). Although an increased Bax level is not sufficient for cell death, it enhances induction of apoptosis. Another p53 target is BID is a BH3-only Bcl2 family member (Sax et al., 2003), whose uncleaved form has a low pro-apoptotic activity but can be cleaved by Caspase-8 and other caspases generating tBid form capable of disrupting mitochondrial membrane (Fig. 6). This cleavage reaction serves as a connection of intrinsic and extrinsic pathways. However, *bid* mutant mice had normal apoptosis after γ-irradiation suggesting a contributory role for Bid in p53-mediated apoptosis. NOXA is another BH3-only Bcl-2 family p53 target involved in apoptosis and tumour suppression. NOXA is induced by p53 after γ-irradiation and under conditions of oncogenic stress, and it loss leads to a significant reduction of apoptotic levels after genotoxic stress (Oda et al., 2000). The most essential BH3-only Bcl-2 family gene for p53-dependent apoptosis is PUMA, which is induced by p53 under a variety of stress conditions (Nakano and Vousden, 2001). Apoptosis induction by Puma requires both Bax and Bak, suggesting that Puma acts upstream of these factors, by neutralizing anti-apoptotic Bcl-2 proteins, and thus helps Bax and Bak multimerise and permeabilize the outer mitochondrial membrane leading to activation of apoptosis (Fig. 6; Chipuk and Green, 2008). Furthermore, loss of PUMA protects cells from p53-mediated apoptosis in mouse and zebrafish (Kratz et al., 2006; Nakano and Vousden, 2001).

Figure 5. An overview of the p53 pathway inputs, signal transduction and outputs.
DNA damage, oncogenes, hypoxia, nutrient depletion and other factors are the stresses activating p53 response. Signal transducers such as ATM, ATR, Chk2 and p14ARF are involved in control of p53 activity by phosphorylation or direct binding. Activity of both p53 and Mdm2 can be regulated by ATM and perhaps other kinases. Regulation of p53-Mdm2 negative feedback loop and of Mdm4, p53 inhibitor, leads to p53 activation. Additional post-translational modifications, histone acetyl transferases (HAT) and cofactor binding regulate the specificity of p53 promoter binding. Subsequent expression of p53 target genes involved in DNA repair (DDB2, DDIT4, GADD45a, TRIM22), cell-cycle arrest (CDKN1A, SFN. TP53I3, CDC25) or apoptosis (PUMA, NOXA, BAX, BID, PIG3) leads to depicted outcomes. The figure was adopted with modifications from Riley et al. (2008).

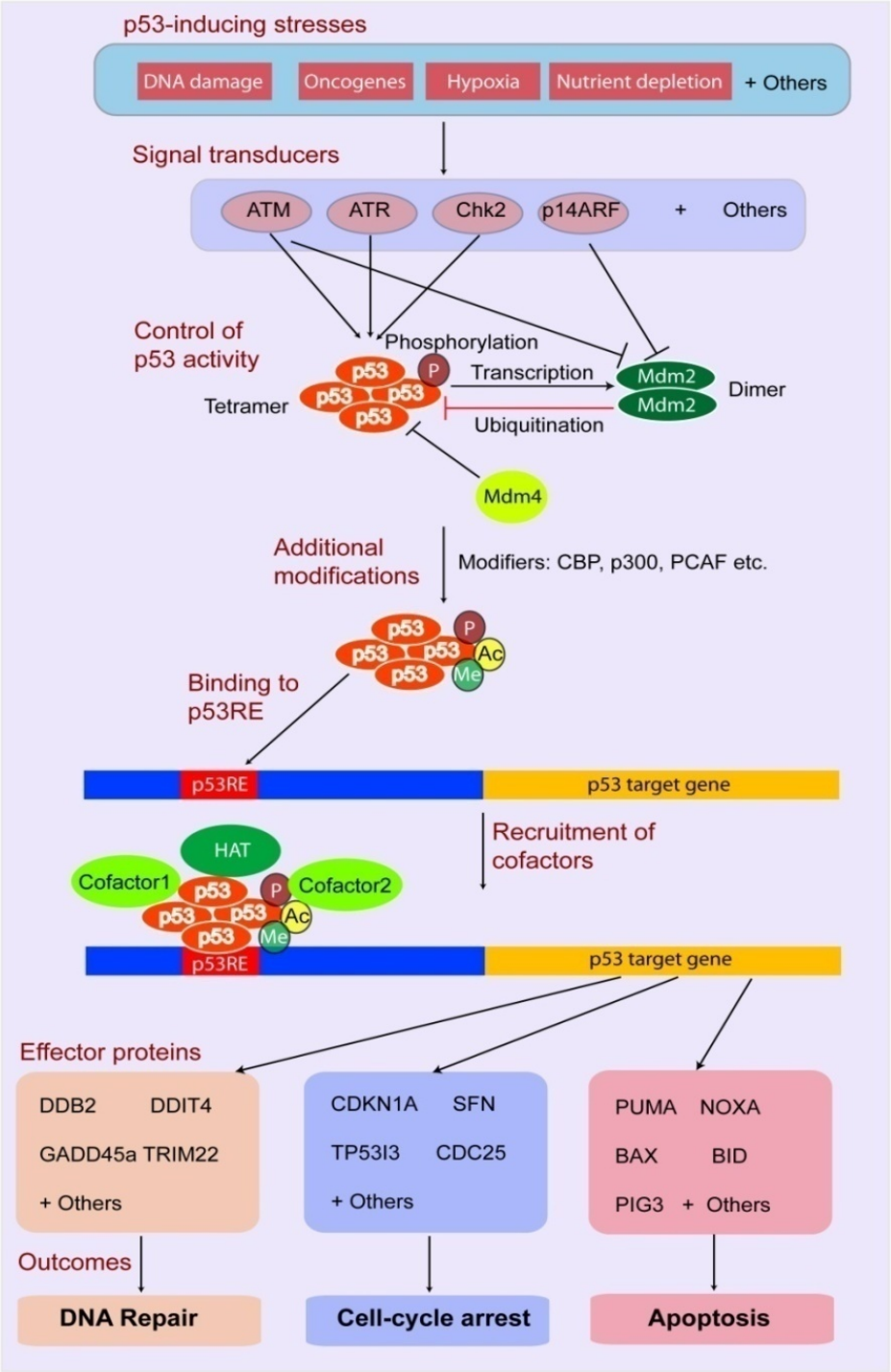
p53-inducing stresses
DNA damage
Oncogenes
Hypoxia
Nutrient depletion
+ Others
Signal transducers
ATM
ATR
Chk2
p14ARF
+ Others
Control of p53 activity
Phosphorylation
Transcription
Mdm2
Mdm2
Dimer
Tetramer
Ubiquitination
Mdm4
Additional modifications
Modifiers: CBP, p300, PCAF etc.
Binding to p53RE
p53RE
p53 target gene
Recruitment of cofactors
HAT
Cofactor1
Cofactor2
p53RE
p53 target gene
Effector proteins
DDB2 DDIT4
GADD45a TRIM22
+ Others
CDKN1A SFN
TP53I3 CDC25
+ Others
PUMA NOXA
BAX BID
PIG3 + Others
Outcomes
DNA Repair
Cell-cycle arrest
Apoptosis

Cells with active p53 typically face a choice between p53-mediated apoptosis and cell cycle arrest. However, the choices of cells with active p53 are often much more complex than this simple binary choice. In different tissues, p53 induction in response to irradiation may occur or not, and even when p53 protein level increases no apoptosis may be induced. The mechanism(s) for these differences is still unknown, although special post-translational modifications of p53 and its co-factor interactions may play a role (Murray-Zmijewski et al., 2008). Several post-translational modifications influence the choice between p53-mediated apoptosis and cell cycle arrest (Das et al., 2008). Ser46-phosphorylated p53 has a higher propensity to activate pro-apoptotic genes than *p21*. After severe DNA damage, p53 becomes acetylated at Lys120 and preferentially activates *Bax* and *Puma*. By contrast, ubiquitination of Lys320 of p53 leads to preferential activation of cell-cycle inhibitory genes by p53. Other known mechanisms for regulating the outcomes of p53 activation are gene-specific chromatin modification and protein cofactor binding to p53.

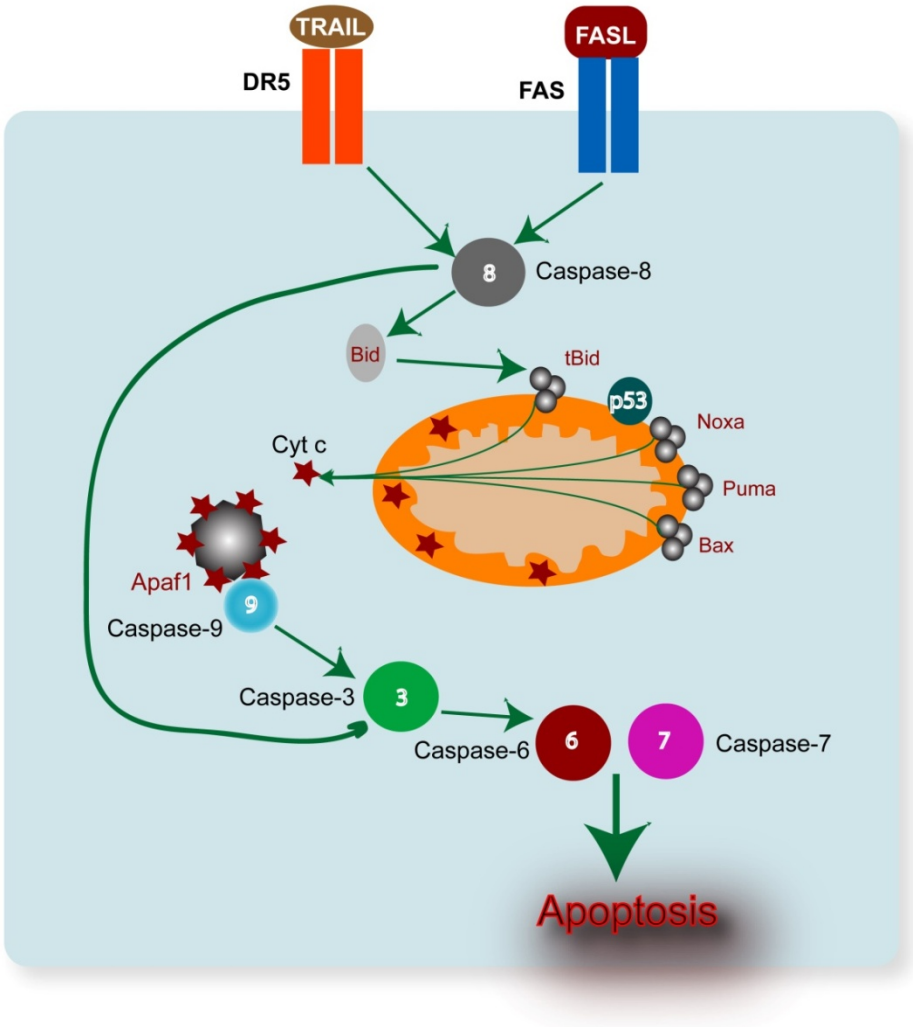

Figure 6. Intrinsic and extrinsic pathways of apoptosis and p53-mediated apoptosis.
Intrinsic pathway of apoptosis is initiated at the outer mitochondrial membrane by Puma, Noxa, Bax, tBid and p53 which induce pore formation in this membrane. These pores allow release of cytochrome C from mitochondria, which can complex with Apaf-1 protein and Caspase9 to form the apoptosome complex. Caspase9 in the apoptosome complex proteolytically activates Caspase3, which in turn activates Caspases6 and 7. Active caspases cleave many proteins to eventually induce apoptosis. p53 regulates the intrinsic pathway of apoptosis by either itself affecting outer mitochondrial membrane permeability or inducing expression of genes which do this (shown in mars red color in this figure). Extrinsic pathway of apoptosis is activated by ligands (such as TRAIL or FASL) binding to their receptors, death receptors. Ligand-bound death receptors become activated, complexes of adaptor molecules assembled on them activate Caspase8, an initiator caspase activating Caspase3. Caspase 8 also cleaves Bid protein transforming it into a highly active BH3-only mitochondria-permebilizing factor. For clarity only the best-investigated factors are shown and their interactions among each other and with anti-apoptotic Bcl-2 proteins are not depicted.

1.8 Evidence for interaction of Hedgehog and p53 pathways

Activation of Hh signaling has oncogenic properties in a number of contexts. To understand how Hh signaling is linked to tumorigenesis, it is necessary to discover the connections between the Hh pathway and other oncogenes and tumour suppressors. p53 is considered the most important tumour suppressor and interacts with many proteins and pathways. Interestingly, Hh signaling is one of p53-interacting signaling pathways. Wetmore and colleagues (2001) have provided the first evidence for a genetic interaction of p53 and Shh signaling pathway in the context of medulloblastoma development. Mice or humans heterozygous for *patched* mutation (*patched*$^{+/-}$) show a strongly increased incidence of medulloblastoma most likely due to an increased level of Hh signaling. The authors also found that *p53* loss in *patched*$^{+/-}$ background leads 95 % of mice to develop medulloblastoma compared to only 14 % of *patched*$^{+/-}$*p53*$^{+/-}$ mice. *p53* also interacts genetically with *Sufu*, a negative regulator of Shh signaling (Lee et al., 2007). While *Sufu*$^{+/-}$ heterozygote mice did not develop medulloblastoma with higher frequency, *Sufu*$^{+/-}$ *p53*$^{+/-}$ heterozygotes had medulloblastoma incidence of 58 %, suggesting that activated Hh signaling can cause medulloblastoma development if not controlled by p53. In basal cell carcinoma (BCC) mutations in *patched* and *p53* are found with a higher incidence (Kim et al., 2002; Reifenberger et al., 2005). Moreover, in gliomas requiring Hh signaling for development and maintenance (Clement et al., 2007) *p53* mutations are the most frequent genetic alterations (Ohgaki and Kleihues, 2007). Cancer stem cells in glioma tumours present activated Hh signaling due to higher expression of Gli1, which is required for cancer stem cell self-renewal and overall tumour proliferation and survival. Studies of genetic interactions give important clues for further research but do not provide mechanistic explanations of the observed phenomena. A recent study by Stecca and Ruiz i Altaba (2009) described a negative feedback loop between p53 and Gli1 in the mouse, which helps explain the genetic interaction of p53 and Shh signaling. The authors observed that p53 can inhibit Gli1-mediated proliferation, neurosphere formation and positive transcriptional regulation in luciferase assays. p53 also promoted cytoplasmic localization of Gli1, which interferes with its normal nuclear localization and may direct Gli1 to proteosomal degradation. Closing the loop, Gli1 overexpression led to a striking increase of Mdm2 expression and down-regulation of p53 in the mouse brain and several cell lines (Stecca and Ruiz iAltaba, 2009). These results are

consistent with the previously reported finding that Hh signaling can negatively regulate p53 pathway (Abe et al., 2008).

1.9 Zebrafish as a model system

Different organisms have been used as model systems for understanding fundamental biological problems and pathologies. More precisely, a model system can be defined as an organism with useful features together with information resources and powerful experimental tools, which enable convenient and productive research. The zebrafish (*Danio rerio*) as a model system was established in early 1980s by George Streisinger and co-workers. In the last 20-30 years zebrafish has become very popular due to the fact that it is a vertebrate of small size with relatively short life cycle and rapid external development, high number of progeny and can be easily maintained in the lab. Moreover, the embryo is transparent, a property important for *in vivo* microscopy, and transgenic technologies enable imaging of a variety of cells and processes in the zebrafish embryos. Finally, forward and reverse genetic approaches are available to uncover and characterize gene functions.

1.10 Aims of this thesis

The work presented here aimed to investigate the role of Shh in controlling proliferation and cell survival. Shh and Fgf signalling pathways are good candidate mechanisms how to control proliferation during limb development, since they are both known to directly regulate proliferation in other contexts. However, it has been an open question whether and how they work together to regulate proliferation of limb bud cells. I set out to investigate this question using *shh*$^{-/-}$ mutant analysis, pharmacological inhibition of Hh and Fgf signaling and activation of Fgf signaling using recombinant FGF protein.

Shh is known to provide survival signals in a way that is yet unknown. My aim was to investigate the existence of a common mechanism underlying the survival function of Shh in different tissues. I have identified p53 pathway as the apoptosis-inducing mechanism in *shh*$^{-/-}$ mutant and created a reporter to study p53 activation. Another aim was to confirm that normal Hh signaling pathway is required to control p53 activaty. Since p53 also affects cell cycle progression, I aimed to understand how p53 affects proliferation and differentiation of retinal progenitor cells in the absence of Shh.

2 RESULTS

2.1 Shh and Fgf signaling pathways in regulating fin bud cell proliferation

2.1.1 Loss of Shh signaling leads to reduction of cell cycle gene expression correlating with Fgf signaling status

In order to investigate the role of Shh in regulating cell-cycle progression in the pectoral fin buds, I analyzed the expression of G1- and S-phase cell-cycle genes in the pectoral fin buds of zebrafish *shh*$^{-/-}$ mutants. Analysis was focused on *cyclinD1*, *pcna* and *mcm5*, which are generally used as markers of proliferating cells in zebrafish (Shepard et al., 2004; Ryu et al., 2006). Expression of *cyclinD1* is necessary for G1-progression and S-phase entry, while *pcna* and *mcm5* are necessary for DNA replication during S-phase (Ohtani, 1999). As a control, I analyzed expression of *replication protein A1* gene (*ra1*), which is expressed constitutively in all cells of the fin bud. At 32 hpf, *cyclinD1*, *pcna*, *mcm5* and *ra1* are expressed at very similar levels in wild-type and in *shh*$^{-/-}$ mutant fin buds (Fig. 7C-F, I-L). Since expression of the Shh target *patched1* (*ptc1*) (Concordet et al., 1996) is absent from *shh*$^{-/-}$ mutant fin buds at all stages (Fig. 7A, M), these results indicate that expression of G1- and S-phase cell-cycle genes is independent of Shh at 32hpf. Examination of these cell-cycle genes at 38hpf, however, reveals that *cyclinD1*, *pcna*, and *mcm5* expression are lost in *shh*$^{-/-}$ mutant fin buds, while *ra1* remains unaltered (Fig. 7O-R, V-X), suggesting that cell-cycle progression becomes dependent on Shh signaling at later stages. Since the expression of Fgf ligands in the AER depends on Shh activity (Capdevila and Izpisúa Belmonte, 2001; Neumann et al., 1999), I also tested whether the activity of the Fgf signaling pathway in *shh*$^{-/-}$ mutant fin buds correlates with the observed reduction in cell-cycle gene expression. Using the Fgf-target *pea3* as a marker for Fgf signaling (Roehl and Nüsslein-Volhard, 2001), I find that *pea3* expression in *shh*$^{-/-}$ mutant pectoral fin buds is identical to wild-type fin buds at 32hpf, but is strongly reduced at 38hpf (Fig. 7B, H, N, U). This result is consistent with the observation that Shh is necessary for maintenance of Fgf expression in the AER, and suggests a correlation between the activity of Fgf signaling and the expression of cell-cycle genes in *shh*$^{-/-}$ mutant fin buds. Taken together, these results show that expression of G1- and S-phase cell-cycle genes is initially normal in *shh*$^{-/-}$ mutant pectoral fin buds, but is later lost, and that this shift correlates with a similar loss of Fgf signaling activity at later stages.

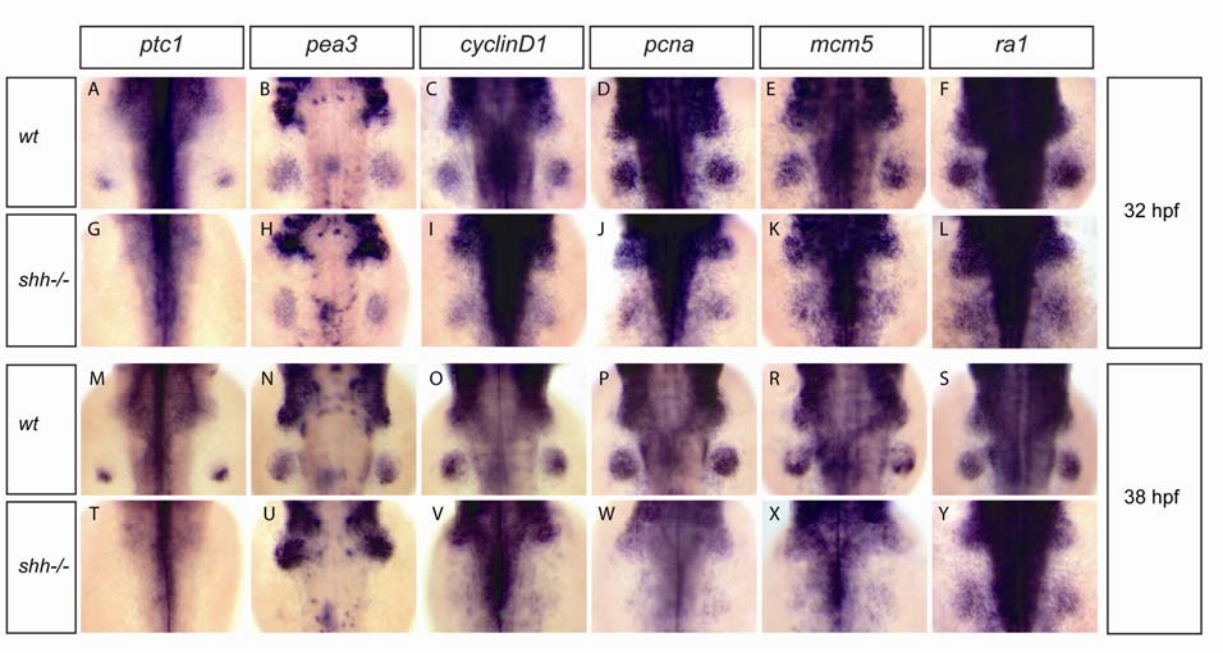

Figure 7. G1- and S-phase cell-cycle gene expression in fin buds of *shh*$^{-/-}$ mutant correlates with the Fgf signaling status.
Wild-type embryos and *shh*$^{-/-}$ mutant embryos at 32 hpf (A-L) and 38 hpf (M-Y) were analysed for expression of the Shh target *patched1(ptc1)* (A, G, M; T), the Fgf target *pea3* (B, H, N, U), the cell-cycle genes *cyclinD1*, *pcna,* and *mcm5* (C-E, I-K, O-R, V-X), and *replication protein A1*(*ra1*) (F, L, S, Y). The Shh target *ptc1* was expressed in the posterior part of wild-type fin buds at 32 and 38 hpf stages (A, M), but its expresssion was absent in *shh*$^{-/-}$ mutant fin buds (G, T). The Fgf signaling target *pea3* was expressed at comparable levels in wild-type and *shh*$^{-/-}$ mutant fin buds at 32 hpf stage (B, H). At 38 hpf *pea3* was still strongly expressed in the wild-type fin buds (N), but almost completely absent in the *shh*$^{-/-}$ mutant fin buds (U). *cyclinD1*, *pcna* and *mcm5* were expressed strongly in both wild-type and *shh*$^{-/-}$ mutant fin buds at 32 hpf stage (C-E, I-K). At 38 hpf these genes were still strongly expressed in the wild-type fin buds (O-R), but downregulated in the *shh*$^{-/-}$ mutant fin buds (V-X). Expression of *ra1* was similar in both wild-type and *shh*$^{-/-}$ mutant fin buds at 32 and 38 hpf stages.

Since the loss of G1- and S-phase cell-cycle genes in *shh*$^{-/-}$ mutant fin buds occurs relatively late, and only after Fgf signaling is lost, selective inhibition of Hh signaling using the plant alcaloid cyclopamine (Incardona et al., 1998) was employed to determine the time period of inhibition necessary to affect cell-cycle progression. Cyclopamine inhibits the action of Smoothened protein, which transduces the Hh signal after it becomes released from

Patched1-mediated inhibition (Chen et al., 2002). The use of cyclopamine allows inhibition of Hh signaling for varying periods of time, and thereby temporal control over the signaling inhibition. My aim was to find duration of cyclopamine treatment sufficient to inhibit Hh signaling, but leaving Fgf signaling largely unaffected, thereby uncoupling the two pathways from each other. I find that a 6-hour treatment from 34 to 40 hpf with 100 µM cyclopamine is sufficient to inhibit *ptc1* expression almost completely (Fig. 8A, D), but has little effect on expression of the Fgf-target *pea3* (Fig. 8B, E). Likewise, this treatment has little or no effect on *cyclinD1*, *pcna*, *mcm5* and *ra1* expression (Fig. 8C, G-I, F, J-L). By contrast, however, a 13-hour cyclopopamine treatment from 34 to 47 hpf leads to loss of both *ptc1* and *pea3* expression (Fig. 9A, B, D, E), and also leads to strong reduction of *cyclinD1*, *pcna*, and *mcm5* expression, but without affecting *ra1* (Fig. 9C, G-I, F, J-L). These results show that loss of Shh signaling leads to loss of cell-cycle gene expression only after a 13-hour delay, indicating that this is likely to be an indirect effect. Since after this delay period cell-cycle gene expression loss correlates closely with reduction of Fgf signaling in response to Shh inhibition, Fgfs are very good candidates for mediating the effect of Shh on cell-cycle progression in the fin bud.

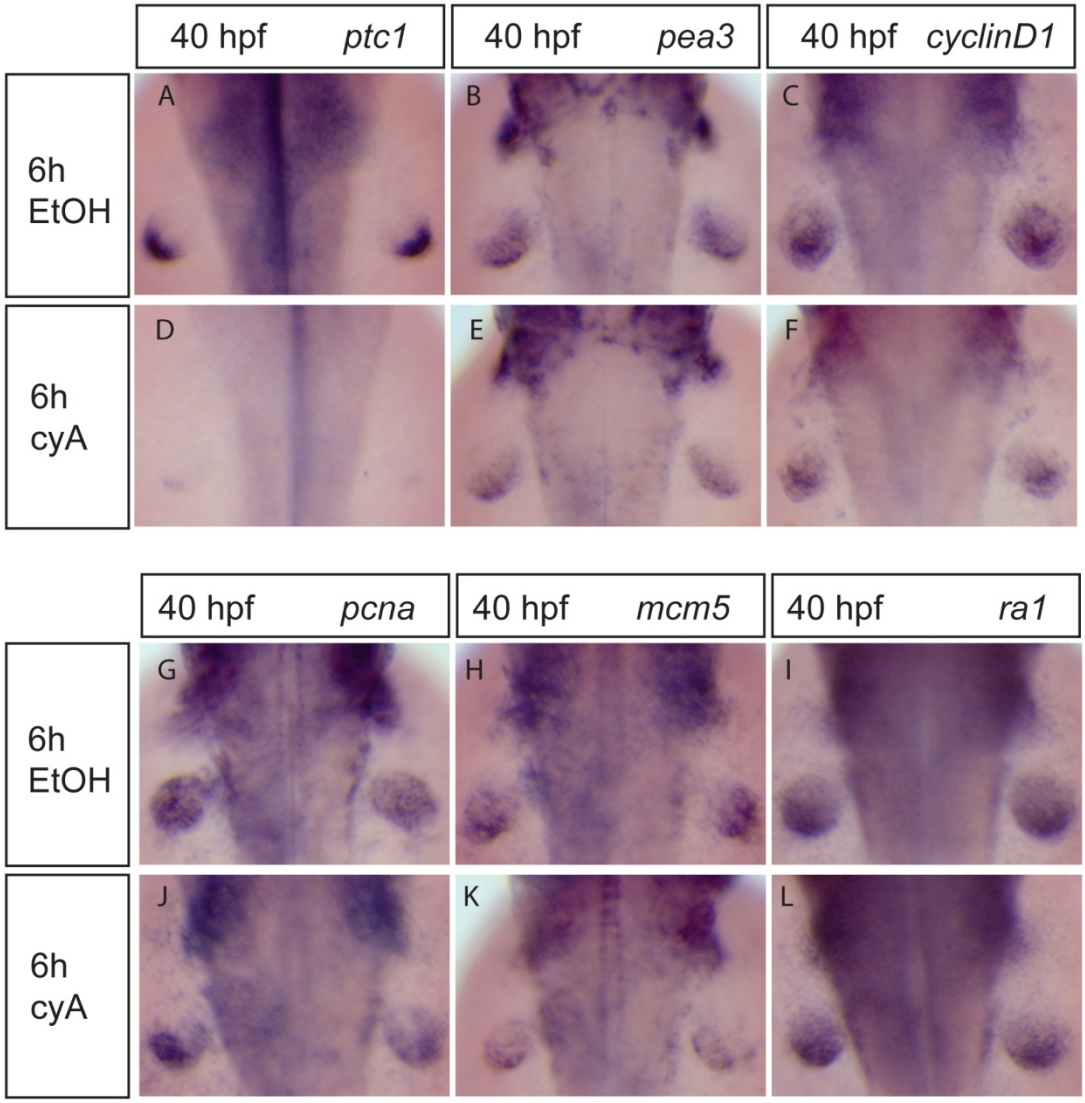

Figure 8. Cyclopamine inhibition for 6 hours does not strongly affect Fgf signaling and cell-cycle gene expression.
Wild-type embryos were treated with 100 μM cyclopamine (cyA) (D-F, J-L) or with the carrier 0,5 % ethanol (EtOH) (A-C, G-I) for 6 hours from 34 to 40 hpf (A-L) and analysed for the expression of *ptc1*, *pea3*, *cyclinD1*, *pcna*, *mcm5* and *ra1*. Expression of *ptc1* was nearly completely lost after the treatment (A, D). Hh signaling inhibition for 6 hours led to a small change in *pea3* expression in fin buds (B, E). Comparably small changes in expression after the treatment were observed for *cyclinD1*, *pcna*, *mcm5* and *ra1* (C,F; G, J; H, K; I, L).

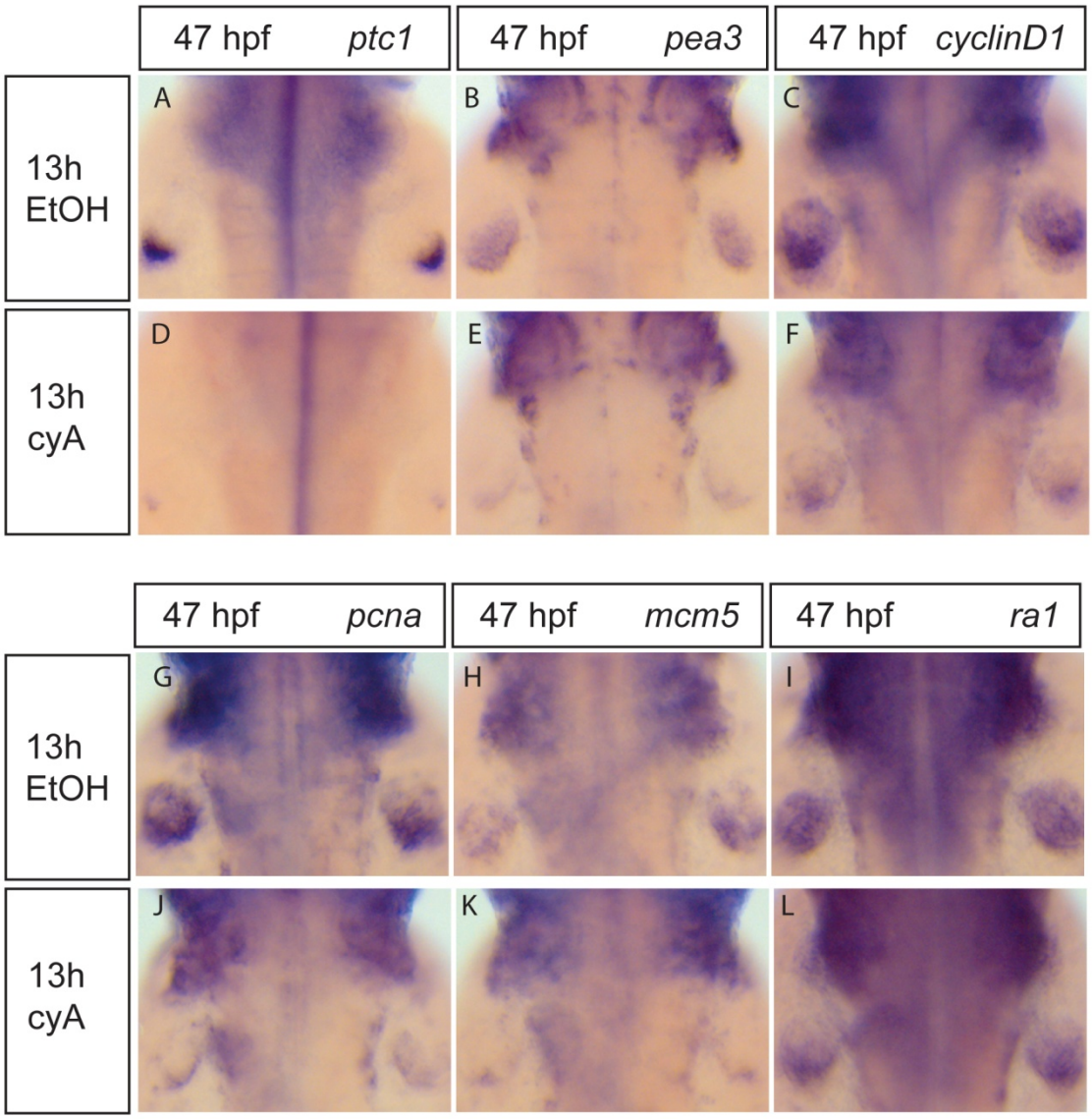

Figure 9. Cyclopamine inhibition for 13 hours is sufficient to inhibit Fgf signaling and cell cycle gene expression.
Wild-type embryos were treated with 100 µM cyclopamine (cyA) (D-F, J-L) or with the carrier 0,5 % ethanol (EtOH) for 13 hours from 34 to 47 hpf (A-C, G-I) and analysed for the expression of *ptc1*, *pea3*, *cyclinD1*, *pcna*, *mcm5* and *ra1*. Expression of *ptc1* was lost after the 13-hour (A, D) inhibition period. After 13-hour Hh signaling inhibition, fin bud *pea3* expression was strongly decreased (B, E). Likewise, expression of *cyclinD1*, *pcna* and *mcm5* in fin buds was strongly downregulated (C, F; G, J; H, K). Expression of *ra1*gene was only mildly affected by 13-hour cyclopamine treatment (I, L).

2.1.2 Fgf signaling inhibition leads to rapid loss of cell-cycle gene expression and proliferation decrease in the fin buds

Following the observation that Hh signaling inhibition strongly affects expression of cell-cycle genes after a 13-hour cyclopamine treatment, I decided to investigate how rapid the response of the same genes is to inhibition of Fgf signaling. For this purpose, I used the chemical inhibitor SU5402, which inhibits signaling by Fgf receptor in mouse cell culture lines (Mohammadi et al., 1997) and in zebrafish embryos (Roehl and Nüsslein-Volhard, 2001). I find that treatment with 10 μM SU5402 for 3 hours between 36 and 39 hpf leads to nearly complete loss of the Fgf-target *pea3* (Fig. 10A, D), while expression of the Shh target *ptc1* is hardly affected (Fig. 10B, E), indicating that, under these conditions, Fgf signaling is blocked whereas Shh signaling is still intact . This 3-hour inhibition of Fgf signaling is sufficient to cause a nearly complete loss of expression of *cyclinD1* (Fig. 10C, F), *pcna* (Fig. 10G, J) and *mcm5* (Fig. 10H, K) in fin buds, while *ra1* (Fig. 10I, L) is unaffected. Interestingly, *cyclinD1*, *pcna*, and *mcm5* expression are also lost from the branchial arch primordia following this treatment (Fig. 10C, F, G, J, H, K). Consistent with the loss of expression of G1- and S-phase genes after 3 hours of SU5402 treatment, the number of cells labelled with 5-bromodeoxyuridine (BrdU) is also strongly reduced in the fin buds under these conditions (Fig. 11A, B). These results show that the effect of Fgf signaling on cell-cycle progression in the fin buds is much more rapid than the effect of Shh signaling, since there is a severe down-regulation of cell-cycle genes already after 3 hours of Fgf signaling inhibition.

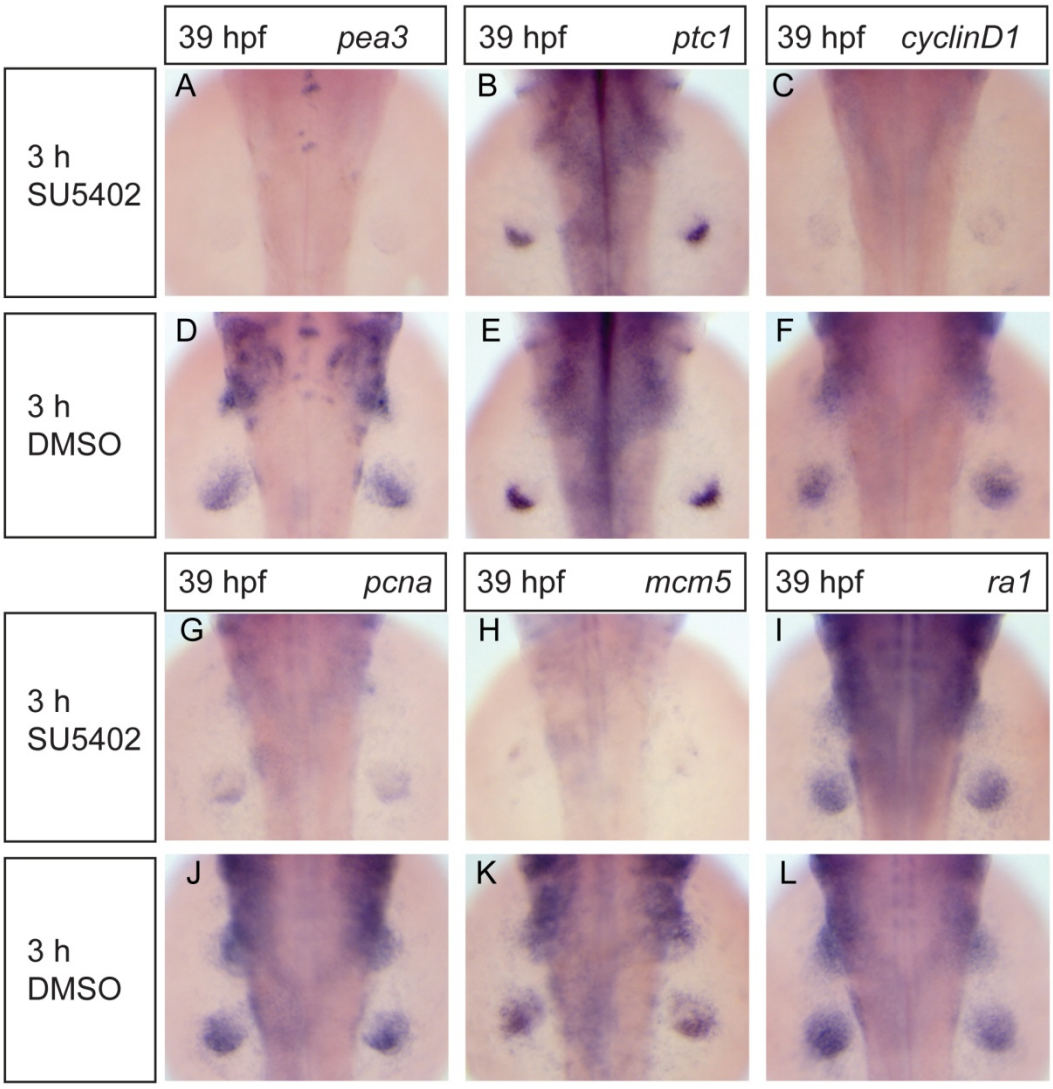

Figure 10. Fgf signaling inhibition leads to loss of G1- and S-phase cell cycle gene expression. Wild-type embryos were treated with 10 μM SU5402 (A-C, G-I) or the carrier 0,125 % DMSO (D-F, J-L) for 3 hours from 36 to 39 hpf. SU5402 treatment strongly downregulated the expression of *pea3* FGF signaling target (A, D), but had only a small effect on *ptc1* expression in fin buds (B, E). SU5402 treatment also caused strong down-regulation of *cyclinD1* (C, F), *pcna* (G, J) and *mcm5* (H, K). Expression of *ra1* was not affected by SU5402 treatment (I, L).

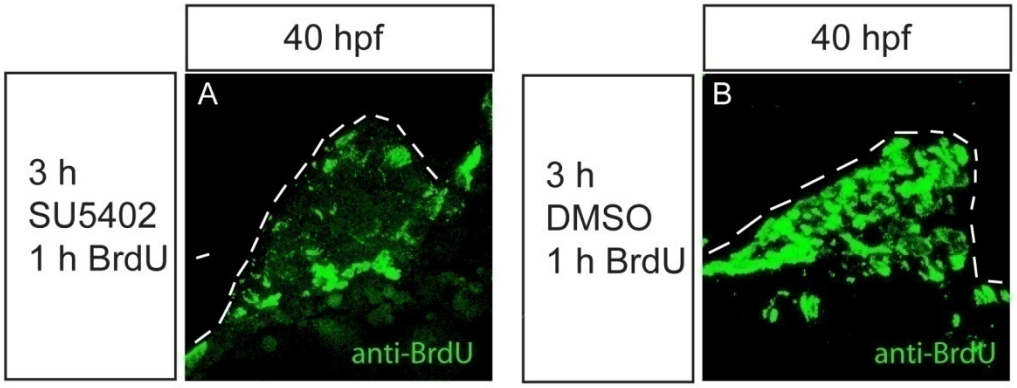

Figure 11. Fgf signaling inhibition reduces proliferation in zebrafish fin buds.
Wild-type embryos were treated with 10 μM SU5402 (A) or 0,125 % DMSO (B) for 3 hours from 36 to 39 hpf. After 3-hour treatment with either SU5402 or DMSO, embryos were injected with 10 mM BrdU solution into the yolk and incubated for 1 hour in the same solutions before fixation. S-phase progression, as revealed by BrdU labeling, was strongly inhibited after SU5402 treatment, in comparison to control embryos (n = 10, at least 2 fin sections per embryo were analysed) (A, B).

Since blockage of Fgf signaling with SU5402 leads to rapid loss of G1- and S-phase gene expression both in the pectoral fin buds and in the branchial arches, I also checked whether Fgf signaling is required for proliferation in other tissues. Therefore, an inhibitor treatment at 20 hpf was performed, at a stage at which many embryonic cells are still proliferative. After 3 hours of treatment with 10 μM of SU5402, expression of *pea3* is almost completely lost in these embryos, but *cyclinD1*, *pcna*, *mcm5* and *ra1* expression is unaltered (Fig. 12A-C, G, H; D-F, I, J). Furthermore, while SU5402 treatment at 36 hpf leads to loss of cell-cycle genes from both the pectoral fin buds and the branchial arches, it has no effect on the same genes expressed in the retina and the optic tectum. These results indicate that Fgf signaling is not generally required for proliferation in the whole embryo, but that it instead directs expression of cell-cycle genes specifically in the pectoral fin buds and in the branchial arches.

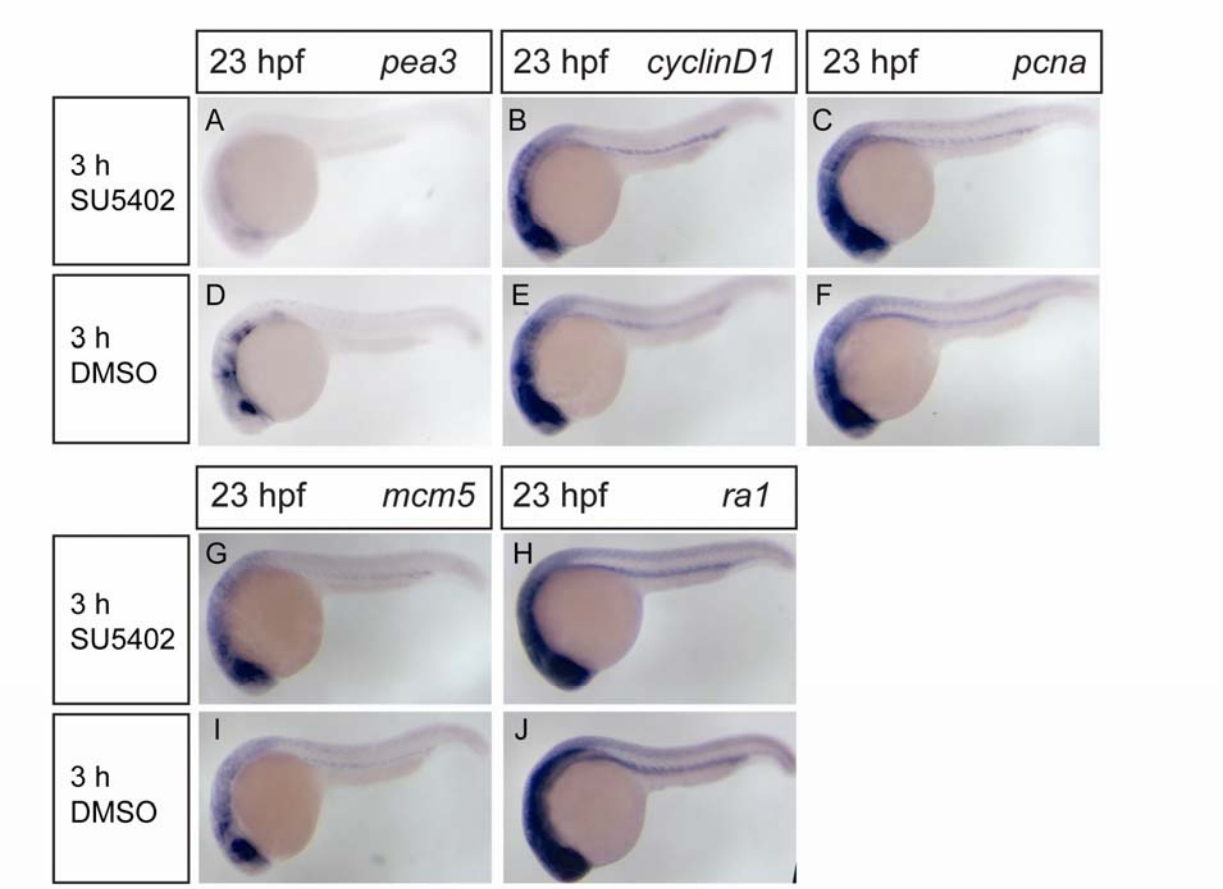

Figure 12. Fgf signaling inhibition at 20 hpf does not lead to global reduction of cell-cycle gene expression.
Wild-type embryos were treated with 10 µM SU5402 (A-C, G,H) or 0,125 % DMSO (D-F, I, J) for 3 hours from 20 to 23 hpf. SU5402 treatment caused a strong downregulation of *pea3* gene expression (A, D), but expression of *cyclinD1*, *pcna*, *mcm5* and *ra1* genes was not changed in SU5402-treated embryos compared to control ones (B, E; C, F; G, I; H, J).

2.1.1 Activation of Fgf signaling in *shh*$^{-/-}$ mutant induces cell-cycle gene expression and proliferation

The results presented so far strongly suggest that Fgf signaling is directly required for cell-cycle progression in zebrafish fin buds, while Shh plays an indirect role via its regulation of Fgf expression. However, since the Shh and Fgf signaling pathways in the limb bud are coupled by a feedback loop mechanism, it is difficult to change the activity of one pathway without affecting the other. Therefore, I decided to use a gain-of-function experiment to uncouple the Fgf pathway completely from the Shh pathway, by providing an ectopic source of Fgf protein in *shh*$^{-/-}$ mutant fin buds, and asking if this ectopic source of Fgf signaling is able

to rescue cell-cycle progression in the absence of Shh. For this purpose, heparin gel beads were soaked with recombinant human FGF4 protein and implanted into fin buds on the right hand side of *shh*$^{-/-}$ mutant embryos at 29-32 hpf. The fin buds on the left hand side were not implanted and served as an internal control in these experiments. Implanted embryos were then grown to 50 hpf and gene expression was analysed by *in situ* hybridisation. I find that FGF4-soaked beads induce *pea3* expression in *shh*$^{-/-}$ mutant fin buds (Fig. 13A). Furthermore, *cyclinD1* (Fig. 13B), *pcna* (Fig. 13C) and *mcm5* (Fig. 13D, D', D'') transcripts are also induced in the fin buds implanted with FGF4-soaked beads. Consistent with these results, I also detect increased incorporation of BrdU in bead-implanted *shh*$^{-/-}$ mutant fin buds, compared to unimplanted fin buds (Fig. 14A, B). Finally, there is increased growth of *shh*$^{-/-}$ mutant fin buds with implanted FGF4-soaked beads (Fig. 13D', D'', 14C, D), further supporting the conclusion that Fgf signaling is able to restore outgrowth in the absence of Shh. This increase in fin size after bead-implantation is somewhat variable and depends on bead position relative to the fin bud, with the largest outgrowth observed when beads are located right inside the bud (Fig 14C, D). Taken together, these results indicate that Fgf signaling is sufficient to direct proliferation in zebrafish fin buds in the absence of Shh.

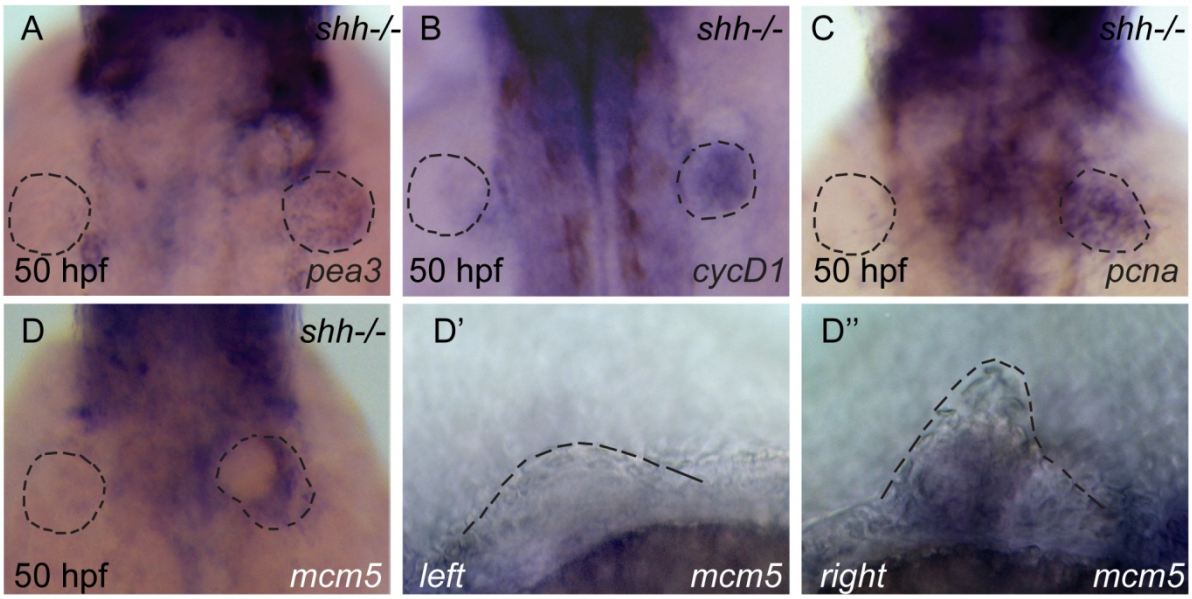

Figure 13. Human FGF4 bead implantation leads to induction of Fgf signaling and cell cycle gene expression in *shh*$^{-/-}$ mutant.
Fin buds on the right hand side of *shh*$^{-/-}$ mutant embryos were implanted with FGF4-soaked heparin beads at 29-32 hpf, grown until 50 hpf and fixed (A-D). *shh*$^{-/-}$ mutant embryos show upregulation of *pea3* (A), *cyclinD1* (B), *pcna* (C) and *mcm5* (D) expression in response to the FGF4-soaked beads on the implanted side. Fin buds are outlined by dotted lines in panels A to D. A non-implanted fin bud on the left hand side shows no *mcm5* expression (D'), while an implanted fin bud on the right-hand side of the same embryo (D'') shows restored *mcm5* expression. Fin buds implanted with FGF4 beads show increased outgrowth (D''), compared to non-implanted control fin buds (D').

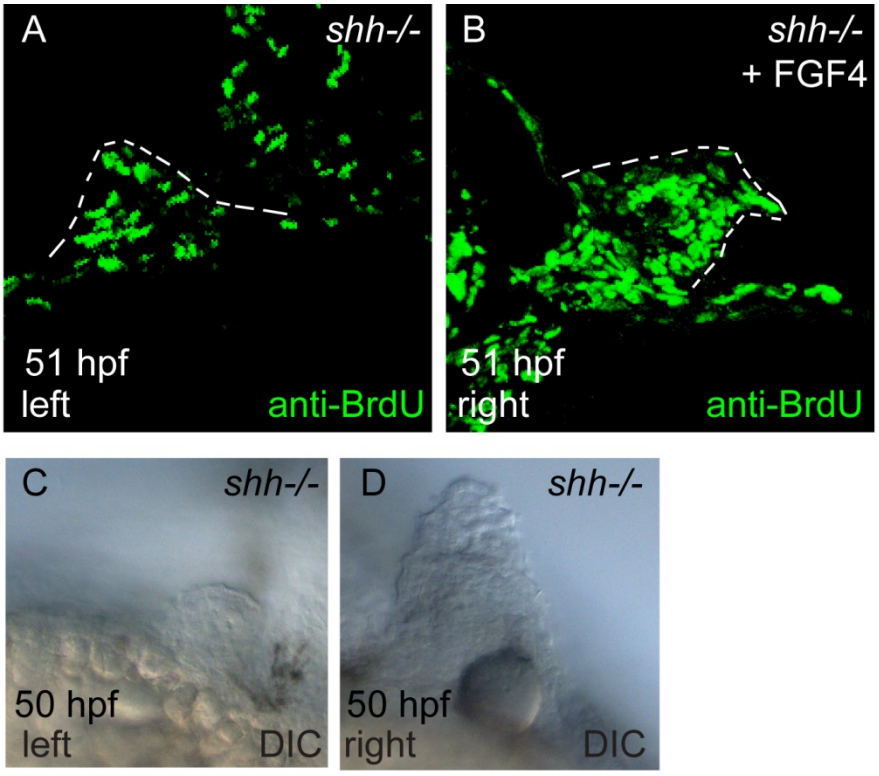

Figure 14. Human FGF4 bead implantation induces fin bud proliferation and outgrowth in *shh*$^{-/-}$ mutant embryos.
Fin buds on the right hand side of *shh*$^{-/-}$ mutant embryos were implanted with FGF4-soaked heparin beads at 29-32 hpf, grown until 50 hpf and fixed (A-D). For anti-BrdU staining, embryos were first implanted and then injected with 10 mM BrdU solution at 38 hpf before fixation at 50 hpf. The non-implanted fin bud shows few BrdU-labeled nuclei (C), while an FGF4 bead-implanted fin bud (D) has extensive BrdU labeling (sections of both sides of 10 bead-implanted embryos were analysed). Fin buds implanted with FGF4 beads show increased outgrowth (D), compared to non-implanted control fin buds (C).

2.2. The mechanism of the survival function of Shh

2.2.1 Apoptotic phenotype of zebrafish *shh*$^{-/-}$ mutant

Previous work on the survival function of Shh leads to the question whether different instances of apoptosis due to loss of Shh signaling share the same mechanism or may have different mechanisms or be secondary consequences of the lack of differentiation signals provided by Shh. To approach this question systematically, I analysed *shh*$^{-/-}$ mutant and wild-type embryos at several stages for apoptosis patterns and levels using whole-mount ApopTag staining, and using fluorescent TdT-mediated dUTP-TMRRed nick end labeling (TUNEL) staining on retinal sections. Representing most of the early zebrafish development, embryos were analysed at 24, 30, 36, 48 and 60 hpf. Mutants in *shh* gene cannot be clearly recognized until around 24 hpf, so 24 hpf was the earliest stage analysed. Apoptosis levels in *shh*$^{-/-}$ mutant were much higher than in wild-type at all stages. Wild-type embryos showed a low-level stereotypic pattern of apoptosis (Fig. 15D-F, I, J) previously described in zebrafish (Cole and Ross, 2001). At 24 hpf, most of the neural tube of *shh*$^{-/-}$ mutant except for its anterior part contained high numbers of apoptotic cells (Fig. 15A). At 30 and 36 hpf, neural tube apoptosis persisted, but apoptotic cells became localized more dorsally (Fig. 15B, C). Since neural crest cells also undergo apoptosis in the absence of Shh, dorsal apoptotic cells in zebrafish *shh*$^{-/-}$ mutant at 24 and 30 hpf are very likely neural crest cells (Fig. 16A, B). At 48 and 60 hpf, neural tube apoptosis became even more dorsally restricted, its level decreased, and apoptotic cells appeared ín the retina (Fig. 15G, H).

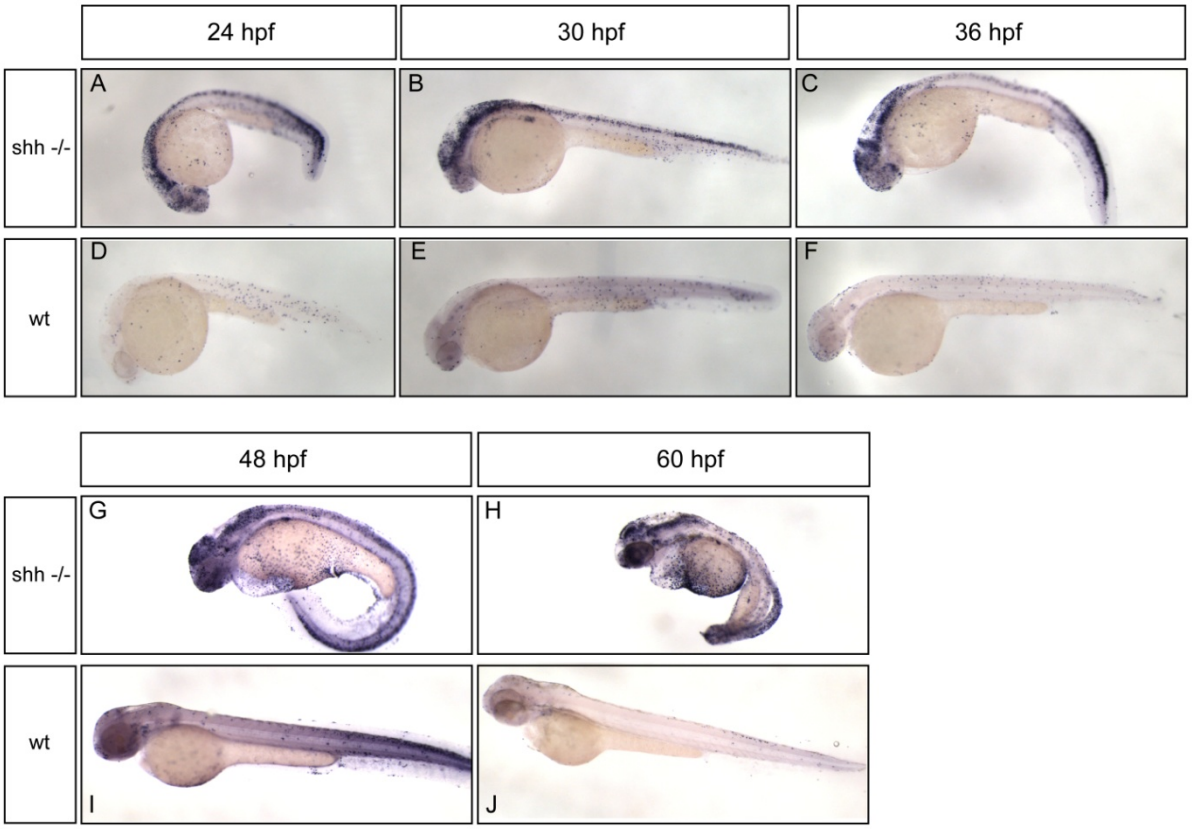

Figure 15. Apoptosis levels in *shh*$^{-/-}$ mutant and wild-type embryos by whole-mount ApopTag staining.
Wild-type (D-F, I, J) and *shh*$^{-/-}$ mutant (A-C, G, H) embryos were stained for apoptotic cells using the ApopTag protocol. At all five stages analysed (24 hpf (A, D), 30 hpf (B, E), 36 hpf (C, F), 48 hpf (G, I), 60 hpf (H, J)) *shh*$^{-/-}$ mutant embryos had dramatically increased levels of apoptosis in the neural tube decreasing over the course of development compared to wild-type. At 48 and 60 hpf stages, high level of retinal apoptosis was also observed in *shh*$^{-/-}$ mutant embryos.

Retinal apoptosis was analysed in *shh*$^{-/-}$ mutant and wild-type embryos at 24, 36, 48 and 60 hpf using TUNEL staining. At 24 hpf, both wild-type and *shh*$^{-/-}$ mutant retinas typically contained very few TUNEL-positive cells (Fig. 16A, E). By contrast, midbrain region of 24 hpf *shh*$^{-/-}$ mutants contained a high number of apoptotic cells (Figure 16A) showing a different timing of apoptosis in the *shh*$^{-/-}$ mutant retina and midbrain. Wild-type and *shh*$^{-/-}$ mutant retinas at 36 hpf were very similar in their low numbers of apoptotic cells and had significant apoptosis in their lenses (Fig. 16B, F). At 48 hpf, apoptosis level in *shh*$^{-/-}$ mutant retinas increased in comparison to that in the wild-type retinas (Fig. 16C, G). Finally, at 60 hpf there is a dramatic difference in apoptotic levels in wild-type and *shh*$^{-/-}$ mutant retinas, with

the mutant retina containing many apoptotic cells (Fig. 16D, H). These results are consistent with the result reported by Neumann and Nüsslein-Volhard (2000) that apoptosis in the *shh*$^{-/-}$ mutant retina is not increased before 48 hpf. The distinct timing of apoptosis in different regions of *shh*$^{-/-}$ mutant embryos may suggest different apoptotic mechanisms or reflect differences in Shh expression requirements for cell survival in different tissues, but the same mechanism of apoptosis induction.

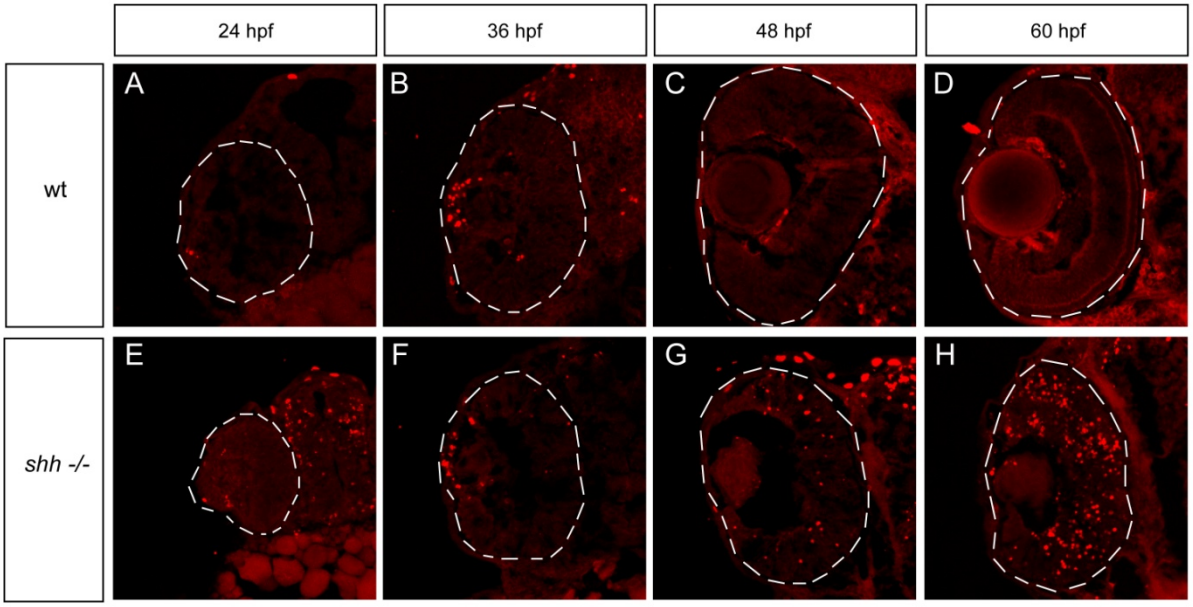

Figure 16. Retinal apoptosis in zebrafish *shh*$^{-/-}$ mutant and wild-type embryos during development.
Wild-type (A-D) and *shh*$^{-/-}$ mutant (E-H) retinal sections were TUNEL stained. The following stages were analysed: 24 hpf (A, E), 36 hpf (B, F), 48 hpf (C, G) and 60 hpf (D, H). There is an increase in retinal apoptosis level in *shh*$^{-/-}$ mutant over the course of development, whereas in wild-type there is no such increase.

2.2.2 Anti-apoptotic factor expression in *shh*$^{-/-}$ mutant

Apoptosis is generally induced when pro-apoptotic factors outweigh anti-apoptotic factors in a cell. One model to understand apoptosis induction is that of the death threshold, which suggests that cumulative influence of both pro- and anti-apoptotic factors matters and the final outcome may not be attributed to a single factor (Lowe et al., 2004). Bcl2 family consists of both pro- and anti-apoptotic factors, and their balance is essential for cell survival. Zebrafish contains 12 pro-apoptotic and 5 anti-apoptotic bcl-2 family genes, which were functionally characterized by Kratz and colleagues (2006). Bcl2, Bcl2l, Mcl1a and Mcl1b were

confirmed as pro-survival factors, and Mcl1 proteins were found to be essential for cell survival during early embryonic development. As a first step toward understanding apoptosis in *shh*$^{-/-}$ mutant, I analysed expression of these anti-apoptotic Bcl2 family genes in wild-type and *shh*$^{-/-}$ mutant embryos. *Bcl2*, *bcl2l, mcl1a* and *mcl1b* all have a broad expression pattern in both wild-type and *shh*$^{-/-}$ mutant embryos consistent with their basic function in regulating apoptosis at the level of mitochondria (Fig. 17). All of these genes are also expressed at very similar levels in wild-type and *shh*$^{-/-}$ mutant embryos suggesting that there is no dramatic change in anti-apoptotic Bcl2 family gene expression in the absence of Shh (Fig. 17). However, it is not possible to exclude some tissue-specific differences in expression of these genes.

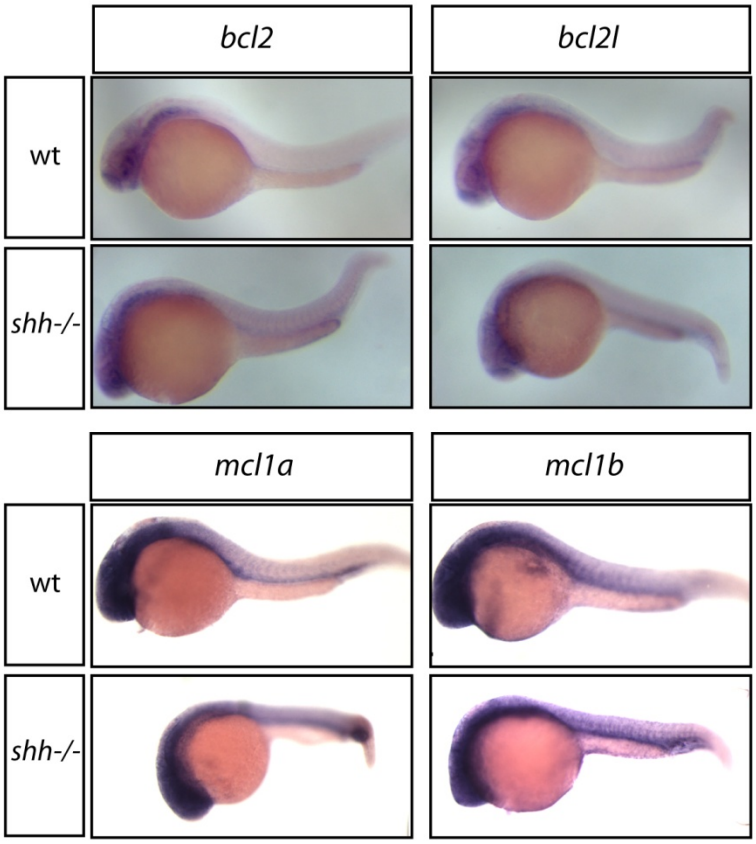

Figure 17. Expression of anti-apoptotic Bcl2 family genes in *shh*$^{-/-}$ mutant versus wild-type zebrafish embryos at 24 hpf.
In situ whole-mount analysis of *bcl2*, *bcl2l*, *mcl1a* and *mcl1b* expression in *shh*$^{-/-}$ mutant and wild-type embryos at 24 hpf

2.2.3 The involvement of p53 pathway in apoptosis in *shh*$^{-/-}$ mutant

Given the lack of clear differences in anti-apoptotic factor expression between *shh*$^{-/-}$ mutant and wild-type embryos, I asked if induction of pro-apoptotic factors may explain increased apoptosis in the developing *shh*$^{-/-}$ mutant embryos. Therefore, I checked if p53 pathway mediates apoptosis in *shh*$^{-/-}$ mutant embryos. Analysis of p53 target gene expression showed that *p53*, *cyclinG1*, *bax1*, *puma* and *p21* are specifically induced in *shh*$^{-/-}$ mutant embryos at 24 hpf (Fig. 18A, D; B, E; C, F; G, I; H, K). Similarly, at 56 hpf, *p53* was up-regulated in the *shh*$^{-/-}$ mutants in the brain, retina and branchial arches (18L, M) relative to wild-type embryos (18N, O). To confirm the results of *in situ* hybridizations, I performed quantitative PCR (qPCR) analyses of p53 target genes on *shh*$^{-/-}$ mutant versus wild-type embryos at 24 hpf and 56 hpf. qPCR clearly showed the induction of *p53*, *mdm2*, *cyclinG1*, *bax1* and *puma* at both stages (Fig. 19). CDK inhibitor gene *p21* had the highest fold induction of expression. Of the pro-apoptotic genes, *bax1* and *puma*, but not *noxa,* were clearly induced in *shh*$^{-/-}$ mutants at both 24 hpf (Fig. 19A) and 56 hpf (Fig. 19B). Puma is one of the most potent inducers of mitochondrial apoptotic pathway and the main pro-apoptotic p53 target in zebrafish and mammals (Kratz et al., 2006; Nakano and Vousden, 2001). Induction of *puma* relative to *bax1* was higher in *shh*$^{-/-}$ mutant embryos at 24 hpf (Fig. 19A) than at 56 hpf (Fig. 19B) correlating with a higher level of apoptosis at 24 hpf than at later stages (Fig. 15). Higher *in situ* and *qPCR* signals for p53 may indicate a higher level of p53 thereby creating a positive feedback loop. However, it was reported that p53 activates an internal promoter of its own gene leading to production of a short p53 isoform *Δ113p53* (Robu et al., 2007). Strongly elevated expression of *Δ113p53* could indeed be detected in *shh*$^{-/-}$ mutant, whereas the level of full-length *p53* cDNA was very similar in both wild-type and *shh*$^{-/-}$ mutant (Fig. 19C). This result rules out the positive feedback loop of full-length p53 expression and suggests that expression of *Δ113p53* occurs similarly in different cases of p53 activation.

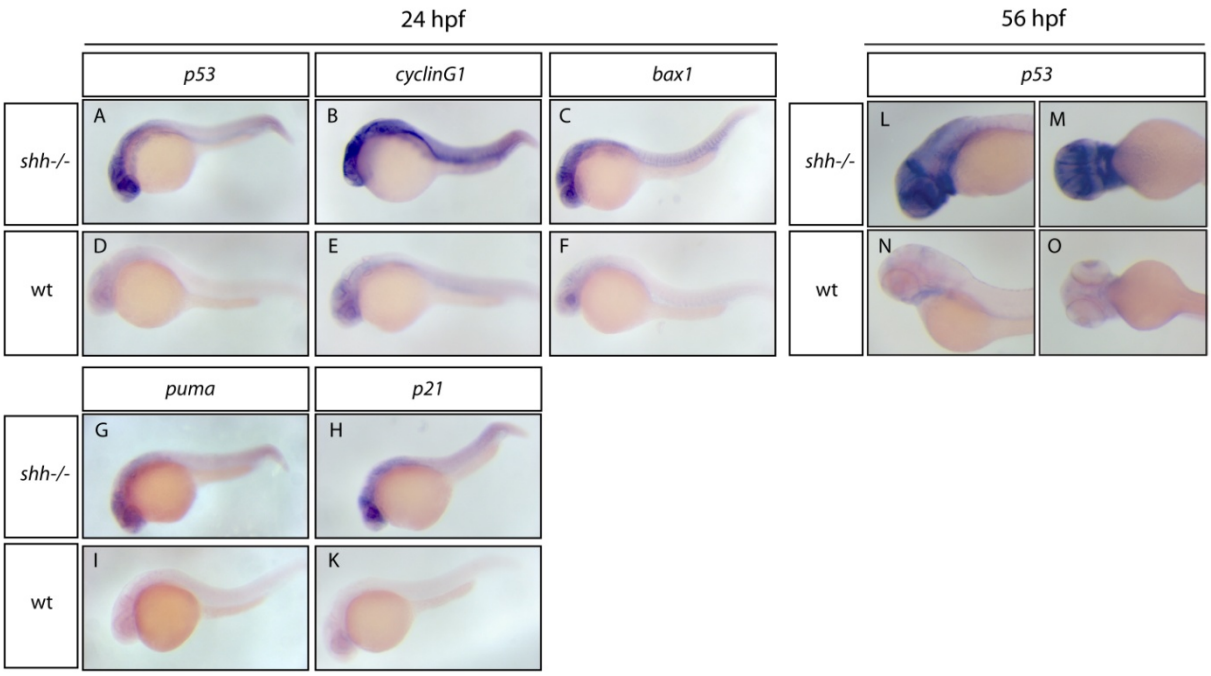

Figure 18. Expression of p53 target genes in 24 and 56 hpf *shh*$^{-/-}$ mutant versus wild-type. 24 hpf wild-type and *shh*$^{-/-}$ mutant embryos were *in situ* hybridised with probes against *p53* (A, D), *cyclinG1* (B, E), *bax1* (C, F), *puma* (G, I) and *p21* (H, K). These p53 target genes are expressed at a higher level in *shh*$^{-/-}$ mutant, and higher expression occurs in neural tube, retina and somites. 56 hpf wild-type and *shh*$^{-/-}$ mutant embryos were also hybridized with the probe against *p53* gene (L, M, N, O). The hybridizations show increased expression of *p53* in *shh*$^{-/-}$ mutant embryos (L, M) compared to wild-type ones in some brain regions, retina and branchial arches.

Timing of ectopic apoptosis due to genetic defects can help understand the reasons for its induction. High level of apoptosis in the *shh*$^{-/-}$ mutant occurs at 24 hpf, when morphological defects of the mutant are striking. In order to understand apoptosis and p53 activation timing better, I performed *in situ* hybridisation against *p53* and ApopTag staining on embryo clutches from heterozygous *shh*$^{+/-}$ parents at 1 somite, 6 somite, 8 somite, 10 somite, 12 and 14 somite stages (Fig. 20). Increased apoptosis and induced *p53* expression could be first identified in *shh*$^{-/-}$ mutant embryos at the 10 somite stage (Fig. 20M-P) and then progressed as development proceeded. Consistent with the requirement of Shh for survival in many different tissues, *p53* expression and apoptosis occurred in a broad pattern (Fig. 20). Another notable observation is that the onset of p53 activation and apoptosis in *shh*$^{-/-}$ mutant occur rapidly and at a defined developmental time point since 8 somite (Fig. 20I-L) and 10 somite (Fig. 20M-P) stages are separated by only around 1 hour. These results show that

control of p53 activity by Shh signaling starts early in development before most cells exited the cell cycle and differentiated.

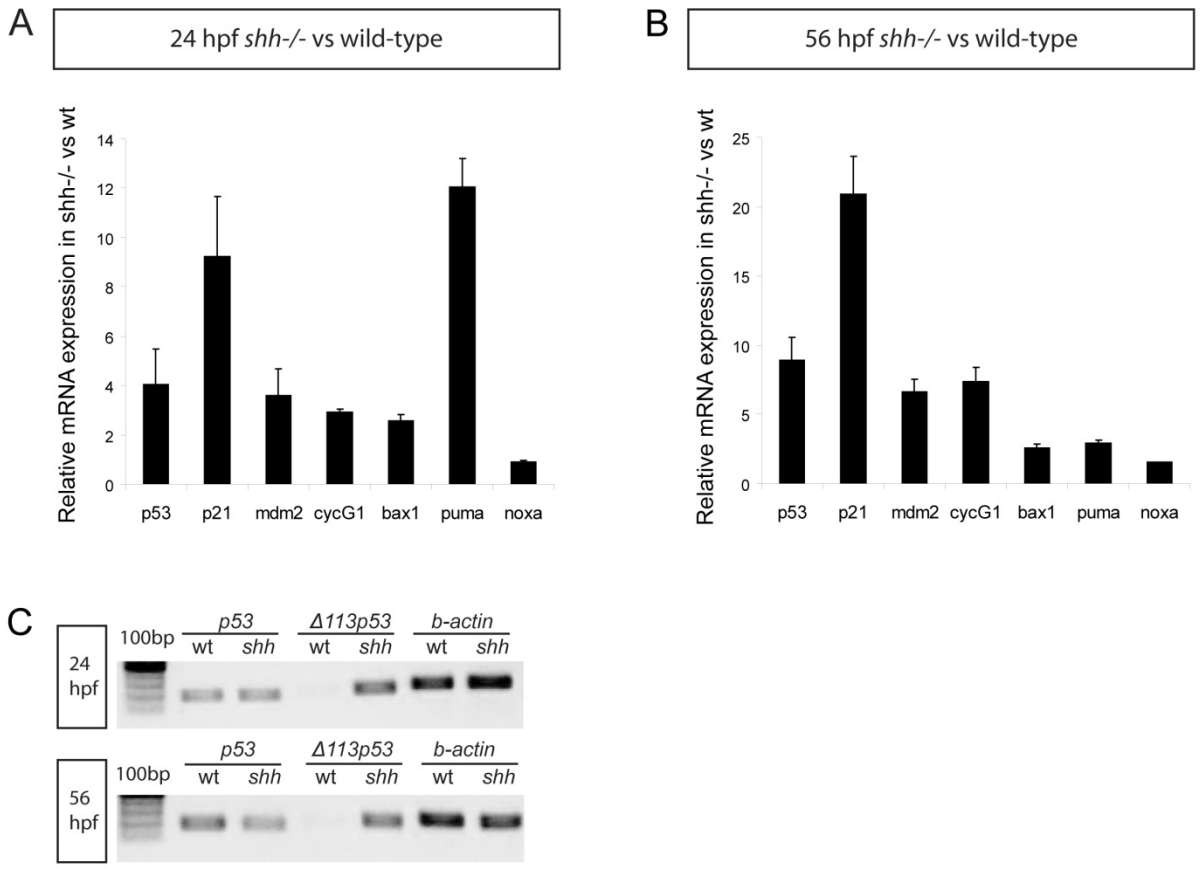

Figure 19. Quantitative PCR analysis of p53 target activation and p53 isoform expression in *shh*$^{-/-}$ mutant embryos**.**

qPCR analyses were performed at 24 and 56 hpf (A, B). qPCR assays for *p53, p21, mdm2, cyclinG1, bax1, puma, noxa* and *gapdh* were performed on both wild-type and *shh*$^{-/-}$ mutant embryos, and expression of p53 targets was normalized using *gapdh* expression as a reference gene. The panels show p53 target gene expression in mutant embryos relative to that in wild-type siblings (A, B). All p53 targets except *noxa* show up-regulation. qPCR assays were performed on three different clutches of embryos and standard deviations are shown.

C. Semiquantitative PCR for full length p53, *Δ113p53* and *β-actin* expression in wild-type and *shh*$^{-/-}$ mutant at 24 hpf and 56 hpf. *p53* is expressed at similar levels in both wild-type and *shh*$^{-/-}$ mutant, whereas *Δ113p53* is expressed at a much higher level in *shh*$^{-/-}$ mutants. PCR was normalized using *β-actin* expression.

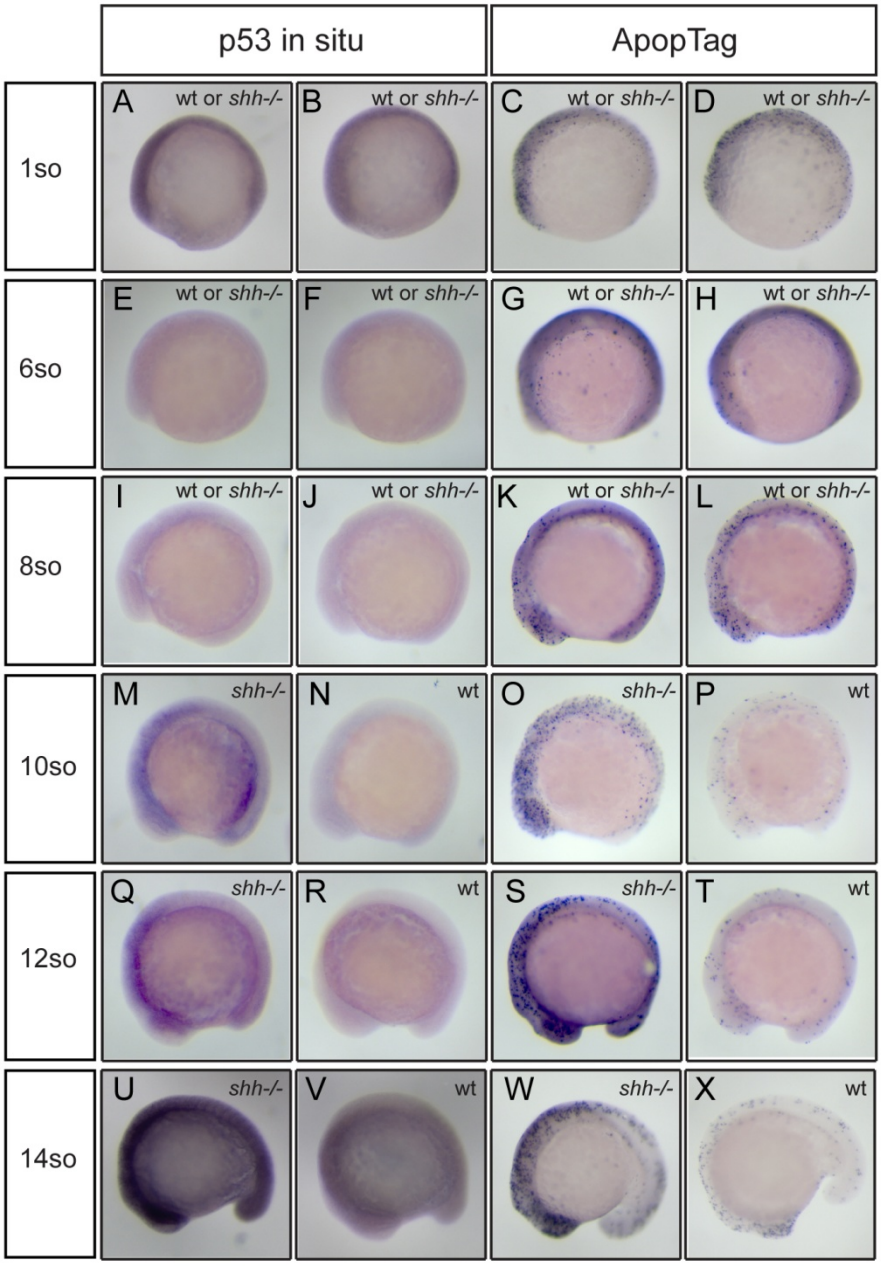

Figure 20. Onset of increased *p53* expression and apoptosis in *shh*$^{-/-}$ mutant occurs during somitogenesis.
p53 in situ was used to identify time points with activated p53 protein (A, B, E, F, I, J, M, N, R, S, V, W). ApopTag staining was used as an assay for apoptosis (C, D, G, H, K, L, P, Q, T, U, X, Y). The following stages were analysed 1so (A-D), 6so (E-H), 8so (I-L), 10so (M-P), 12so (Q-T), 14so (U-X). At early stages it was not possible to identify the genotype of the embryos. From 10somite stage on, *shh*$^{-/-}$ mutant embryos could be identified based on higher *p53* expression and ApopTag staining because they made one quarter of the batch. The stainings were repeated two times and 40 embryos were analysed for each staining.

Expression analysis clearly showed activation of p53 pathway in *shh*$^{-/-}$ mutant. To confirm p53 pathway's importance for apoptosis in *shh*$^{-/-}$ mutant, I performed p53 morpholino oligonucleotide (MO) knock-down (Nasevicius and Ekker, 2000). MO against *p53* gene were used previously to knock down p53 expression during early zebrafish development (Langheinrich et al., 2002). Injection of p53 morpholino but not of control morpholino could indeed suppress elevated apoptosis in *shh*$^{-/-}$ mutant at 24 hpf without affecting levels of normal developmental apoptosis (Fig. 21A). At 56 hpf in *shh*$^{-/-}$ mutant exhibits an increased level of apoptosis in the retina, which could be suppressed by MO knock-down of p53 but not by control MO (Fig. 21B). p53 generally activates intrinsic apoptotic pathway, which is inhibited by Bcl2 family proteins. To confirm the importance of the intrinsic apoptotic pathway, I expressed EGFP-bcl2 or EGFP mRNA in *shh*$^{-/-}$ mutant and wild-type embryos. Indeed, EGFP-bcl2 successfully suppressed elevated apoptosis in *shh*$^{-/-}$ mutant at 24 hpf, whereas EGFP did not have any effect (Fig. 21C). This result suggests that p53-mediated apoptosis in *shh*$^{-/-}$ mutant occurs via the intrinsic pathway. However, a number of studies in tissue-culture systems showed that Bcl2 overexpression may lead to inhibition of p53 transcriptional activity (Froesch et al., 1999; Beham et al., 1997; Ryan et al., 1994). Such a situation would obscure our results by suppressing p53 pathway upstream of its effects on mitochondria. Therefore, I also analysed expression of p53 targets *p53* and *cyclinG1* after injection of EGFP-bcl2 or EGFP mRNA and failed to find any differences in expression of the p53 targets in these experimental conditions (Fig. 21D). Therefore, it is unlikely that in this system overexpression of EGFP-bcl2 can block p53 transcriptional activity.

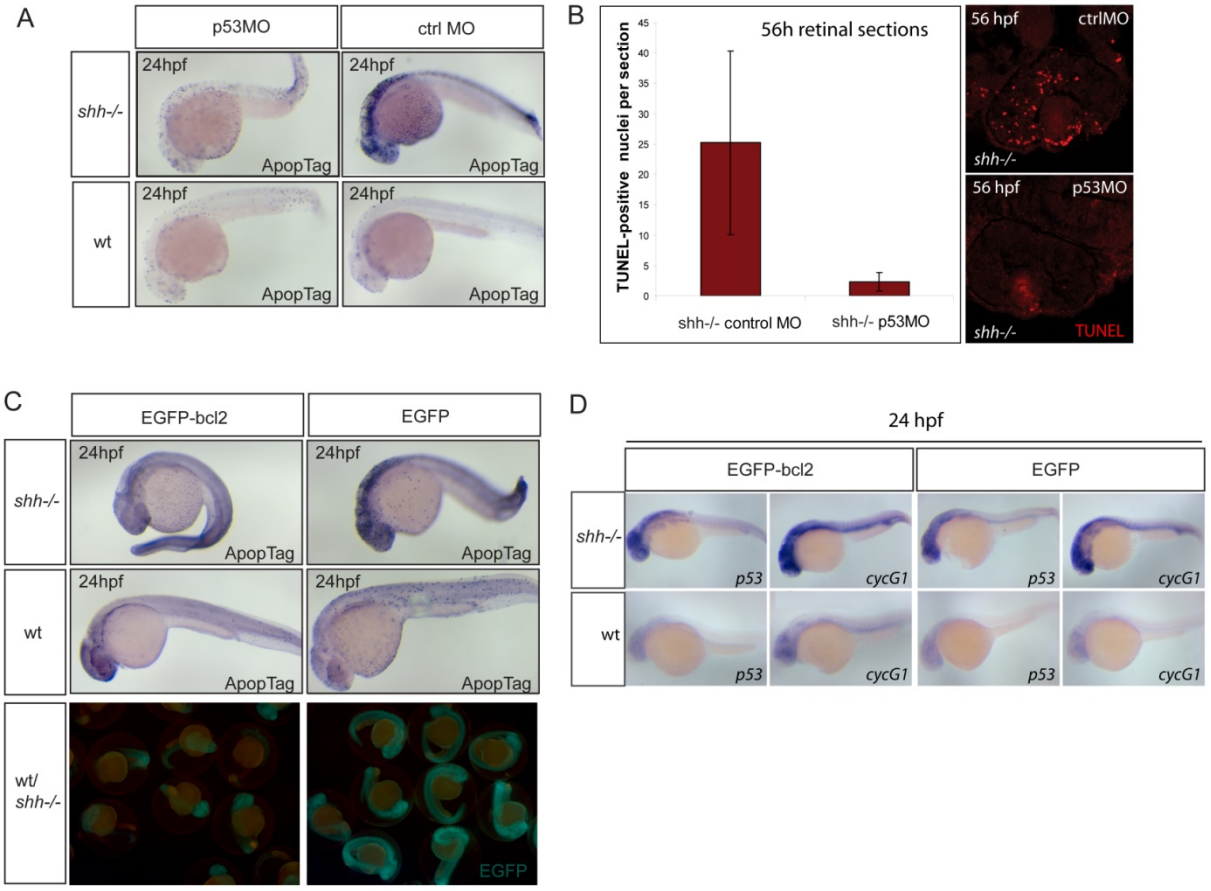

Figure 21. p53 mediates apoptosis in *shh*$^{-/-}$ mutant by intrinsic apoptosis pathway.
A. Elevated apoptosis observed in in *shh*$^{-/-}$ mutant at 24 hpf could be suppressed by injection of p53 morpholino but not of control morpholino.
B. Retinal apoptosis observed in in *shh*$^{-/-}$ mutant at 56 hpf could be suppressed by injection of p53 morpholino but not by injection of control morpholino (n = 10 and 40 sections for *shh*$^{-/-}$ mutant injected with p53 morpholino; n = 10 and 34 sections for in *shh*$^{-/-}$ mutant injected with control morpholino).
C. Apoptosis in in *shh*$^{-/-}$ mutant could be suppressed by injection of EGFP-bcl2 mRNA but not by injection of EGFP RNA. Injection of EGFP-bcl2 also reduces the level of normal developmental apoptosis.
D. The level of expression of *p53* and *cyclinG1* in both in *shh*$^{-/-}$ mutant and wild-type embryos was not affected by injection of EGFP-bcl2 mRNA relative to the control injection of EGFP mRNA.

2.2.4 *shh*$^{-/-}$ *p53*$^{-/-}$ double mutant phenotypes

p53 requirement for apoptosis occurring due to *shh* loss could be shown using morpholino knock-down. However, MO have limited perdurance and mostly exert their effects during the first 2 days of development. Thus, it is difficult to study late effects of gene loss

using morpholino knock-downs. Furthermore, genetic null mutations are generally perceived superior to morpholino knock-down for loss-of-function experiments. Therefore, to confirm the role of p53 in apoptosis in *shh*$^{-/-}$ mutant and to study the late effects of *p53* loss on the phenotype of *shh*$^{-/-}$ mutant, *p53*^{zdf1} mutation (Berghmanns et al., 2005), a null mutation of *p53,* was genetically combined with *shh*^{t4} null mutation. The double mutant *shh*$^{-/-}$*p53*$^{-/-}$ was protected from ectopic apoptosis in *shh*$^{-/-}$ mutant at 24 hpf, but normal apoptosis was not affected (Fig. 22A). I also checked the levels of apoptosis in the retina of wt, *shh*$^{-/-}$ and *shh*$^{-/-}$ *p53*$^{-/-}$ embryos at 72 hpf and found that the high level of apoptosis observed in *shh*$^{-/-}$ mutant at 72 hpf was successfully suppressed by *p53* loss (Fig. 22B).

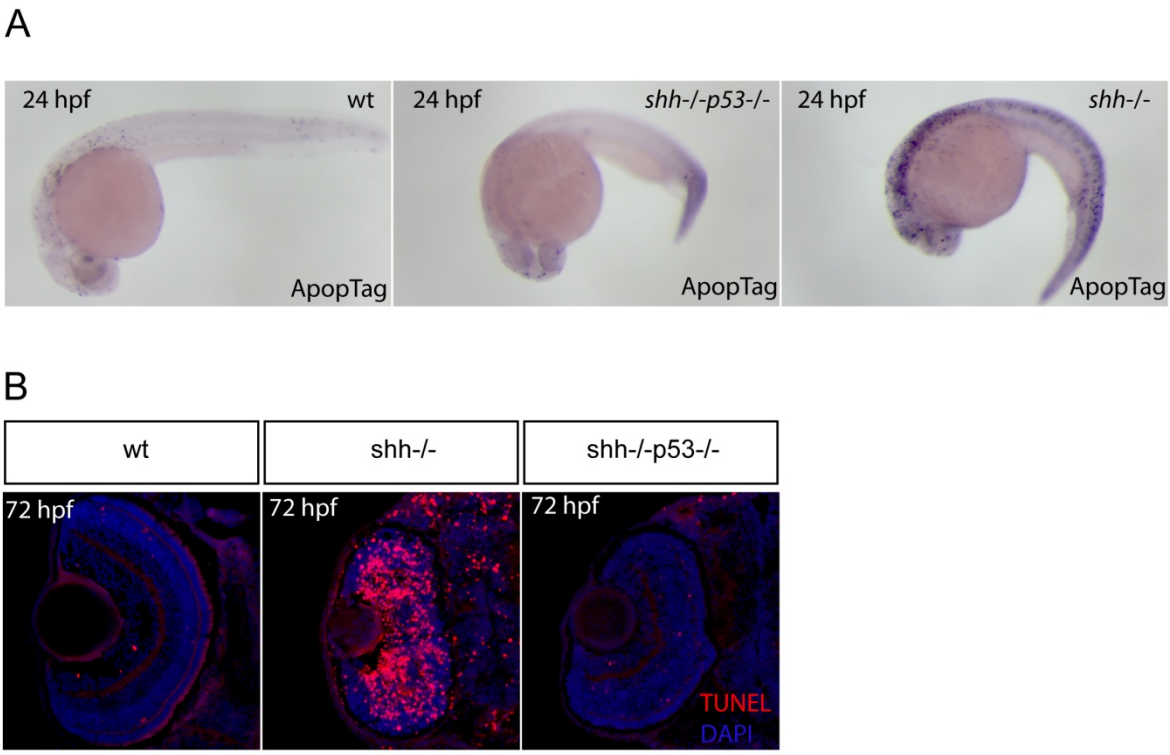

Figure 22. Rescue of apoptosis in *shh*$^{-/-}$ mutant by loss of *p53*.
Apoptosis staining at 24 hpf and at 72 hpf in wt, *shh*$^{-/-}$ and *shh*$^{-/-}$*p53*$^{-/-}$ is shown in this figure. Apoptosis was assayed in whole-mount in 24 hpf embryos using ApopTag staining (A) and on retinal sections in 72 hpf embryos using TUNEL staining (B). A. Elevated apoptosis in *shh*$^{-/-}$ relative to wild-type is rescued by *p53* loss in *shh*$^{-/-}$*p53*$^{-/-}$ B. Highly elevated retinal apoptosis in *shh*$^{-/-}$ relative to wild-type is likewise rescued by *p53* loss in *shh*$^{-/-}$*p53*$^{-/-}$. The figure shows representative pictures. All stainings were performed on at least 6 embryos for each genotype.

When cells survive due to suppression of apoptosis, the most interesting question is what fate they acquire. Acquisition of particular fates during development is tightly linked to

the cell-cycle exit of differentiating cell precursors. Therefore, another interesting question is whether p53 affects failure of cell-cycle exit in the retina of *shh*$^{-/-}$ mutants. In zebrafish retina, Shh signaling was proposed to serve as a differentiation and cell-cycle exit signal in addition to being a survival factor (Masai et al., 2005; Shkumatava et al., 2004; Shkumatava and Neumann, 2005). Therefore, I wanted to suppress retinal apoptosis and examine whether p53 contributes to the differentiation phenotype of *shh*$^{-/-}$ mutant zebrafish embryos. Another important goal is to identify p53-independent effects of Shh on retinal differentiation and retinal progenitor cell-cycle exit. To achieve these goals, retinal sections of wt, *shh*$^{-/-}$ and *shh*$^{-/-}$*p53*$^{-/-}$ mutant embryos were stained with antibodies against retinal differentiation markers. Retinal ganglion cells (RGCs) identified by anti-zn5 staining were present in retinas of embryos of all three genotypes, but they appeared more abundant in *shh*$^{-/-}$*p53*$^{-/-}$ retinas (Fig. 23A-C). A subset of amacrine cells identified by anti-parvalbumin antibodies were found in large numbers in the inner plexiform layer of the wild-type retina (Fig. 23D), whereas *shh*$^{-/-}$ mutant retina has none of these cells (Fig. 23E). Strikingly, *shh*$^{-/-}$*p53*$^{-/-}$ embryos show a partial rescue of amacrine cell differentiation (Fig. 23F). Another more widely expressed marker of differentiated amacrine cells is GAD67, whose staining revealed a high number of amacrine cell in the wild-type retina (Fig. 23M) and their virtual absence in the *shh*$^{-/-}$ retina (Fig. 23N). In the *shh*$^{-/-}$*p53*$^{-/-}$ retina the number of GAD67-positive amacrine cells strongly increased compared to the *shh*$^{-/-}$ retina (Fig. 23O). Differentiation of red-green cone and rod photoreceptors is normal in wild-type embryos (Fig. 23G, J), whereas in *shh*$^{-/-}$ cells of these types are almost completely absent (Fig. 23H, K). As in the case of amacrine cells, differentiation of photoreceptors is rescued in *shh*$^{-/-}$*p53*$^{-/-}$ mutant (Fig. 23I, L). These results imply that p53 prevents differentiation of all cell types in the *shh*$^{-/-}$ mutant retina. However, differentiation of two other cell types was not rescued in the *shh*$^{-/-}$*p53*$^{-/-}$ mutant retina. Müller glia is an abundant late-differentiating cell type which is required to maintain the environment inside the retina. A high number of these cells were present in the wild-type retina at 72 hpf (Fig. 24A) in contrast to the *shh*$^{-/-}$ mutant retina where Müller glia were absent (Fig. 24B). This differentiation defect could not be rescued by *p53* loss (Fig. 24C). Bipolar cells are a retinal cell type involved in signal transduction during light perception, which was identified by antibodies against PKCα in the wild-type retina at 72 hpf (Fig. 24D). The *shh*$^{-/-}$ mutant retina lacked bipolar cells (Fig. 24E) and this bipolar cell differentiation defect could not be

rescued in *shh*$^{-/-}$*p53*$^{-/-}$ mutant retina (Fig. 24F). Taken together, these data suggest that previously described retinal differentiation defects of *shh*$^{-/-}$ mutants (Shkumatava et al., 2004) in the cases of amacrine cells and photoreceptors are mediated by p53.

Figure 23. Rescue of photoreceptor and amacrine cell differentiation in *shh*$^{-/-}$ mutant by *p53* loss.
The figure shows photos of stained retinal sections from 72 hpf wild-type (wt) (A, D, G, J, M), *shh*$^{-/-}$ (B, E, H, K, N) and *shh*$^{-/-}$*p53*$^{-/-}$ mutants (C, F, I, L, O). The sections are oriented with their anterior side to the top. All sections are stained with phalloidin-Alexa568 to visualize the overall lamination of the retina. Antibody against zn5 antigen (zn5) labels retinal ganglion cells in the retina. Wild-type embryos (A) have both ganglion cell layer and the optical nerve labeled. Ganglion cell layer is also relatively normal in *shh*$^{-/-}$ mutant (B), and loss of *p53* in *shh*$^{-/-}$*p53*$^{-/-}$ mutant leads to a significant increase in the intensity of zn5 staining (C). Amacrine cells are successfully labeled in wild-type retina with an antibody against parvalbumine (D), but are normally absent in *shh*$^{-/-}$ mutant (E). In *shh*$^{-/-}$*p53*$^{-/-}$ mutant a significant number of them appears (F) due to rescue of differentiation. Antibody staining against Zpr1 protein expressed in red-green double cones identifies the photoreceptors in wild-type embryos (G), their lack in *shh*$^{-/-}$ mutant (H) and rescue of their differentiation in *shh*$^{-/-}$*p53*$^{-/-}$ mutant (I). Antibody staining against Zpr3 protein expressed in rod photoreceptors identifies them in wild-type embryos (J), their lack in *shh*$^{-/-}$ mutant (K) and rescue of their differentiation in *shh*$^{-/-}$ *p53*$^{-/-}$ mutant (L).

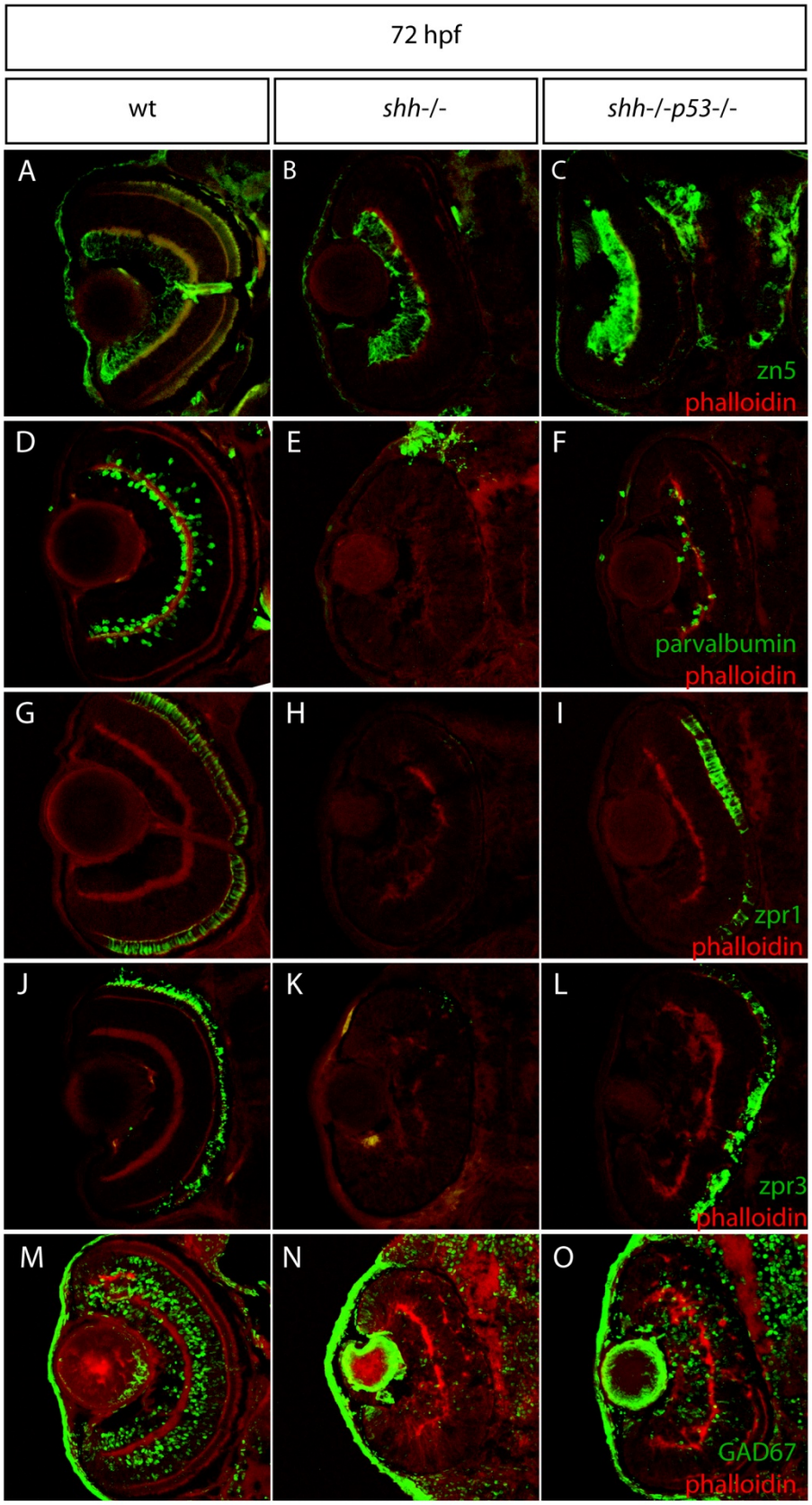
72 hpf
wt
shh-/-
shh-/-p53-/-
A
B
C
zn5
phalloidin
D
E
F
parvalbumin
phalloidin
G
H
I
zpr1
phalloidin
J
K
L
zpr3
phalloidin
M
N
O
GAD67
phalloidin

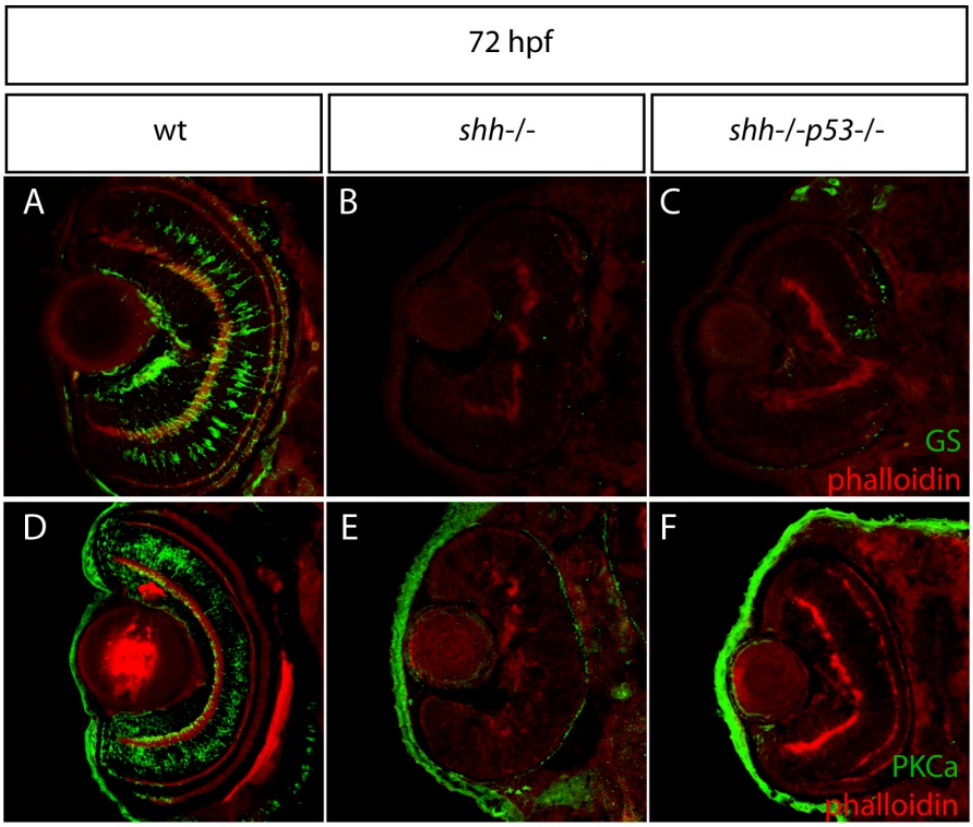

Figure 24. Loss of *p53* does not rescue differentiation of Müller glia cells and bipolar cells in the retina of $shh^{-/-}$ mutants.
Staining against glutamine synthetase, a marker for Müller glia, reveals a high number of these cells in wild-type embryos (A). In both $shh^{-/-}$ and $shh^{-/-}p53^{-/-}$ mutants (B, C) there are very few of Müller glia. Staining against PKCα, a marker of bipolar cells in the retina, identifies these cells in the wild-type embryos (D), but no bipolar cells are present in appropriate retina regions in either $shh^{-/-}$ and $shh^{-/-}p53^{-/-}$ mutants (E, F). All stainings were performed on at least 6 embryos for each condition and representative pictures are shown.

Since loss of *p53* rescued differentiation in the $shh^{-/-}$ mutant retina, a question arises whether p53 affects cell-cycle exit in the retina. A likely possibility is that *p53* loss induced cell-cycle exit of the precursor cells which later differentiated. According to this view, p53 would be responsible for failure of cell-cycle exit in the $shh^{-/-}$ mutant retina. An alternative view that failure of cell-cycle exit can induce p53 activation in the $shh^{-/-}$ mutant retina is attractive but is not consistent with the available data since p53 activation is a much earlier event than cell-cycle exit in the retina. To confirm the first possibility, I decided to directly analyze S-phase progression using the BrdU incorporation assay in the wt, $shh^{-/-}$ and $shh^{-/-}$

p53$^{-/-}$ mutant retinas. BrdU incorporation assays were performed at 48 and 56 hpf, since at these stages cell-cycle exit in the retina is being completed. Indeed, at 48 hpf wild-type retina contains BrdU-positive cells not only at the retinal margin but also at the basal surface of the retina (Fig. 26A) and by 56 hpf all cells except cells in the marginal zone exit the cell cycle (Fig. 26B). In the *shh*$^{-/-}$ mutant retina, high numbers of cells remained in S-phase at both stages (Fig. 26A, B). Interestingly, in the *shh*$^{-/-}$*p53*$^{-/-}$ mutant retina the pattern and extent of cell-cycle exit are very similar to the wild-type situation (Fig. 26A, B). Since cell-cycle exit in the zebrafish retina is induced by *p57kip2* expression, I checked if this gene is expressed in *shh*$^{-/-}$ mutant upon loss of *p53*. In fact, at 38 hpf, strong *p57kip2* expression was present in large areas of wild-type and *shh*$^{-/-}$*p53*$^{-/-}$ mutant retinas, but was absent from the *shh*$^{-/-}$ mutant retina (Fig. 25C). By contrast, *p53* was highly expressed only in the *shh*$^{-/-}$ mutant retina and was nearly absent in wild-type and *shh*$^{-/-}$*p53*$^{-/-}$ mutant retinas (Fig. 25C). These striking results suggest that the cell-cycle exit defect in the *shh*$^{-/-}$ mutant retina is clearly dependent on the p53 function. Since p53 is well known to inhibit cell cycle progression, it is possible to predict that the cell-cycle exit defect in the *shh*$^{-/-}$ mutant retina may not be a case of ectopic uncontrolled proliferation but rather a cell cycle block in S-phase. Supporting this prediction requires a way to label cells with activated p53 to better understand their cell cycle properties and eventual progression to apoptosis.

Figure 25. Loss of *p53* rescues cell cycle exit defect in *shh*$^{-/-}$ mutant.
S-phase progression in wild-type, *shh*$^{-/-}$ and *shh*$^{-/-}$*p53*$^{-/-}$ mutants at 48 and 56 hpf was studied by BrdU labeling. Confocal sections are shown with the anterior side to the top.
A. At 48 hpf most cells in the wild-type retina have already exited the cell cycle. In the *shh*$^{-/-}$ mutant retina, however, cell cycle exit is almost completely absent. By contrast, cell-cycle exit in the *shh*$^{-/-}$*p53*$^{-/-}$ mutant retina is much more advanced and quite similar to the situation in the wild-type retina.
B. At 56 hpf in the wild-type retina BrdU-positive cells are found only in the ciliary marginal zone (CMZ) and in the *shh*$^{-/-}$ mutant retina cells still failed to exit the cell cycle. Like in the wild-type retina, cells of *shh*$^{-/-}$*p53*$^{-/-}$ mutant have mostly exited the cell cycle and proliferative cells are located only in the CMZ.
C. *In situ* hybridizations against *p57kip2* and *p53* in wild-type, *shh*$^{-/-}$ mutant and *shh*$^{-/-}$*p53*$^{-/-}$ mutant retinas.

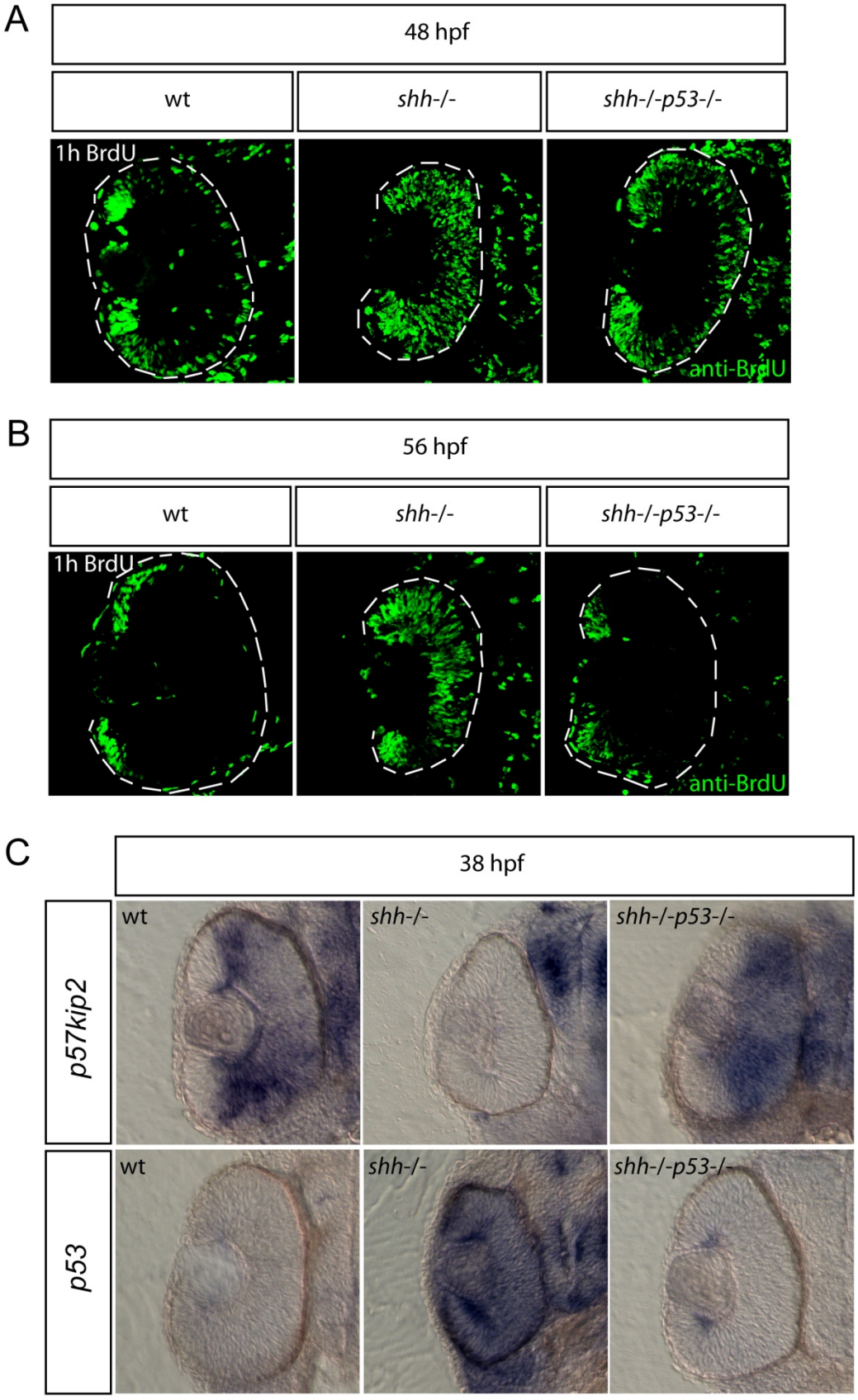
A
48 hpf
wt
shh-/-
shh-/-p53-/-
1h BrdU
anti-BrdU
B
56 hpf
wt
shh-/-
shh-/-p53-/-
1h BrdU
anti-BrdU
C
38 hpf
p57kip2
p53
wt
shh-/-
shh-/-p53-/-

2.2.5 Hedgehog pathway activation rescues apoptosis in *shh*$^{-/-}$ mutants

The results so far demonstrate that p53 is essential for elevated apoptosis in the *shh*$^{-/-}$ mutant. However, it is not yet clear how the absence of Shh signaling activates p53 pathway. Abe et al. (2008) suggested the existence of an unknown factor inhibiting p53 pathway, which can be induced by Gli-mediated Hh signaling activation. Since their work was performed on human and mouse cell lines, I wanted to confirm if this conclusion would also apply to the situation of *shh* genetic loss in zebrafish. Protein kinase A (PKA) is a negative regulator of Hh signal transduction from Smo to Gli transcription factors in vertebrates. To better understand the connection between *shh* loss and p53 activation *in vivo*, I activated canonical Hh/Gli signaling pathway by injection of dominant-negative PKA GFP fusion (dnPKA-GFP) mRNA (Hammerschmidt et al., 1996; Ungar and Moon, 1996) into progeny of fish heterozygous for *shh* deletion. Given the limited stability of this mRNA, I chose to analyse the phenotypes due to dnPKA-GFP over-expression at 12 somites stage, when *shh*$^{-/-}$ mutant embryos already show elevated expression of p53 target genes and a high level of apoptosis. Indeed, overexpression of dnPKA-GFP led to a high level of *ptc1* expression in 52 out of 61 (85 %) embryos (Fig. 26A, N), whereas 9 out of 61 (15 %) which probably received little mRNA showed normal uninduced expression of *ptc1* for wild-type and *shh*$^{-/-}$ mutant, respectively (Fig. 26B, C, N). All of EGFP-injected embryos showed an uninduced level of expression, of which 16 out of 61 (26 %) embryos showed *shh*$^{-/-}$ mutant level of *patched1* expression (Fig. 26E) and 45 out of 61 (74 %) had wild-type level of expression (Fig. 26D, N). p53 pathway activity after either dnPKA-GFP or EGFP over-expression was assessed by an *in situ* staining for *cyclinG1*, a well-characterized p53 target gene. Only 5 out of 45 (11 %) dnPKA-GFP injected embryos expressed *cyclinG1* at a perceptibly higher level than the rest 40 embryos (Fig. 26F, G, N), and the difference between these two categories of embryos was slight. By contrast, injection of EGFP mRNA didn't lead to a decrease in proportion of *shh*$^{-/-}$ mutant embryos with high expression of *cyclinG1* (15 out of 57 (26 %)) (Fig. 26I, N). In the case of EGFP-injected embryos, the difference of *cyclinG1* expression between wild-type and *shh*$^{-/-}$ mutant embryos was very pronounced (Fig. 26H, I). Consistent with its effect on *cyclinG1* expression, dnPKA-GFP also led to a reduction in the number of embryos with elevated apoptosis levels (5 out of 65 (7,7 %)) (Fig. 26K, N) compared to 17 out of 66 (26 %) in the EGFP-injected sample (Fig. 26M, N) and the number of apoptotic cells in dnPKA-GFP-injected embryos was smaller than

in EGFP-injected ones. The number of embryos with a low level of apoptosis correspondingly increased to 60 out of 65 (92 %) in the dnPKA-GFP injected sample (Fig. 26J, N) compared to 49 out of 66 (74 %) in the EGFP-injected sample (Fig. 26L, N).

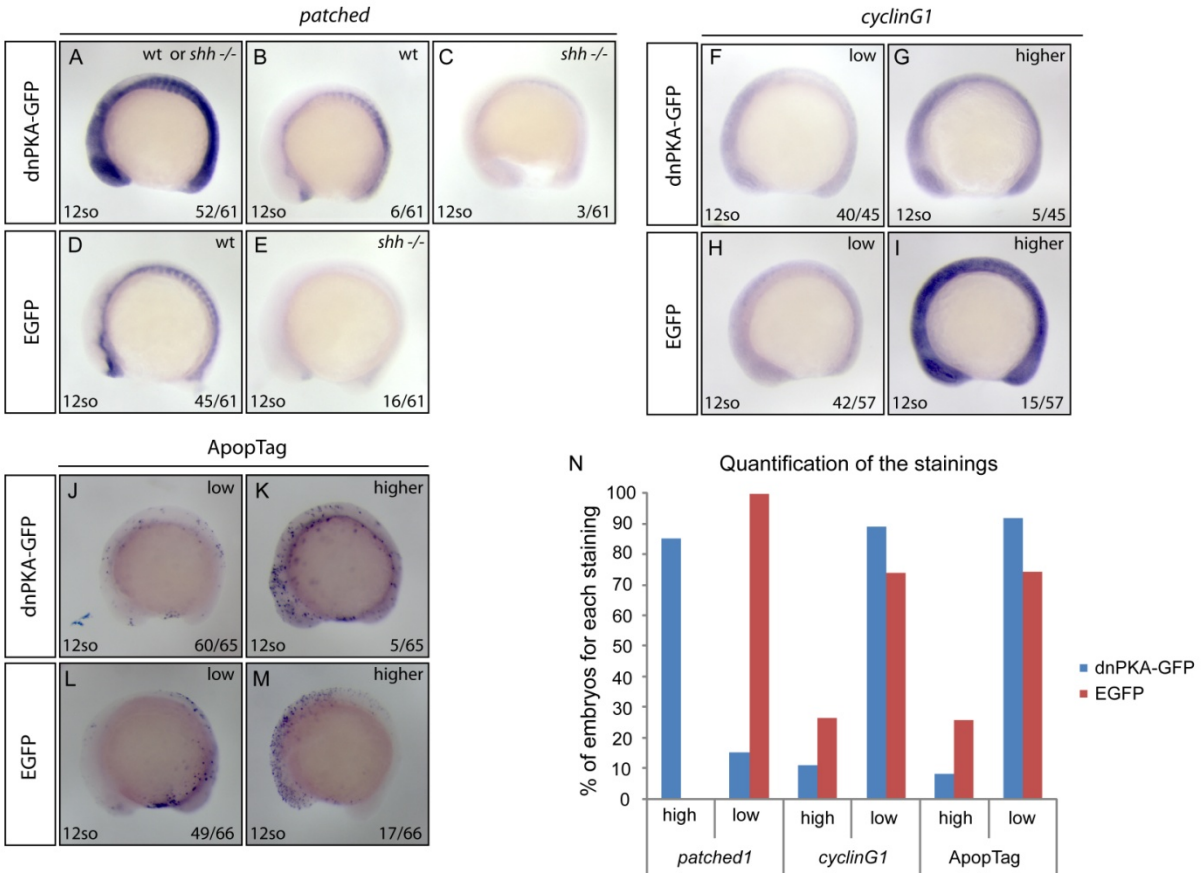

Figure 26. Hh signaling activation by dnPKA-GFP decreases p53 target *cyclinG1* expression and suppresses apoptosis in *shh*$^{-/-}$ mutant embryos.
Embryos at the 12 somite stage from *shh*$^{+/-}$ parent fish were injected with either dnPKA-GFP (A-C, F, G, J, K, N) or EGFP mRNA (D, E, H, I, L, M, N) and *in situ* stained for *patched1* (A-E), target gene of Hh signaling, and for *cyclinG1* (F-I), p53 target gene, and ApopTag staining was performed to characterize the level of apoptosis (J-M). Injection of dnPKA-GFP mRNA led to expression of *patched1* at a high level in most embryos (A) compared to a few embryos which received little dnPKA-GFP mRNA (B, C) and EGFP-injected embryos (D, E). Few of the embryos injected with dnPKA-GFP showed a higher level of *cyclinG1* expression (G) and this level was not very different from that of the majority of embryos (F). The difference of *cyclinG1* expression after EGFP mRNA injection in higher-expressing (I) and lower-expressing (H) embryos was very large. ApopTag staining of EGFP-injected shows that around one quarter of embryos have a much higher level of apoptosis (M) than most of the embryos with a low level of apoptosis (L). Injection of dnPKA-GFP mRNA leads to a strong decrease in the number of embryos with increased apoptosis and its level (K) and a decrease in low-apoptosis proportion of embryos (J). Summary of the results of this experiment (N) shows two categories for each staining: high and low, which in the case of *patched1* staining indicate ectopic activation of Hh signaling or lack thereof and in the cases of *cyclinG1* and ApopTag indicate relative levels of gene expression and apoptotic cell numbers, respectively. Proportions of embryos with the presented phenotypes are shown in the lower right corner of each image. The results presented are representative of three independent experiments.

2.2.6 Creating and characterizing zebrafish p53 reporter line

Our ability to study gene expression using *in situ* hybridization (ISH) is important to study gene transcripts in developing embryos. However, ISH does not allow real-time analysis of cells expressing particular transcripts and is difficult to combine with many antibody stainings and other histochemical methods. Advent of fluorescent proteins has overcome this problem by enabling researchers to create reporter systems based on particular promoters driving expression of genes encoding fluorescent proteins. My aim was to develop a transgenic p53 reporter to study the behavior and characteristics of cells with active p53. I implemented a strategy similar to the one previously employed by Zhang et al. (2001). Human 2.4 kb CDKN1A promoter encoding p21 was used as the basis for the p53 reporter, 13 copies of the optimal p53 binding sites (PG13) (Kern et al., 1992) were inserted in front of this promoter as an enhancer. Tol2kit transgenic system (Kwan et al., 2007) was then used to assemble the final construct. In short, PG13p21 promoter, nlsEGFP and polyA DNA parts were assembled by recombination inside the destination vector used for transposon-based transgenesis (Fig. 27). The destination vector additionally provided EGFP transgene specifically expressed in the heart, which facilitates transgenic embryo screening and identification of carrier fish.

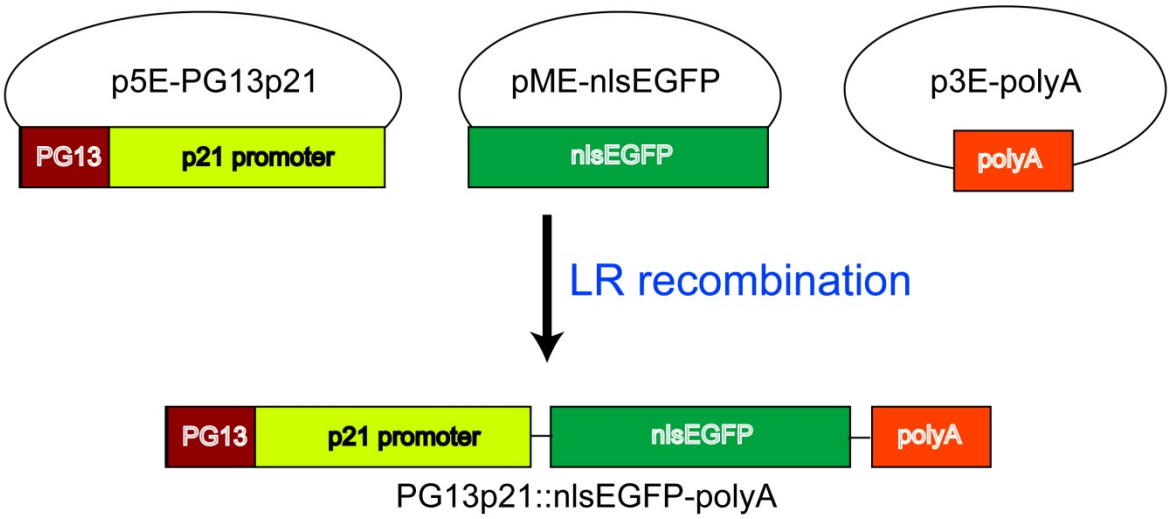

Figure 27. The Tol2kit-based strategy to make PG13::nlsEGFP-polyA p53 reporter.
5' entry vector containing human *p21* promoter with PG13 enhancer, middle entry vector encoding nlsEGFP and 3' entry vector containing polyA signal were LR recombined with pDestCG2 vector (not shown), which serves as a carrier of the construct for transgenesis. LR recombination resulted in PG13p21::nlsEGFP-polyA construct inside the pDestCG2, which provides attachment sites for the transposase and a transgenic marker for positive embryo screening.

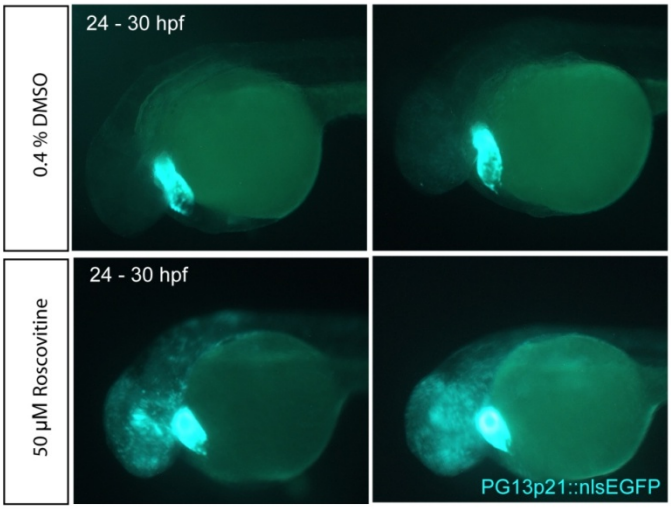

Figure 28. Activation of PG13p21::nlsEGFP p53 reporter by treatment with roscovitine.
Wild-type embryos carrying PG13p21::nlsEGFP transgene were incubated for 6 hours at 24 hpf with either 50 µM roscovitine or 0.4 % DMSO in E3 medium. DMSO-treated embryos did not show any significant expression of the reporter (the upper panel), but Roscovitine was quite effective in inducing p53 reporter expression (the lower panel). All embryos show green-heart transgenesis marker. The experiment was repeated two times and 20 embryos were used for each treatment.

The p53 reporter zebrafish transgenic line represents a potentially general tool to study p53 activation and regulation. Studies of p53 in zebrafish employed camptothecin, a genotoxic drug, or roscovitine, an Mdm2 inhibitor, to activate p53 (Langheinrich et al., 2005; Lee et al., 2007). I chose treatment with roscovitin to verify activation of the p53 reporter. Treatment with roscovitine for 6 hours at 24 hpf could efficiently induce p53-mediated apoptosis, which was prevented by p53 knockdown (Langheinrich et al., 2005). Wild-type embryos carrying the p53 reporter transgene were incubated either with 50 μM roscovitine or 0.4 % DMSO as a control for 6 hours starting at 24 hpf. As a result, p53 reporter expression was strongly up-regulated in the brain and retina of the roscovitine-treated but not of control DMSO-treated embryos (Fig. 28). This result confirms the utility of the p53 reporter transgenic line in the context of drug-induced p53 activation and suggests that this line is a valuable tool for other investigations of p53 function.

2.2.7 p53 reporter activation in *shh*$^{-/-}$ mutant

The next step to characterize the utility of the newly-generated p53 reporter was to introduce it into *shh*$^{-/-}$ mutant. After obtaining PG13p21::nlsEGFP *shh*$^{+/-}$ fish, expression of the p53 reporter was photographed in *shh*$^{-/-}$ mutant and wild-type embryos at 24, 30, 36 and 48 hpf (Fig. 29). At all stages analysed wild-type embryos had a low background level of the p53 reporter expression consistent with previous observations that p53 activation is normally under tight control. By contrast, at all analysed stages the level of the p53 reporter expression in *shh*$^{-/-}$ mutants was high. At 24 hpf, *shh*$^{-/-}$ mutants had a very broad expression of the p53 reporter in the retina, neural tube and somites. Over the next 24 hours of development, expression of the p53 reporter in *shh*$^{-/-}$ mutants becomes restricted to midbrain and retina regions (Fig. 29). These changes in p53 reporter expression are most certainly caused by the clearance of cells by p53-mediated apoptosis. To confirm the specificity of the p53 reporter induction in *shh*$^{-/-}$ mutant embryos, I knocked down p53 expression using morpholino oligonucleotides. High level of p53 reporter expression in *shh*$^{-/-}$ mutant at 24 hpf was readily inhibited by p53 MO but not by control MO injection (Fig. 30). This result confirms that p53 is essential to mediate the expression of its transcriptional activity reporter transgene.

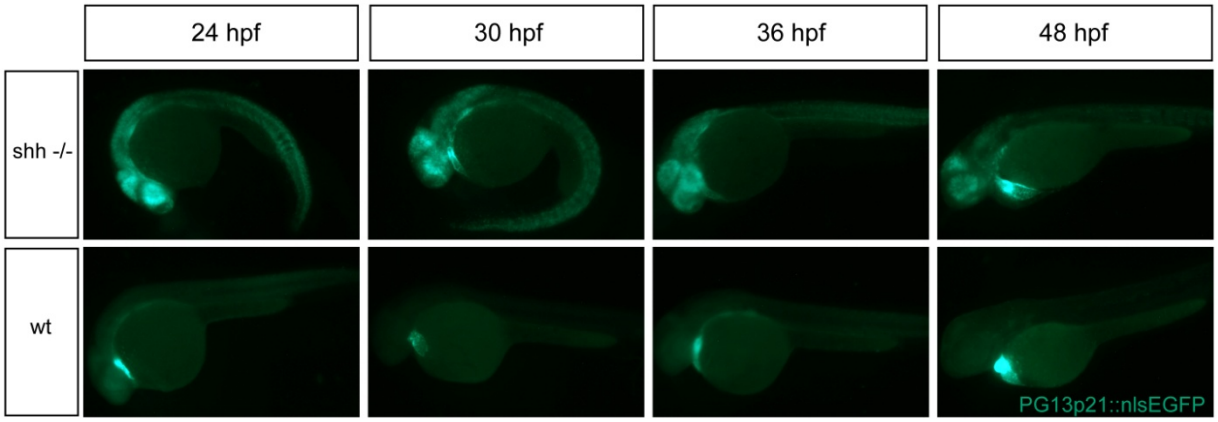

Figure 29. p53 reporter PG13p21::nlsEGFP expression in wild-type and *shh*$^{-/-}$ mutant embryos during development.
Wild-type and *shh*$^{-/-}$ mutant embryos carrying PG13p21::nlsEGFP p53 reporter were photographed at 24, 30, 36 and 48 hpf. Expression of the p53 reporter is highly elevated in mutant embryos in the retina, nervous system and somites in comparison to the p53 reporter expression in wild-type at all stages.

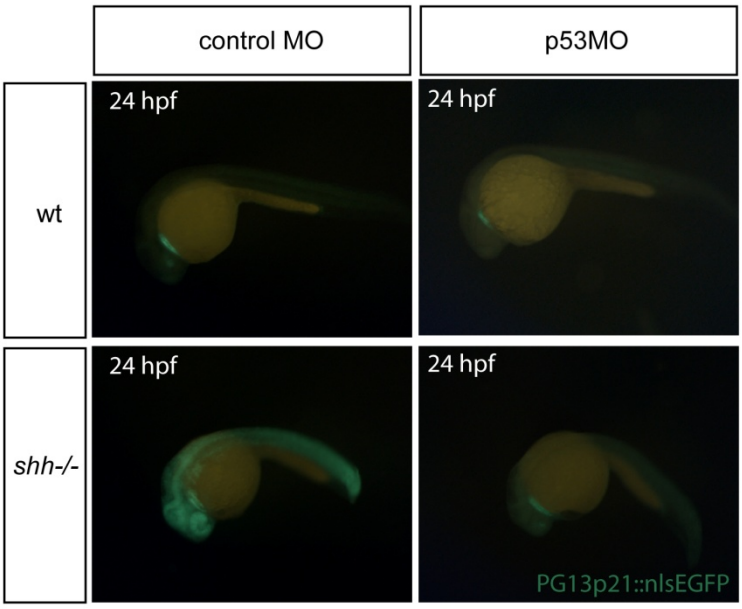

Figure 30. p53 knock-down inhibits PG13p21::nlsEGFP reporter expression in *shh*$^{-/-}$ mutant embryos at 24 hpf.
Progeny of heterozygous *shh*$^{-/-}$ embryos carrying PG13p21::nlsEGFP was injected with either p53 morpholino or control morpholino and the reporter was imaged at 24 hpf.

Shh exerts its effects on cell survival in specific regions of the developing embryo, whereas expression of the p53 reporter seems ubiquitous. To verify whether different cells

express p53 reporter at different levels, I injected H2BmRFP1 mRNA into oocytes carrying p53 reporter and analysed hindbrain and midbrain regions of wild-type and *shh*$^{-/-}$ at 24 hpf. Wild-type embryos expressed almost no p53 reporter in either hindbrain or midbrain (Fig. 31). By contrast, many cells expressed p53 reporter in *shh*$^{-/-}$ mutants in hindbrain and midbrain regions (Fig. 31A, B). p53 reporter nlsEGFP is expressed at very different levels in different cells in *shh*$^{-/-}$ mutant embryos as is clearly seen in a hindbrain section by very different relative levels of nlsEGFP and H2BmRFP1 (Fig. 31A). To understand whether p53 reporter expression was consistent with the embryo regions requiring Shh for cell survival, I analysed p53 reporter expression and apoptosis by TUNEL staining in different embryo regions at 24 hpf on embryo cryosections (Fig. 32). Especially striking was expression of the p53 reporter in the neural tube. Midbrain, hindbrain and spinal cord expressed nlsEGFP in *shh*$^{-/-}$ mutant p53 reporter fish and had a high number of TUNEL-positive cells (Fig. 33B, C, D). By contrast, in the *shh*$^{-/-}$ retina despite the pronounced expression of p53 reporter there was no elevated apoptosis at 24 hpf. This result is interesting and unexpected, because the spread of *shh* expression in the retina starts at 28 hpf (Neumann and Nüsslein-Volhard, 2000). Activation of p53 in *shh*$^{-/-}$ mutant retinal cells before 28 hpf indicates a requirement of Shh perception at an earlier stage to control p53 activity. In the absence of Shh, neural crest cells undergo apoptosis (Ahlgren and Bronner-Fraser, 1999). Consistently, some p53 reporter-positive cells in the midbrain section (Fig. 32B) are located in the lateral regions characteristic of neural crest cells. In the spinal cord section (Fig. 32D) p53 reporter labels somite cells, which may be sclerotome or muscle cells requiring Shh for their survival (Borycki et al., 1999). I then analysed apoptosis wild-type and *shh*$^{-/-}$ mutant carrying p53 reporter at 56 hpf by staining with TUNEL. Sections of wild-type embryos contained very little signal for p53 reporter and TUNEL staining and most signal was due to auto-fluorescence (Fig. 33). By contrast, all the sections from *shh*$^{-/-}$ mutant had a strongly increased level of apoptosis and p53 reporter expression. Especially strong apoptosis and p53 reporter expression were detected in the *shh*$^{-/-}$ mutant retina (Fig. 33A). This observation is different from the result at 24 hpf, when *shh*$^{-/-}$ mutant retina had very little apoptosis, and suggests that accumulation of pro-apoptotic factors eventually induces cell death in the *shh*$^{-/-}$ mutant retina. Midbrain and hindbrain regions of *shh*$^{-/-}$ mutants at 56 hpf also contained many apoptotic and p53 reporter-positive cells, which is similar to the situation in the *shh*$^{-/-}$ mutant at 24 hpf (Fig. 33B, C). Taken together, the results at 24 and 56

hpf in *shh*$^{-/-}$ mutant suggest that p53 reporter- positive cells persist during development and gradually become cleared by apoptosis rather than die simultaneously at a defined time point.

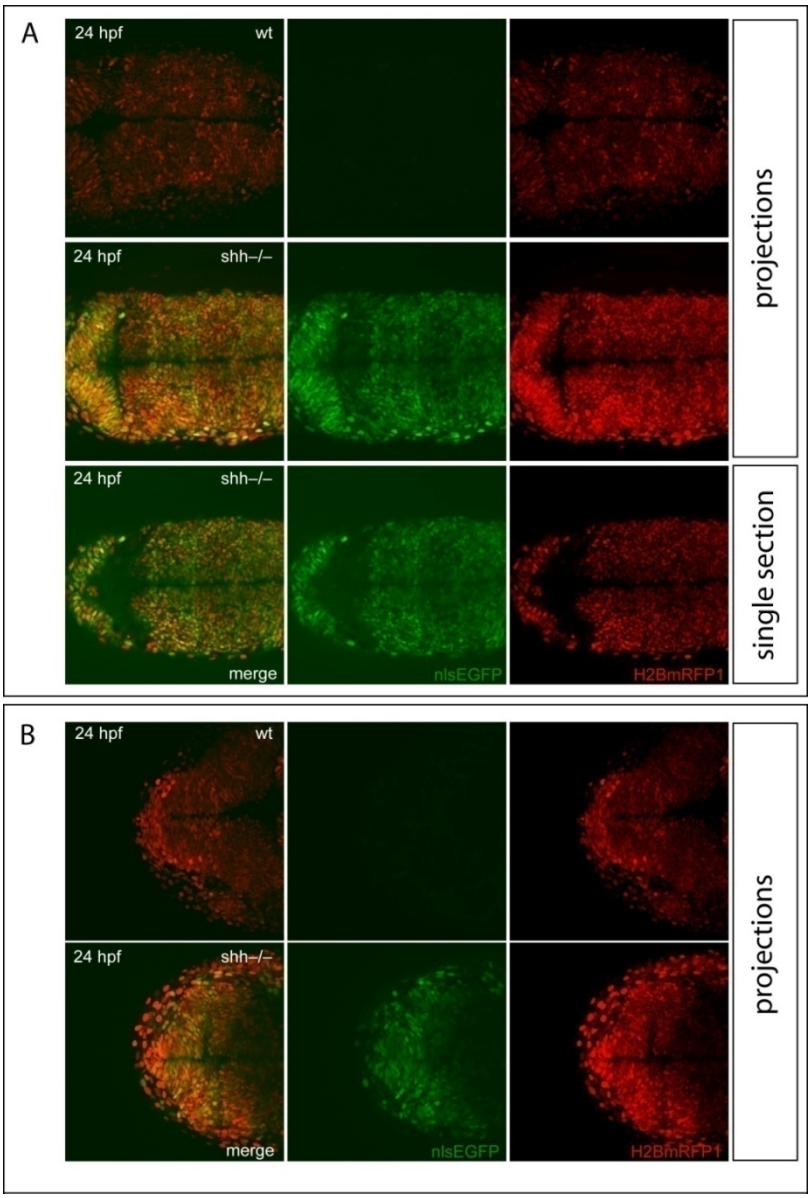

Figure 31. Cell-specific levels of PG13p21::nlsEGFP reporter expression in brain regions of wild-type and *shh*$^{-/-}$ mutant embryos at 24 hpf.
A. Hindbrain regions of the wild-type and *shh*$^{-/-}$ embryos containing PG13p21::nlsEGFP p53 reporter and injected H2BmRFP1. For the *shh*$^{-/-}$ mutant embryo, both image stack projection and single section images are shown.
B. Midbrain regions of the wild-type and *shh*$^{-/-}$ embryos containing PG13p21::nlsEGFP p53 reporter and injected H2BmRFP1.

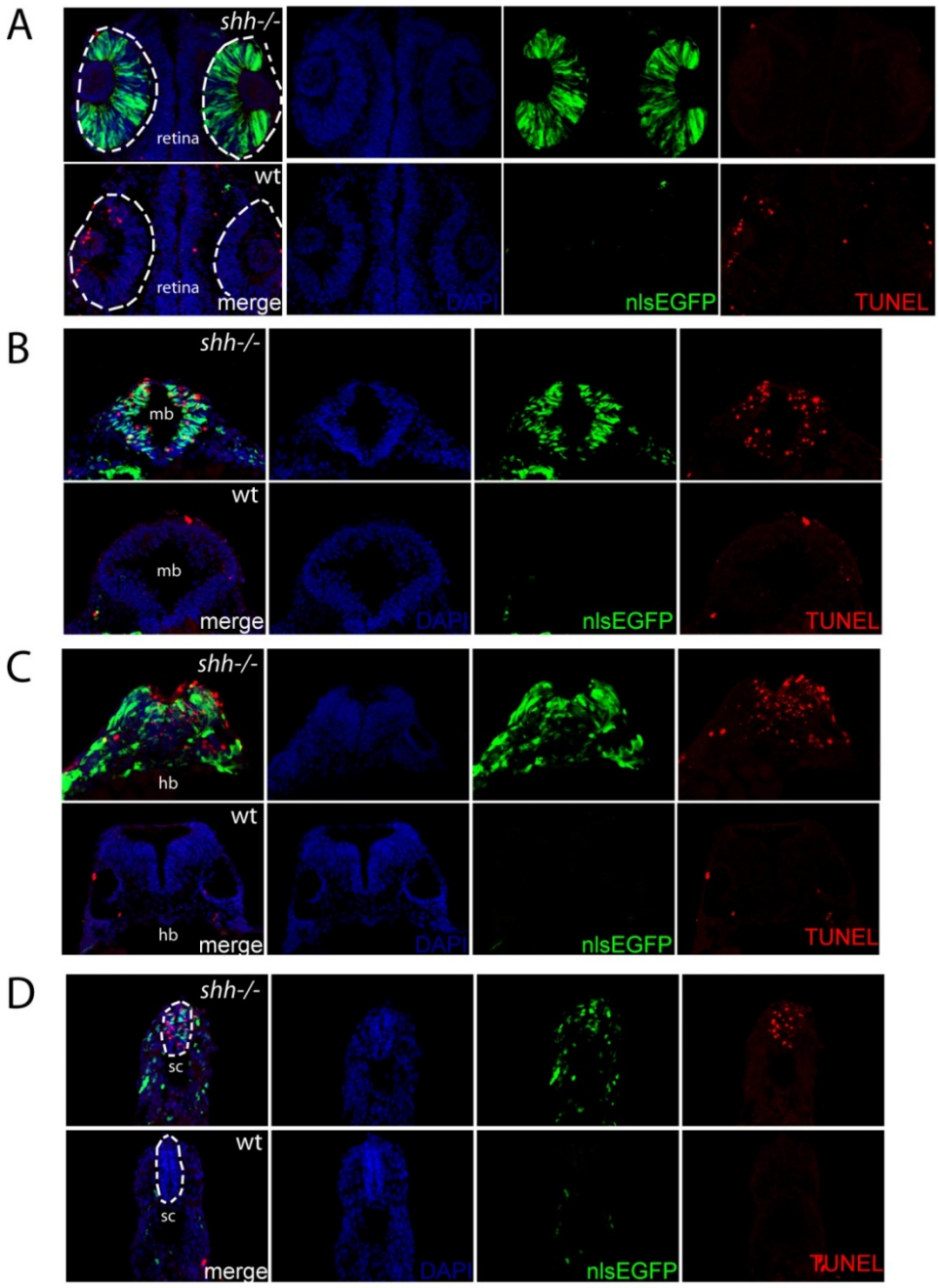

Figure 32. p53 reporter expression and apoptosis in *shh*$^{-/-}$ mutant and wild-type at 24 hpf.
24 hpf wild-type and *shh*$^{-/-}$ embryos carrying p53 reporter transgene (PG13p21::nlsEGFP) were transversally sectioned and stained with TUNEL and DAPI, nlsEGFP signal is endogeneous (A-D). A. Sections of *shh*$^{-/-}$ and wild-type retinas show that p53 reporter is expressed at a high level in *shh*$^{-/-}$ retina, but there is no increase in apoptosis. B. Transverse sections of midbrain regions of *shh*$^{-/-}$ and wt. C. Transverse sections of hindbrain regions of *shh*$^{-/-}$ and wt. D. Transverse sections of hindbrain regions of *shh*$^{-/-}$ and wt. In midbrain (B), hindbrain (C) and spinal cord (D) p53 reporter expression highly correlates with increased apoptosis and a proportion of p53 reporter positive cells are also TUNEL-positive.

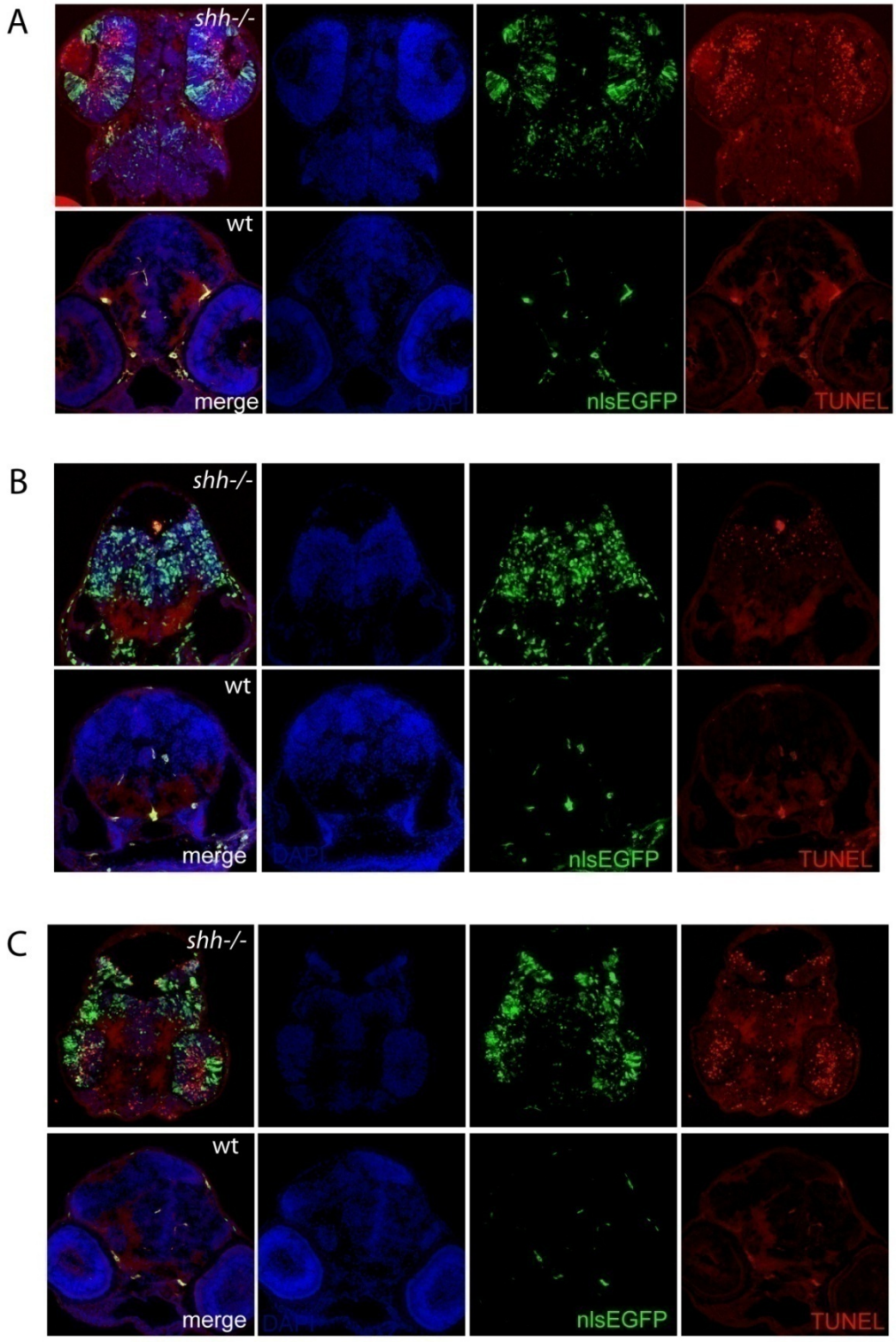

Figure 33. p53 reporter expression and apoptosis in *shh*$^{-/-}$ mutant and wild-type at 56 hpf. 56 hpf wild-type and *shh*$^{-/-}$ embryos carrying p53 reporter transgene (PG13p21::nlsEGFP) were transversally sectioned and stained with TUNEL and DAPI, nlsEGFP signal is endogeneous (A-C). A. Retinal section. B. Hindbrain section. C. Midbrain section.

2.2.8 p53 reporter-positive cells in *shh*$^{-/-}$ mutant are positive for apoptotic markers

Since p53 is known to induce apoptosis, it is very important to characterize apoptotic phenotype in p53 reporter-positive cells. p53 reporter is usually expressed in the embryo regions with elevated levels of apoptosis as revealed by TUNEL staining (Figs 32, 33). However, since TUNEL is quite a late marker of apoptosis many TUNEL-positive cells in *shh*$^{-/-}$ mutants lack detectable p53 reporter expression. This is most likely due to protein degradation in the dying cells and longer persistence of apoptotic cell death. An alternative possibility of p53-independent apoptotic cell death can be excluded because *p53* loss efficiently suppresses apoptosis in the *shh*$^{-/-}$ mutant. To characterize the apoptotic phenotype of p53 reporter-positive cells, I stained 24 hpf *shh*$^{-/-}$ mutant embryos with TUNEL or anti-activeCaspase3. Wild-type embryos were not used for these stainings because they contain extremely few p53 reporter positive cells. Although in the *shh*$^{-/-}$ mutant there were many TUNEL-positive cells, few of them were also positive for p53 reporter nlsEGFP (Fig. 34A). In double-positive cells, TUNEL signal occupied the center of the cell and p53 reporter nlsEGFP was located at the cell periphery. This result contrasts with the normally nuclear localization of nlsEGFP, but the cytoplasmic localization of p53 reporter nlsEGFP is consistent with nuclear breakdown in the apoptotic cells (Kramer et al., 2008). Next I wanted to see whether p53 reporter co-localizes with activeCaspase3. The number of activeCaspase3-positive cells in the hindbrain of *shh*$^{-/-}$ mutants was much lower than that of TUNEL-positive cells (Fig. 34B) suggesting a much shorter persistence of Caspase3 activity in apoptotic cells. Strikingly, in most examined cells cytoplasmic activeCaspase3 was clearly co-localised with p53 reporter nlsEGFP (Fig. 34B). This result confirms that cell death program is activated in cells with active p53.

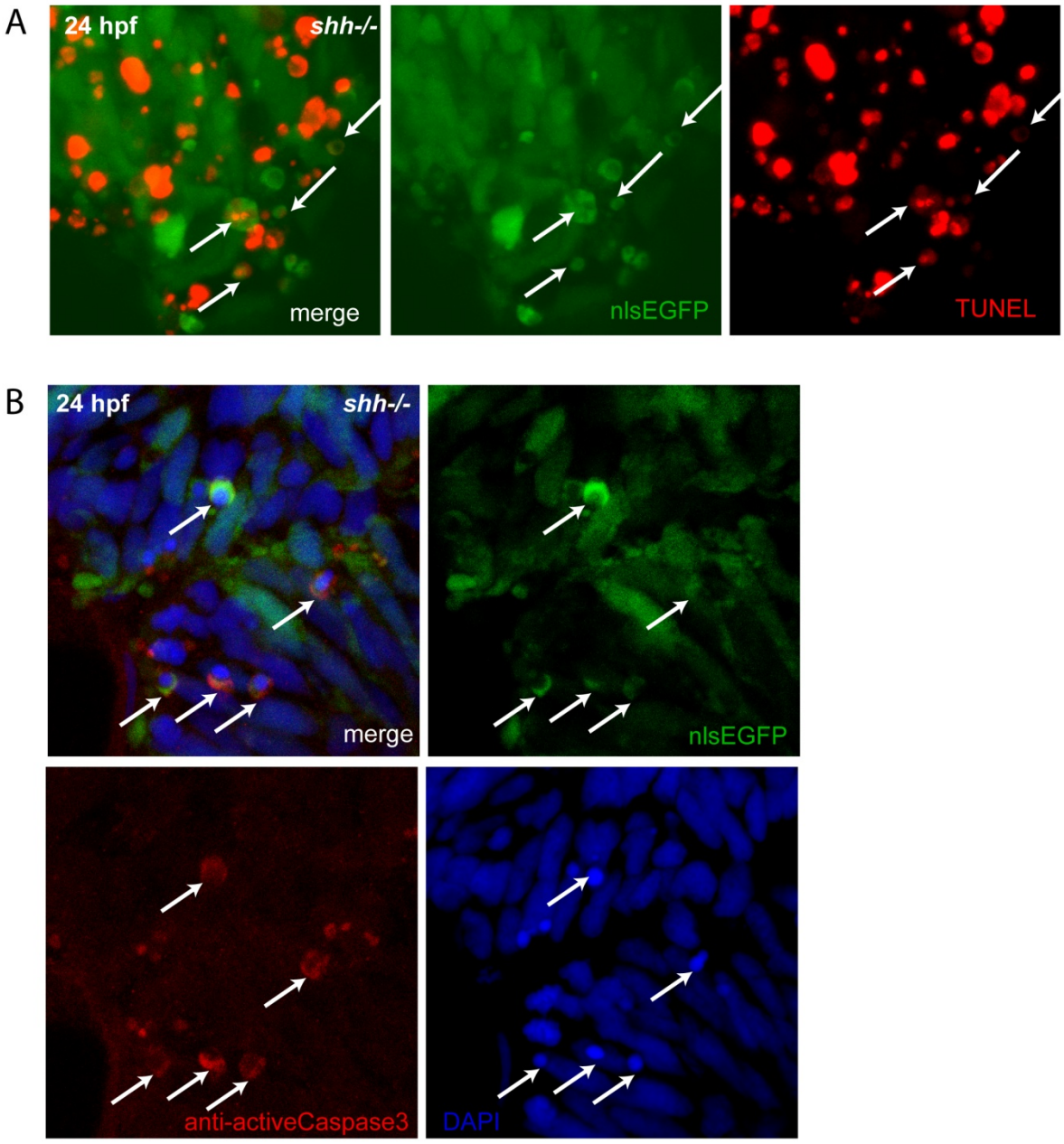

Figure 34. Co-localisation of apoptotic markers with p53 reporter expression.
A. Labeling p53 reporter nlsEGFP-positive cells with TUNEL. In some cells, TUNEL and nlsEGFP are present. These cells are labeled with arrows.
B. Anti-activeCaspase3 labeling of p53 reporter nlsEGFP-positive cells. Cells undergoing apoptosis but not small apoptotic corpses have both nlsEGFP and activeCaspase3 in the cytoplasm (labeled with arrows). DAPI staining shows that activeCaspase3-positive cells have condensed nuclei.

2.2.9 Cell cycle behavior of p53 reporter-positive cells in *shh*$^{-/-}$ mutant

Development of the PG13p21::nlsEGFP p53 reporter zebrafish transgenic line allows a better understanding of how cells with activated p53 behave *in vivo*. In particular, this line enabled a better, easier and more versatile visualization of cells with active p53 as described in previous sections. Additionally, cell-cycle behavior of p53 reporter-positive cells can be studied (Zhang et al., 2001). Observations of cell-cycle exit rescue in *shh*$^{-/-}$ retina by *p53* loss raise a question how cell cycle is regulated by p53 in the absence of Shh. Since p53 can induce cell-cycle arrest, one can explain the cell-cycle exit experiments (Fig. 26) by proposing that p53 inhibits cell cycle progression of retinal progenitors in the absence of Shh. To address this hypothesis, I used Fluorescence-activated cell sorting (FACS) method to analyse cell cycle properties of p53 reporter-positive cells. For FACS analysis, cell cycle distribution was determined using Propidium Iodide (PI) DNA staining since cells have different DNA contents in different cell cycle stages. Natural EGFP fluorescence was used to sort p53 reporter-positive cells. Thus, it is possible to compare cell cycle distributions of different cell populations directly. I applied the PI/EGFP-based FACS analysis to wild-type and *shh*$^{-/-}$ mutant embryos at 48 and 56 hpf, the stages used for the cell cycle exit experiment, expecting this analysis to help me understand the influence of p53 on retinal progenitor cell cycle progression. For this experiment the best samples would be dissected eyes. However, since it is technically challenging to obtain sufficient numbers of dissected eyes from zebrafish embryos, I used embryo heads for FACS-based experiments. In the case of *shh*$^{-/-}$ mutants, eyes contain a high proportion of all p53 reporter-positive cells in the head, which makes FACS likely to provide information on p53 reporter activation in the retina. FACS data show light scattering properties of the cells allowing correct cell populations to be selected for analysis as shown in Fig. 35A for 48 hps *shh*$^{-/-}$ mutants. PI and EGFP staining signals enable determination of cell cycle distributions of all cells (All cells), GFP-positive (GFP+) and GFP-negative (GFP-) cells for both wild-type and *shh*$^{-/-}$ mutant heads (Fig. 36). At 48 hpf in *shh*$^{-/-}$ mutant p53 reporter-positive cells have a very low G2/M cell percentage at 3 %, whereas 21.7 % of *shh*$^{-/-}$ mutant GFP– cells, 13.5 % of all *shh*$^{-/-}$ mutant cells and 11.5 % of wild-type cells were mitotic (Fig. 36B). This very low G2/M cell percentage in *shh*$^{-/-}$ mutant heads was accompanied by a higher S-phase proportion and a slightly higher G1-phase percentage relative to other samples (Fig. 36B). At 56 hpf, cell cycle distribution of p53 reporter-positive *shh*$^{-/-}$ mutant cell remained

similar to that at 48 hpf with G2/M proportion of 4.5 %. However, at 56 hpf there was a dramatic reduction in G2/M proportions most probably due to cell-cycle exit in wild-type and *shh*$^{-/-}$ p53 reporter-negative cell populations, making all populations similar in their mitotic indices. Moreover, the S-phase percentages of p53 reporter-positive and negative cells in *shh*$^{-/-}$ mutants at 56 hpf became similar. Nevertheless, the FACS data clearly indicate that p53 reporter-positive cells in *shh*$^{-/-}$ mutants are defective in cell-cycle progression and completing mitoses required for birth of differentiated cells at 48 hpf.

Figure 35. FACS analysis of cell cycle distribution of cells with active p53 reporter in wild-type and *shh*$^{-/-}$ mutant heads.
Heads of wild-type and *shh*$^{-/-}$ embryos carrying PG13p21::nlsEGFP reporter were dissociated to single cells to analysed using flow cytometry. DNA was stained using propidium iodide and EGFP fluorescence was detected directly.
A. Example of FACS data for 48 hpf *shh*$^{-/-}$ PG13p21::nlsEGFP. In the upper row, the left-most panel shows the distribution of cells according to their scatter properties. The middle panel shows the PI staining distribution (FL3A vs FL3W). The right panel shows the distribution of EGFP signal (FL1H) relative to the DNA PI staining signal (FL3W). The lower row of panels shows cell cycle distributions of cells with different levels of p53 reporter expression. The left panel shows cell cycle distribution of all cells in the sample, where peaks in different shadings correspond to cells with different DNA content. The middle panel shows cell cycle distribution of p53 reporter-positive cells, where notable shortage of G2-phase/mitotic cells is evident. The left panel shows the cell cycle distribution of p53 reporter-negative cells.
B. Cell cycle phase quantification of wild-type and *shh*$^{-/-}$ head samples at 48 and 56 hpf. Mutant samples are classified into All cells, GFP+ and GFP-, and the data for wild-type samples is presented as All Cells. G1, S and G2/M cell cycle phases and sub-G1 are the categories distinguished on the basis of PI DNA staining. Left panel shows samples at 48 hpf and the right panel shows 56 hpf samples. FACS experiments were repeated 3 times at both 48 and 56 hpf and representative data are shown.

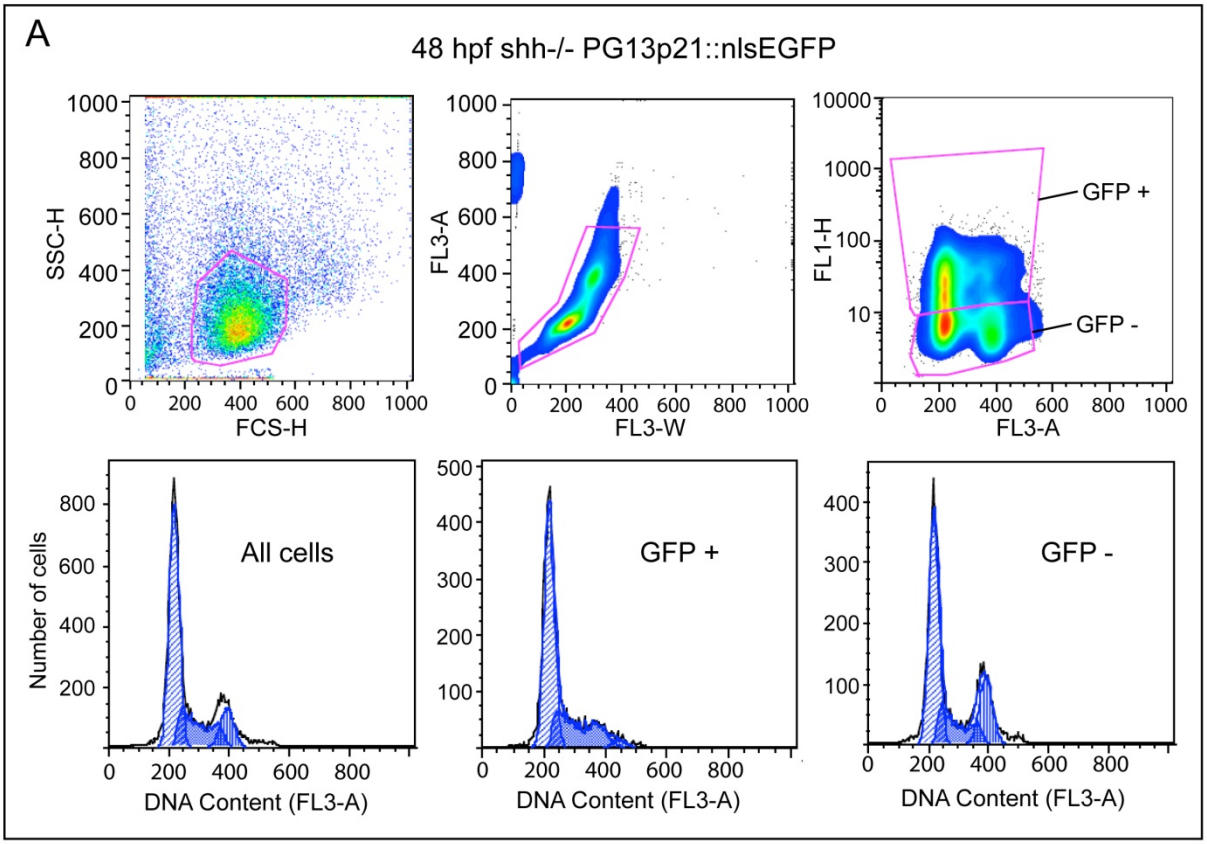
A
48 hpf shh-/- PG13p21::nlsEGFP
SSC-H
FCS-H
FL3-A
FL3-W
FL1-H
FL3-A
GFP +
GFP -
Number of cells
All cells
GFP +
GFP -
DNA Content (FL3-A)
DNA Content (FL3-A)
DNA Content (FL3-A)

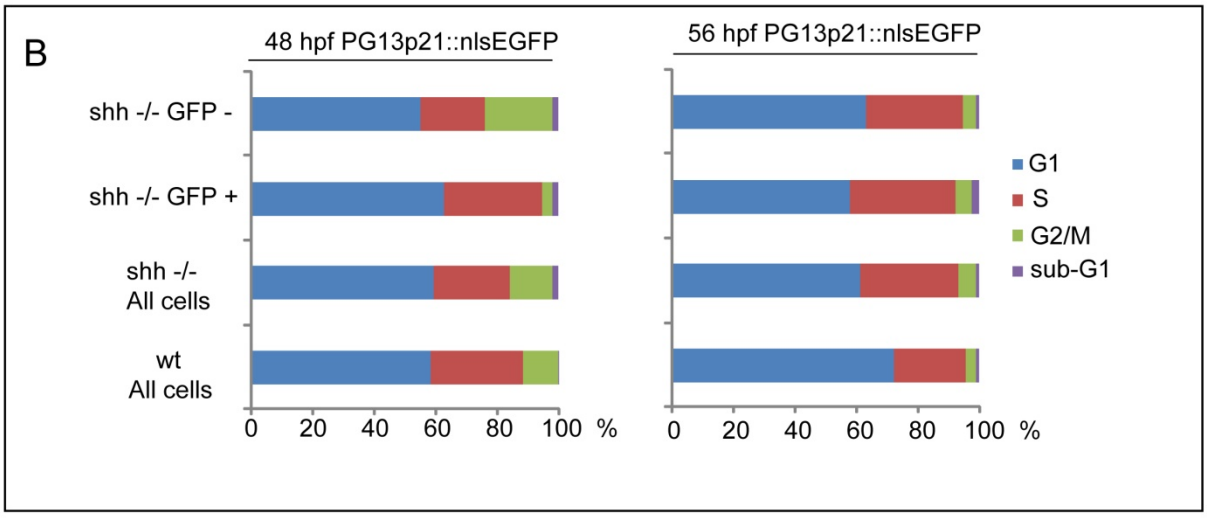
B
48 hpf PG13p21::nlsEGFP
56 hpf PG13p21::nlsEGFP
shh -/- GFP -
shh -/- GFP +
shh -/-
All cells
wt
All cells
G1
S
G2/M
sub-G1
%
%

2.2.10 p53 regulates proliferation in the *shh*$^{-/-}$ mutant retina

Information about cell cycle behaviour of p53 reporter-positive cells in *shh*$^{-/-}$ mutant obtained using FACS is important, but it doesnt't provide direct information on how these cells behave in the retina. Therefore, a direct analysis of the cell cycle progression of retinal cells had to be done. As a first step, BrdU labeling of S-phase cells was performed on wild-type and *shh*$^{-/-}$ mutant retinas at 48 hpf. In the wild-type retina, there are very few p53 reporter-positive cells and they are BrdU-negative (Fig. 36). By contrast, *shh*$^{-/-}$ mutant retina contains many p53 reporter-positive cells and nearly all of them are BrdU-positive, whereas some p53 reporter-positive cells present in the brain are BrdU-negative (Fig. 36). This result contrasts with the FACS data in whole-head cell populations since in the retina p53 reporter-positive cells have a low G1-phase proportion. It also suggests that in other head regions of *shh*$^{-/-}$ mutants, p53 reporter-positive cells may be predominantly in G1-phase. Therefore, cell-cycle regulation by p53 in the absence of Shh may be tissue-specific.

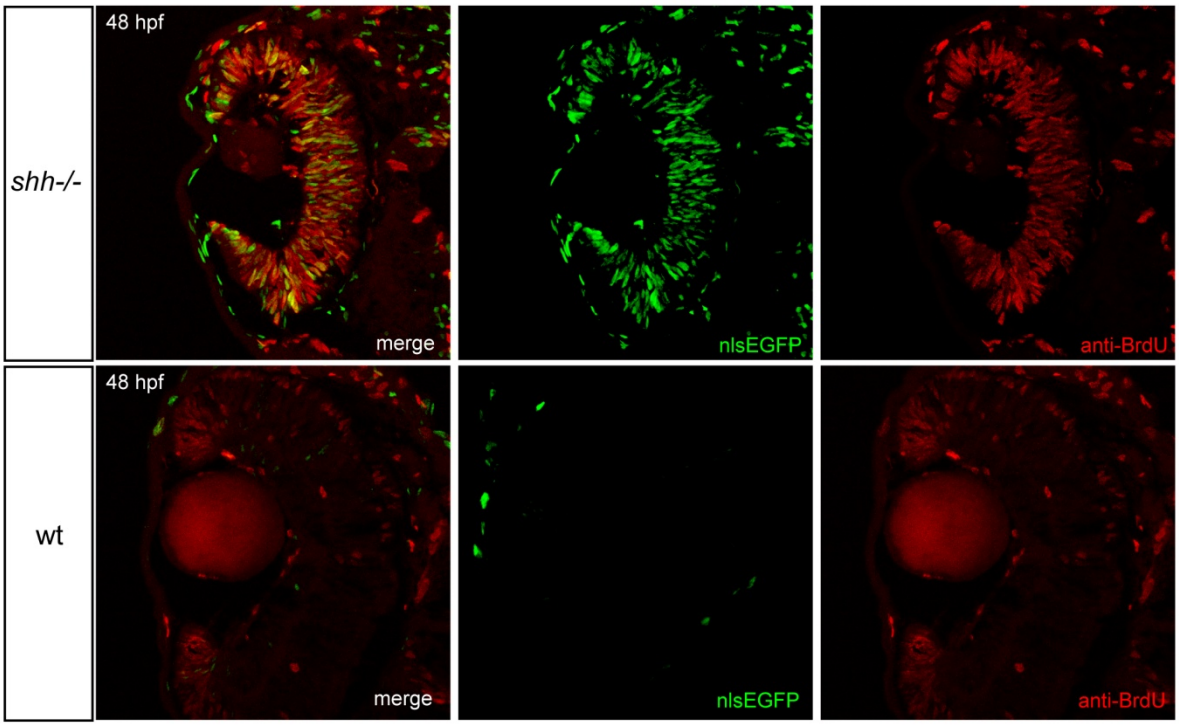

Figure 36. BrdU labeling of 48 hpf wild-type and *shh*$^{-/-}$ mutant retinas carrying p53 reporter. Retinal cryosections of wild-type and *shh*$^{-/-}$ mutant embryos labeled with 1-hour BrdU pulse were stained with anti-BrdU and anti-GFP antibodies. Image stacks were obtained using confocal microscopy and projected.

Since FACS-based experiments showed that p53 reporter-positive cells have defects in their progression into G2-phase and mitosis, I next analysed this aspect of cell cycle progression in the *shh*$^{-/-}$ mutant retina. Staining cells for Ser10-phosphorylated form Histone3 (pH3) enables studies of mitotic cell populations, since pH3 is a reliable marker for cells in late G2-phase and mitosis (Hendzel et al., 1997). pH3 also lends itself well to quantification of proliferation due to relatively low numbers of positive cells. In addition pH3 can be co-localised with the EGFP signal from the p53 reporter transgene. Using these tools, I analysed cell cycle progression of retinal cells during neurogenesis at 34 and 48 hpf. At 34 hpf, in the wild-type retina there is ongoing neurogenesis and the level of proliferation is still high, whereas in *shh*$^{-/-}$ mutants neurogenesis is defective and the rate of retinal mitosis is lower than in their wild-type siblings (Stenkamp et al., 2002). Wild-type retina at 48 hpf is completing neurogenesis, and a high number of cells are going through their final mitoses. To investigate the influence of p53 on retinal proliferation in the *shh*$^{-/-}$ mutant, I first studied co-localisation of pH3 with p53 reporter nlsEGFP in wild-type and *shh*$^{-/-}$ mutant retinas at 34 and 48 hpf (Fig. 37A). At both stages, wild-type embryos had very few cells expressing p53 reporter. By contrast, in the *shh*$^{-/-}$ mutant retina at both 34 and 48 hpf most cells were p53 reporter-positive (Fig. 37A). The number of pH3-positive retinal cells was clearly smaller in the *shh*$^{-/-}$ mutant than in the wild-type at both 34 and 48 hpf (Fig. 37A). Moreover, some mitotic cells in the *shh*$^{-/-}$ mutant retina were p53 reporter-negative suggesting that not all mitotic cells experienced p53 influence (Fig. 37A). However, these co-localisation data are not very useful to quantify the influence of p53 on cell cycle progression in the *shh*$^{-/-}$ mutant retina because p53 reporter nlsEGFP nuclear signal becomes cytoplasmic in mitosis and may not co-localise with pH3 chromatin signal. In addition, wild-type and *shh*$^{-/-}$ mutant p53 reporter-negative cell populations are different and there is some variation in p53 reporter expression in different cells and embryos. Therefore, as a more direct approach I used genetic inactivation of *p53* to understand its role in cell cycle regulation in the *shh*$^{-/-}$ mutant retina. At 34 and 48 hpf stages, I obtained samples of wild-type, the *shh*$^{-/-}$ mutant and the *shh*$^{-/-}$ *p53*$^{-/-}$ embryos and stained retinal sections with anti-pH3 antibody to identify mitotic cells and with DAPI to visualize cell DNA. At both 34 and 48 hpf there were fewer mitotic cells in the *shh*$^{-/-}$ mutant than in the wild-type retina with the difference less striking at 48 hpf than at 34 hpf (Fig. 37B). Strikingly, in the double *shh*$^{-/-}$ *p53*$^{-/-}$ mutant there was a clear increase in mitotic cell numbers and

retina size at both 34 and 48 hpf (Fig. 37B). To normalize mitotic cell numbers with respect to the total cells in the retina, mitotic and total cells were counted for each retinal section image and mitotic cell percentages were calculated. In the first experiment at 34 hpf, wild-type retina contained 13,9 % (Standard Devation(SD) = 1,53 %) pH3-positive cells, *shh*$^{-/-}$ mutant retina had 7,13 % (SD=1,48%), which is almost 2 times fewer (Fig. 37C). By contrast, 34 hpf *shh*$^{-/-}$ *p53*$^{-/-}$ retinas had 11,5 % (SD=1,79%) pH3-positive cells, which is statistically different from the *shh*$^{-/-}$ mutant retinal mitotic rate (t-test P<0,001) and almost reached the wild-type mitotic rate (Fig. 37C). This result suggests that in the absence of Shh decreased proliferation in the retina is due to p53 activity. Another possibility is that *p53* loss by itself is sufficient to increase retinal proliferation. Most evidence in the literature suggests that p53 regulates proliferation only under conditions of stress or upon its ectopic activation. However, to address this possibility, I repeated analysis of mitotic rates at 34 hpf in wild-type, *p53*$^{-/-}$, *shh*$^{-/-}$ and the *shh*$^{-/-}$ *p53*$^{-/-}$ retinas (Fig. 37D). Clearly, *p53* loss on its own is not sufficient to increase the mitotic rate, since mitotic rates of the wild-type retina (11,8 %, SD=1,73 %) and *p53*$^{-/-}$ mutant retina (12,02 %, SD=1,46 %) are not statistically different (t-test, P=0,67). In the second experiment at 34 hpf, the mitotic rate in the *shh*$^{-/-}$ mutant retina (7 %, SD=1,38 %) was also significantly lower than in the wild-type retina (t-test, P<0,001). Showing the rescue of retinal proliferation, the mitotic rate of the *shh*$^{-/-}$ *p53*$^{-/-}$ retina (12,1 %, SD=1,9 %) was even slightly higher than the wild-type retinal mitotic rate, but the difference was not significant (t-test, P=0,55). I then checked proliferation at 48 hpf in wild-type, *shh*$^{-/-}$ and the *shh*$^{-/-}$ *p53*$^{-/-}$ retinas (Fig. 37E). Mitotic rates in wild-type and *shh*$^{-/-}$ mutant retinas were 11,1 % (SD – 2 %) and 7,16 % (SD – 1,25 %), respectively, and significantly different from each other (t-test, P<0,001) (Fig. 37E). Similar to the results at 34 hpf, loss of *p53* in the *shh*$^{-/-}$ mutant (*shh*$^{-/-}$ *p53*$^{-/-}$) retina led to a striking increase in the mitotic rate to 11,6 % (SD – 1,54 %), which is a complete rescue of mitosis since the difference between wild-type and *shh*$^{-/-}$ *p53*$^{-/-}$ mitotic rates is not significant (t-test, P= 0,34). The results at both 34 and 48 hpf conclusively demonstrate that p53 is responsible for decreased mitotic rates in the *shh*$^{-/-}$ mutant retina during neurogenesis.

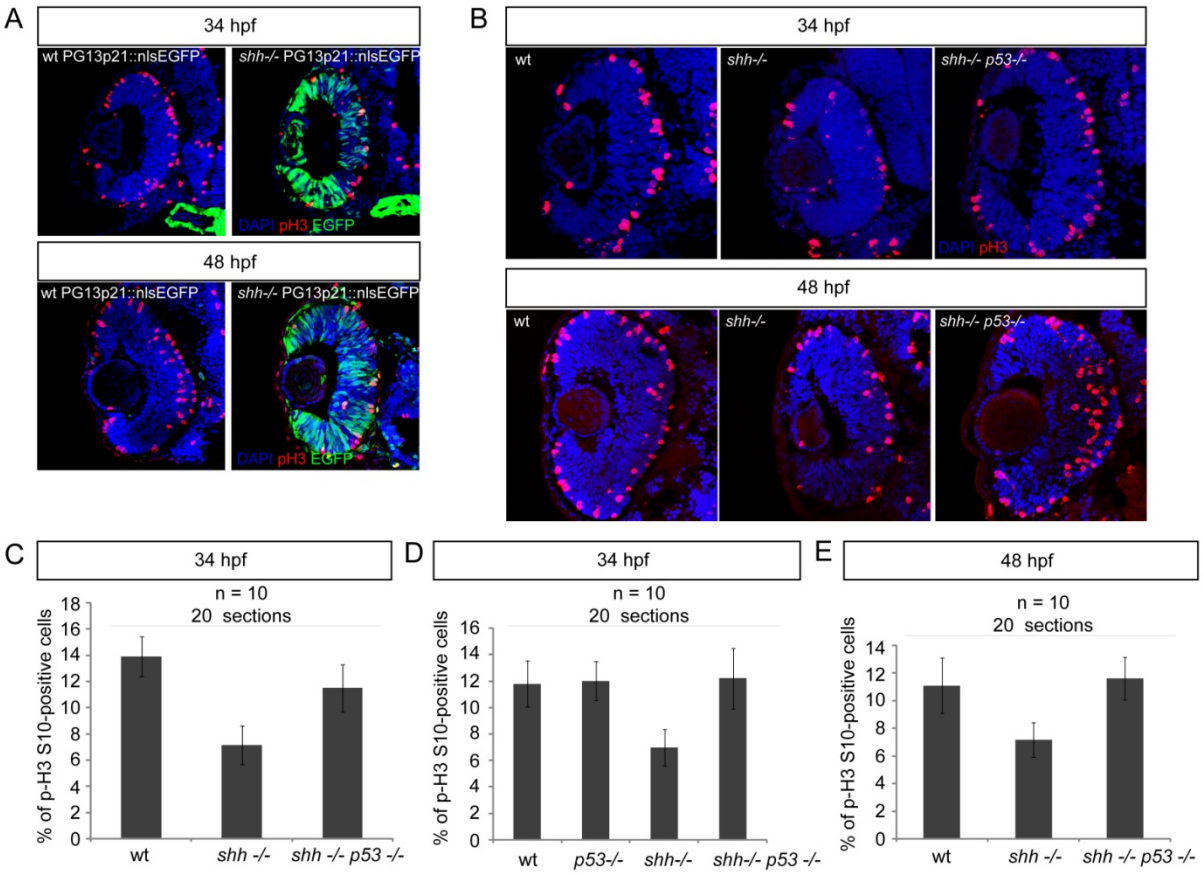

Figure 37. p53 regulates mitotic rate in *shh*$^{-/-}$ mutant during neurogenesis.
A. pH3 staining of PG13p21::nlsEGFP p53 reporter retinas. Wild-type and *shh*$^{-/-}$ mutant at 34 and 48 hpf were analysed. At both stages, wild-type retinas had a high level of mitotic cells and no expression of p53 reporter. By contrast, at the same stages mutant retinas had a lower number of mitotic cells and most retinal cells were p53 reporter-positive. Not all mitotic cells in the *shh*$^{-/-}$ mutant retinas were clearly p53 reporter-positive.
B. pH3 / DAPI staining of wild-type, *shh*$^{-/-}$ and *shh*$^{-/-}$ *p53*$^{-/-}$ retinas at 34 and 48 hpf. At both stages, mitotic rate in the *shh*$^{-/-}$ retina was lower that in the wild-type retina. In the *shh*$^{-/-}$ *p53*$^{-/-}$ retina the mitotic rate almost reached that of wild-type retina.
C. Statistical analysis of pH3/DAPI stainings in wild-type, *shh*$^{-/-}$ and *shh*$^{-/-}$ *p53*$^{-/-}$ retinas at 34 hpf, which are shown in B. 10 embryos and 20 retinal sections were analysed for each genotype.
D. Statistical analysis of the second pH3/DAPI staining experiment in wild-type, *p53*$^{-/-}$, *shh*$^{-/-}$ and *shh*$^{-/-}$ *p53*$^{-/-}$ retinas at 34 hpf. 10 embryos and 20 retinal sections were analysed for each genotype.
E. Statistical analysis of pH3/DAPI stainings in wild-type, *shh*$^{-/-}$ and *shh*$^{-/-}$ *p53*$^{-/-}$ retinas at 48 hpf, which are shown in B. 10 embryos and 20 retinal sections were analysed for each genotype.

3 Discussion

3.1 Direct and indirect regulation of proliferation by Shh in different contexts

The cell-cell signaling events that direct vertebrate limb development have been the subject of intense research for more than a hundred years. This provides an excellent foundation for investigating the mechanisms whereby pattern formation is integrated with proliferation. This integration means that signaling pathways involved in patterning also exert their effects on proliferation. In this project, I have focused on two of the main signals important for patterning and growth of the vertebrate limb: the Shh and Fgf signaling pathways. While both signals are crucial for outgrowth of the limb bud, it has been very challenging to uncouple these signals from each other, since expression of Shh depends on Fgf signaling, and vice versa. For example, while AER ablation experiments have been interpreted as causing failure of limb outgrowth because they lead to loss of Fgf gene expression in the limb bud (Fallon et al., 1994; Niswander et al., 1993; Dudley et al., 2002), AER ablation simultaneously leads to loss of Shh expression from the ZPA (Niswander et al., 1994; Laufer et al., 1994), and so cannot be used to separate the effect of Fgf signaling on proliferation from the effect of Shh signaling. In order to overcome this situation, I have used a combination of loss-of-function and gain-of-function experiments in the zebrafish model system to uncouple Shh from Fgf signaling in the pectoral fin bud, and have assessed the effect of each signal on fin bud cell cycle gene expression and proliferation independently of the other signal.

My results show that the effect of Shh on proliferation during limb development is indirect, and is mediated by its effect on Fgf expression in the AER. Inhibition of Shh signaling leads to loss of cell cycle progression only after a relatively long delay period of around 13 hours, which correlates with a concomitant loss of Fgf signaling. Inhibition of Fgf signaling, on the other hand, leads to disruption of cell cycle progression very rapidly, after only 3 hours of inhibitor treatment, and this occurs even though activity of the Shh pathway is still present. This rapid effect of Fgf on cell-cycle progression suggests a direct transcriptional response of cell-cycle genes to the Fgf pathway in the limb bud, which is consistent with the direct mitogenic effect of Fgf signaling shown for several cell types in tissue culture.

Since Hh signaling has also been shown to have a direct mitogenic effect on some cell types, it is perhaps surprising that Shh directs proliferation indirectly in the vertebrate limb

bud. However, there is at least one previous example of such an indirect effect of Hh signaling on proliferation. During *Drosophila* wing development, Hh is necessary for growth of the wing imaginal disc, but this effect is mediated via the Hh-dependent expression of Decapentaplegic (Dpp), a member of the Tgf-β family of secreted signaling proteins (Roy and Ingham, 2002; Burke and Basler, 1996; Martín-Castellanos and Edgar, 2002). Furthermore, the proliferative response of different cell types to Hh is clearly context-dependent, and Hh signaling can even function as a negative regulator of the cell-cycle in some cell types (Neumann, 2005). Interestingly, this negative effect of Hh signaling on proliferation also appears to be indirect in some cases. In the rodent colonic epithelium, for example, Hh signaling stimulates cell-cycle exit by antagonizing the Wnt pathway (van den Brink et al., 2004). In the *Drosophila* retina, on the other hand, Hh signaling has both positive and negative effects on cell-cycle progression (Firth and Baker, 2005). Cell-cycle arrest of cells in front of the retinal differentiation wave depends on Hh signaling in combination with Dpp, while cell-cycle re-entry behind the wave front also depends on Hh signaling, but in this case mediated by the Notch signaling pathway (Firth and Baker, 2005; Baonza and Freeman, 2005).

My results also show a context-dependent effect of Fgf signaling on cell-cycle progression. Thus Fgf signaling is clearly essential for cell-cycle progression in the pectoral fin buds and in the branchial arches, since expression of G1- and S-phase cell-cycle genes in these tissues is lost after only 3 hours of inhibition of the Fgf pathway. Inhibition of Fgf signaling fails to affect cell cycle progression in other organs, however, such as the retina and the optic tectum, or at earlier stages of development. The Fgf signaling pathway is therefore not a global mitogenic signal in the zebrafish embryo, but instead directs proliferation in a highly tissue-specific manner. Altogether, the evidence thus indicates that both the Hh and Fgf pathway affect cell cycle progression in some cell types but not in others, and that this effect can be either direct or indirect. The control of cell-proliferation in multicellular organisms can therefore only be understood in a context-dependent manner, and my results help to shed light on this question in the context of the vertebrate limb bud. The molecular mechanisms by which different cell types respond distinctly to the same signal are still poorly understood, but will undoubtedly be unravelled by future research.

3.2 Interaction of p53 and Shh in regulation of cell survival, cell cycle exit, and differentiation

3.2.1 p53 mediates apoptosis in the absence of Shh in zebrafish

During development cell number is controlled not only by the rate of proliferation, but also by the rate of cell death. Since Shh has been implicated in the regulation of apoptotic cell death, I examined the role played by zebrafish Shh in directing apotosis during organogenesis. In this project I focused on the elevated apoptosis in the neural tube and retina of the *shh*$^{-/-}$ mutant. I asked if lower Bcl2 family gene expression in the *shh*$^{-/-}$ mutant can be the reason for cell death. However, no striking differences in expression of Bcl2 family genes *bcl2*, *bcl2l*, *mcl1a* and *mcl1b* were found between wild-type and *shh*$^{-/-}$ mutant embryos (Fig. 17). Although I cannot exclude some tissue-specific expression differences between wild-type and *shh*$^{-/-}$ mutants, these results suggest that Shh signaling does not regulate expression of anti-apoptotic Bcl2 family genes globally. Another possibility is that Shh regulates survival through a different mechanism. However, activation of Hh signaling can induce expression of *Bcl2* gene in mouse keratinocytes (Bigelow et al., 2004), chick spinal cord (Cayuso et al., 2006) and mouse lymphoma cells, where Hh signaling is required for survival through maintenance of Bcl2 expression (Dierks et al., 2007).

Further expression analyses showed that p53 target genes such as *p53* itself, *p21*, *mdm2*, *cyclinG1*, *bax1*, *puma* were up-regulated in the *shh*$^{-/-}$ mutant relative to wild-type through most of development as confirmed by *in situ* hybridization and qPCR assays (Figs. 18, 19). Up-regulation of *p53* gene expression occurred by p53-mediated transcription from an internal promoter generating a short *p53* transcript encoding an inactive p53 isoform (Chen et al., 2005; Robu et al., 2007). p53 is indeed required for elevated apoptosis in the absence of Shh, since morpholino knockdown of p53 rescued apoptosis in the neural tube and in the retina of the *shh*$^{-/-}$ mutant (Fig. 21). Over-expression of EGFP-bcl2 (Langenau et al., 2005) also rescued elevated apoptosis in the *shh*$^{-/-}$ mutant showing that intrinsic apoptotic pathway is activated. In contrast to the studies showing that Bcl2 can inhibit p53 activity (Froesch et al., 1999; Beham et al., 1997; Ryan et al., 1994), p53 target gene expression remained normal after EGFP-bcl2 over-expression (Fig. 21), which suggests that effects of Bcl2 on p53 activity may be species- or tissue-specific. This result is also consistent with my observation that Bcl2

family gene transcription is unaffected by loss of Shh. These results suggest that Shh is necessary to inhibit the activity of p53 but it is unclear how direct this inhibition is. To address this question, I then studied the onset of p53 pathway activation and elevated apoptosis in the *shh*$^{-/-}$ mutant, which turned out to happen at the 10somite stage (Fig. 20). The broad pattern of p53 target gene expression and apoptosis in the *shh*$^{-/-}$ mutant at the 10somite stage argues against the idea that cells die due to differentiation failure, since few cells in the wild-type express neuronal differentiation marker HuC at this stage (Kok et al., 2007). Early requirement of Shh for cell survival during development is consistent with the suggestion that Hh signaling affects cell survival independently from and earlier than affecting cell fate (Cayuso et al., 2006).

The results above raise a question whether p53 activity can be suppressed by Hh signaling activation. Indeed, activation of Hh signaling using dnPKA-GFP can effectively suppress p53 target gene expression and apoptosis in the *shh*$^{-/-}$ mutant at the 12somite stage (Fig. 26). As this thesis project was in progress, Abe et al. (2008) provided evidence that Hh signaling regulates stability of p53 by activating Mdm2 in human cell lines probably through induction of an unknown Mdm2-activating factor. Stecca and Altaba (2009) characterized the interaction between p53 and Gli1, a downstream Hh signaling mediator, in wild-type chick neural stem cells. These authors found that Gli1 can suppress p53 activity by up-regulating Mdm2 level. They also showed that p53 can interfere with Gli1 functions, which creates a negative feedback loop. These studies are consistent with and support my observations that p53 mediates apoptosis in the absence of Shh, and that Shh is required to control p53 activity *in vivo*. Due to lack of antibodies against zebrafish Mdm2, I could not determine if Hh signaling up-regulates Mdm2 level in zebrafish. Nevertheless, since p53 activity can be inhibited by Hh signaling activation in human cell lines, chick neural stem cells and zebrafish embryos, the same mechanism is likely involved.

Concerning p53 regulation, the question is whether Hh signaling is required for establishment or maintenance of p53 activity control. Due to the localized nature of Shh expression, it is unlikely that cells would require persistent Shh signaling to maintain p53 activity control. Another possibility is that Shh is required to maintain control of p53 activity only during a certain period of development. Shh is not involved in the earliest stages of p53 control since p53 can already be activated in late gastrulation (Kratz et al., 2006), which is

much earlier that 10somite stage. However, p53 activity control appears to become dependent on Shh signaling after the onset of Shh expression.

3.2.2 p53 regulates proliferation and differentiation in the *shh*$^{-/-}$ mutant retina

The insight that p53 is essential for apoptosis due to *shh* loss allows investigating how apoptosis suppression affects proliferation and differentiation. The retina was chosen as a system to examine these aspects of apoptosis suppression. To suppress apoptosis throughout development of *shh*$^{-/-}$ mutants, double *shh*$^{-/-}$ *p53*$^{-/-}$ mutants were generated. Elevated apoptosis was suppressed in these double mutants both in the neural tube at 24 hpf and in the retina at 72 hpf (Figs. 21, 22). I then studied how suppression of apoptosis affects differentiation in the *shh*$^{-/-}$ mutant retina. In fact, in the *shh*$^{-/-}$ *p53*$^{-/-}$ mutant retina, RGC staining is strongly increased, many amacrine cells, which are absent in the *shh*$^{-/-}$ mutant retina, appear and both cone and rod photoreceptors are nearly completely rescued (Fig. 23). However, differentiation of bipolar and Müller glia cells was not rescued in the *shh*$^{-/-}$ *p53*$^{-/-}$ mutant (Fig. 24). These results show that Shh is required not for differentiation of most retinal cell types, but simply to promote survival of retinal progenitor cells. In contrast, no rescue Müller glia differentiation in the *shh*$^{-/-}$ *p53*$^{-/-}$ mutant retina supports previous work in the mouse showing that Shh is required for Müller glia development (Wang et al., 2002). Several previous studies in zebrafish have addressed how suppression of p53-mediated apoptosis affects retinal differentiation. In zebrafish mutants of DNA polymerase delta 1 subunit (*pold1*) many cells die of apoptosis, and suppression of apoptosis in the retina by *p53* knockdown rescues eye size and morphology (Plaster et al., 2006). Yamaguchi and colleagues (2008) found that in the case of the zebrafish *primase1* mutant *p53* knockdown led to the rescue of amacrine cell and photoreceptor differentiation. By contrast, *p53* knockdown in *chromatin assembly factor 1b* (*caf1b*) mutant did not lead to rescue of retinal differentiation (Fischer et al., 2007). Differentiation rescue by loss of *p53* activity in the *shh*$^{-/-}$ mutant retina is similar to the p53 knockdown results in *pold1* and *primase1* mutants. However, Shh likely affects differentiation by regulating p53 activity and through other mechanisms, whereas mutations of *pold1* or *primase1* were proposed to induce genotoxic damage. By contrast, *caf1b* is required for both cell survival and differentiation of most cell types. Although p53 inhibits retinal

differentiation in the *shh*$^{-/-}$ mutant, it promotes differentiation in mouse embryonic stem cells after DNA damage by decreasing Nanog expression (Lin et al., 2005), and reduces spontaneous differentiation of human stem cells (Qin et al., 2007). Thus, the effect of p53 on differentiation is strongly context-dependent.

p53 loss in the *shh*$^{-/-}$ mutant rescues two aspects of retinal proliferation: cell-cycle exit of retinal cell progenitors (Fig. 25) and mitoses during neurogenesis (Fig. 37). Moreover, cyclin-dependent kinase inhibitor *p57kip2* expression is rescued in the *shh*$^{-/-}$ *p53*$^{-/-}$ mutant retina (Fig. 25C), which correlates with normal cell-cycle exit. These findings may represent two sides of the same phenomenon, since active cell-cycle exit must result in more mitoses of differentiating cells. Therefore, rescue of cell-cycle exit may be necessary and sufficient to rescue the mitotic rate in the *shh*$^{-/-}$ mutant retina. However, rescue of the mitotic rate in the *shh*$^{-/-}$ *p53*$^{-/-}$ mutant retina may also result from lack of p53-activated cell cycle inhibitory gene expression. *p57kip2* loss in the *shh*$^{-/-}$ *p53*$^{-/-}$ mutant is required to understand the relative contributions of the two mechanisms. However, since *p57kip2* knockdown results in phenotypes too variable to make clear conclusions, this experiment was not performed. Previous studies of cell-cycle exit in the zebrafish retina (Masai et al., 2005; Shkumatava and Neumann, 2005) showed that *p57kip2* expression is regulated by Hh signaling. My results support this conclusion and uncover that in the *shh*$^{-/-}$ mutant p53 mediates lack of *p57kip2* expression. Thus, a model can be proposed that Hh signaling is required for *p57kip2* retinal expression by controlling activity of p53. Concerning the mechanism of *p57kip2* regulation by p53, there are several studies suggesting that p53-mediated *Notch1* expression may be responsible for lack of *p57kip2* retinal expression. *Notch1* is a p53 target in human keratinocytes (Lefort et al., 2005) and myeloid and lymphoid cells (Secchiero et al., 2009). Moreover, Katoh and Katoh (2008) found that in human and mouse embryonic stem cells Gli2 prevents p53 from activating *Notch1* gene expression, which establishes a connection between p53, Hh and Notch pathways. In zebrafish, *Notch1* homologs are also likely to be p53 targets since they contain optimal p53 binding sites (personal observation). Notch signaling inhibits *p57kip2* expression during zebrafish neural tube development (Park et al., 2005), in pancreas development (Georgia et al., 2006), in the adult intestinal crypts (Riccio et al., 2008) and during eye lense development (Jia et al., 2007). It will be important to check if p53 blocks cell-cycle exit by activating Notch signaling.

3.2.3 p53 reporter expression in tissues requiring Shh for survival

Another important aim in this project was development of a p53 reporter line in zebrafish to study p53 activation. In the *shh*$^{-/-}$ mutant p53 reporter-positive cells were detected in the retina as early as 24 hpf leading to the conclusion that extraretinal Shh signaling is required for control of p53 activity during retinal development, since no Shh is produced in the retina at 24 hpf (Fig. 32). In addition, p53 reporter activation and apoptosis were detected in the midbrain, hindbrain and spinal cord regions of the neural tube (Fig. 32, 33), consistent with the previous studies on the Shh survival function in these tissues (Charrier et al., 2001; Britto et al., 2002). p53 reporter expression but no elevated apoptosis were detected in somites of the *shh*$^{-/-}$ mutant (Fig. 29, 32). However, p53 may mediate apoptosis in the somites of the *shh*$^{-/-}$ mutant at earlier stages, which would make the elevated p53 reporter expression fully consistent with the role of Shh in sclerotome cell survival and myogenic differentiation (Borycki et al., 1999). Locations of p53 reporter-positive cells in the lateral midbrain and of apoptotic cells in streams from the neural tube in whole-mount stainings at 24 hpf suggest their neural crest origin (Figs. 32, 15). These observations agree with the fact that Shh ensures survival of these cells (Ahlgren and Bronner-Fraser, 1999). Taken together, these results show that p53 reporter is detected in most regions, in which Shh plays the cell survival role. p53 reporter-positive cells could also be visualized in terms of their progression through S-phase, mitosis and apoptotic phenotypes (Figs. 34, 36,37). Moreover, FACS sorting of p53 reporter-positive cells enabled studying their cell cycle distribution and helped understand how p53 affects cell cycle progression in the *shh*$^{-/-}$ mutant retina (Fig. 35). Finally, p53 reporter activation could also be induced by p53 activating drugs such as roscovitine (Fig. 28). These results clearly show that the transgenic p53 reporter line is more advantageous than *in situ* hybridizations for detecting expression of p53 target genes, or even than antibodies against p53 (Lee et al., 2008), which are used for visualizing cells with active p53. The current form of the p53 reporter is based on nlsEGFP, but it is certainly possible to replace nlsEGFP with fluorescent proteins of other colours or with degradable fluorescent proteins to obtain a dynamic picture of p53 activity.

3.3 Conclusions and Outlook

Previous studies have shown that both Shh and Fgf signaling are crucial for outgrowth of the vertebrate limb. The results presented here show that the role of Shh in this process is indirect, and is mediated by its effect on Fgf signaling. By contrast, the activity of the Fgf pathway affects proliferation directly and independently of its effect on Shh. These results show that Fgf signaling is of primary importance in directing outgrowth of the limb bud, and clarify the role of the Shh-Fgf feedback loop in regulating proliferation.

The work presented here has also clarified several aspects of the role played by p53 in mediating Shh-directed control of cell survival, cell-cycle exit and differentiation. In the absence of Shh p53 mediates apoptosis in the neural tube and the retina. In the context of the retina, p53 is the mechanism downstream of Shh regulating proliferation, differentiation and survival. It is fascinating that a single mechanism can regulate such different biological processes, and previously Shh would be envisioned to control these processes through distinct mechanisms. On the other hand, there are several different mechanisms downstream of p53 as well, which means that the findings in this thesis point us in the promising direction to search for additional important mechanisms.

The role of Shh-regulated *Bcl2* expression versus p53 pathway control in different cases of Shh-controlled cell survival should be uncovered by future studies. Another interesting question is how p53 pathway activation is controlled temporally and spatially during development in the absence of Shh. Moreover, future research will be necessary to unravel p53-mediated Hh signaling functions in the context of proliferation and differentiation in different model systems and tissues.

4 MATERIALS AND METHODS

4.1 Fish stocks, maintenance and identification

Wild-type *Tupfel Long Fin (TLF)*, *sonic-you*^{t4} (*shh* null mutation, Schauerte et al., 1996) and p53^{zdc1} (Berghmanns et al. (2005); obtained from Schulte-Merker laboratory) heterozygous fish were used. Fish were maintained according to standard protocols. Embryos were grown in E3 embryo medium at 28 ^{o}C with or without the addition of 0.003% 1-phenyl-2-thiourea (PTU) (Sigma, cat# P7629) to inhibit pigmentation. Staging was performed according to hours post-fertilization (hpf) (Westerfield, 1995). Identification of *shh*$^{-/-}$*p53*$^{-/-}$ was performed by first selecting acridine orange-negative embryos and then performing PCR on embryo tails with pairs of the following primers to check the embryos for either wild-type or mutant alleles as described in Berghmanns et al. (2005): p53ID_for: GATAGCCTAGTGCGAGCACACTCTT, p53wtID_rev: AGCTGCATGGGGGGAT and p53mutID_rev: AGCTGCATGGGGGGAA. Alternatively, only PCR genotyping was performed. The *p53* genotype of adult fish was identified using the same PCR assay on fin clips. Fin clips were obtained by anesthesizing adult fish in 0.02 % Tricaine and then cutting small pieces of the caudal fin. All DNA samples for identification were prepared by boiling in 20-50 µl of 50 mM NaOH at 95 ^{o}C for 10 minutes and then neutralizing the resulting lysate with 1M Tris-HCl pH 8.2 as described previously (Meeker et al., 2007).

4.2 Chemicals and solutions

60x stock solution E3 saline:

34,8g NaCl
1,6g KCl
5,8g $CaCl_2$ x $2H_2O$
9,78g $MgSO_4$ x $6H_2O$
H_2O ad 2l
pH 7.2 with NaOH
autoclave
for 1x use 16ml/l + 100µl methylene blue solution

10x loading buffer:

50% glycerol
1x TE
0.25% bromophenol blue
0.25% xylene cyanol

TE:

10 mM Tris/HCl pH 7.4
1mM EDTA pH 8.0

50xTAE:

242 g Tris base
57.1 ml glacial acetic acid
100ml 0.5M EDTA
Add ddH_2O to 1 liter and adjust pH to 8.5.

10xPBS:

70g NaCl;
62.4g Na_2HPO_4 x2H_2O;
3.4g KH_2PO_4
pH7.4

DEPC H_2O:

Di-ethyl pyrocarbonate (DEPC) was dissolved in H_2O at 0.1 %. The solution was incubated overnight at 37 ^oC and then autoclaved.

Acridine Orange

Acridine Orange (Molecular Probes, Invitrogen,cat# A1301) was dissolved at 10 mg/ml in water and used at 1:5000 dilution for live apoptosis staining

4.3 Microinjection of mRNA and morpholino

p53 morpholino (GCGCCATTGCTTTGCAAGAATTG; Langheinrich et al., 2005) was purchased from Gene Tools and was injected into 1-cell stage at 0.5 mM. Five-mismatch control morpholino against *her4* gene (GTACGACTCATTGGTGTCTGTGTTG) was used as a control morpholino. To make RNA for over-expression experiments, required pCS2+ vectors were linearised and transcribed using mMessage mMachine SP6 (Ambion, cat # AM1340). The following plasmids were used to prepare RNA for microinjections:

pCS2+dnPKA-GFP (Moon lab)

pCS2+EGFP

pCS2+EGFP-bcl2 (Look lab)

pCS2+H2BmRFP1 (provided by Gilmour lab)

pCS2+FA Transposase (Tol2kit)

4.4 p53 reporter fish generation

4.4.1p53 reporter construction

Human CDKN1A/p21 2.4 kb promoter was amplified from RPCI-11 Human BAC clone (Imagenes, RPCIB753F15397Q) using the following primers:

HindIII_p21prom_for : AAGCTTGGGCACTCTTGTCCCCCAGG

BamHI_p21prom_rev: GGATCCCTGACTTCGGCAGCTGCTCA

The resulting PCR product was TOPO-cloned into pCR2.1 (Invitrogen) and then subcloned into p5E-MCS vector using HindIII and BamHI restriction sites. The resulting plasmid was named p5E-p21. PG13 enhancer (13 copies of an optimal p53 binding site CCTGCCTGGACTTGCCTGG) was synthesised by GeneArt (custom product). The synthetic PG13 fragment contained KpnI and HindIII restriction sites for directional cloning into p5E-p21. Insertion of PG13 into p5E-p21 resulted into the final 5'-entry vector p5E-PG13p21.

To generate the construct for injection into embryos, p5E-PG13p21 was recombined with pME-nlsEGFP, p3E-polyA and pDestCG2 vectors (Tol2kit, Kwan et al., 2007).

4.4.2 p53 reporter injection and carrier fish identification

pDestCG2-PG13p21::nlsEGFP-polyA plasmid was mixed with FA Transposase RNA to final concentrations 15 ng/µl and 20 ng/µl in DEPC H_2O, respectively. The mix was injected into wild-type oocytes, and injected embryos were grown to adulthood. Subsequently, F0 founder fish were outcrossed into wild-type and *sonic-you* backgrounds to generate F1 transgenic animals, which were used for the experiments and outcrossed once more to generate F2 generation.

4.5 General cloning procedures

4.5.1 RNA purification

For cloning:

To collect total embryo RNA, 30-50 embryos at the required stage were frozen in liquid nitrogen. RNA was then purified using RNeasy Mini kit (Qiagen, cat# 74104) according to the manufacturers' protocol and eluted in DEPC H_2O.

For quantitative and semi-quantitative PCR:

- Transfer embryos (up to 100) to Eppendorf tube. Remove water with glass Pasteur pipette.
- Add 400 µl TRIzol Reagent and directly grind until embryos are dissolved.
- Then add 600 µl TRIzol reagent and mix.
- At this point leave 5 min at room temperature and continue, or freeze the lysate at –20°C.
- Add 200 µl chloroform for each ml reagent and shake the tube vigorously for 15 seconds.
- Leave 5-10 min at room temperature.
- Centrifuge at 12000g for 5 min
- **From now on one should work RNase free!**
- Transfer upper aqueous phase to new tube and precipitate with 0.5 ml isopropanol (for each ml reagent that was initially used)
- Leave 15 min or longer at room temperature.
- Centrifuge at 12000g for 10 min at 4°C.
- Remove supernatant, centrifuge short to collect and remove remaining supernatant.
- Add 1 ml 75% ethanol, vortex, and centrifuge 5 min.
- Remove 75% ethanol. Centrifuge short to collect and remove remaining ethanol. Dry pellet for 5 min at room temperature.
- Dissolve pellet in the desired amount of RNase free water (50µl).

- Measure RNA concentration and run on a gel for short time to verify that degradation has not occurred (The upper 28S band should have twice the intensity of the lower 18S band).

4.5.2 cDNA synthesis

cDNA first-strand synthesis for cloning was performed using SuperScript III Reverse Transcriptase system (Invitrogen, cat# 18080-051) and to prepare cDNA for quantitative PCR Quantitect Reverse Transcription Kit (Qiagen, cat# 205311) was used according to manufacturers' instructions.

4.5.3 Cloning probe template plasmids

Table 1. Primers used to amplify cDNA fragments

Gene	Primer name	Sequence	Template
pcna	pcna_for pcna_rev	cctactccaaactaagaaagcagca atcgggaatccattgaactgg	cDNA
mcm5	mcm5_for mcm5_rev	tggtggaggagaaagcgtcg ggcctcatggattgcgactc	cDNA
ra1	ra1_for t7_ra1_rev	ccattggaggaaacaggaga taatacgactcactatagggcagcgtgtacctggtaagca	cDNA
mcl1a	mcl1a_for mcl1a_rev	tatggctttgagtttggattttagg tgcattgatagccattggc	cDNA
mcl1b	mcl1b_for mcl1b_rev	gagaagaagaaaaaatgtagagttg agcacttcgaaaaggaaaa	cDNA
bcl2l	bcl2l_for t3_bcl2l_rev	tggataaccgtattaccgcc cgcgcaattaaccctcactaaagcactagtcataccaggatc	pDNR-LIB-bcl2l (ZFIN)
bcl2	bcl2_for bcl2_rev	gcgcgtttctatcgtgattt agcatgtgtgcacgtgtttt	cDNA
bax1	bax1_for t3_bax1_rev	tgtacggaagtgttacttctgctc ggatccattaaccctcactaaagggaaggccgcgacctgcagctc	pME18S-FL3-bax1 (ZFIN)
p53	p53_for p53_rev	gaatccccaaaactccacgc ccaaaaagagcaaaactccc	cDNA
mdm2	pME_for: t7_pME_rev:	attaaccctcactaaaggctgctcctcagtggatgttgcctttac taatacgactcactataggcaggttcaggggggaggtgtgg	pME18S-FL3-mdm2 (Imagenes)
puma	puma_for puma_rev	aacaccgctttatatcccct tgtgttcatctgaggccgtg	cDNA
p21	p21_for p21_rev	tcaggtgttcctcagctcct cggaataaacggtgtcgtct	cDNA

4.6 Quantitative Real-time PCR and semiquantitative PCR

cDNA samples prepared using Quantitect cDNA synthesis kit from whole embryos or embryo heads were used for quantitative real-time PCR after a10-fold dilution. SYBR® Green PCR Master Mix (Applied Biosystems, cat# 4309155) was used to prepare qPCR reactions, which were run on the ABI7500 qPCR machine.

Table 2. Primers for PCR assays

Primer name	Sequence	Source
mdm2q_for	gatgcaggtgcagataaagatg	This study
mdm2q_rev	ccttgctcatgatatatttccctaa	This study
p53q_for	cccatcctcacaatcatcact	Kratz et al., 2006
p53q_rev	cacgcacctcaaaagacctc	Kratz et al., 2006
pumaq_for	gaacacacgggttacaaaagac	This study
puma-q_rev	gaaaattcccagagtctgtaagtg	This study
noxaq_for	cgaacctgtgacagaaacttg	Kratz et al., 2006
noxaq_rev	ctgcgcgcactctactaca	Kratz et al., 2006
cycG1-qfor	catctctaaaagaggctctagatgg	This study
cycG1-qrev	cacacaaaccaggtctccag	This study
bax1_qfor	gcaagttcaactggggaaga	This study
bax1_qrev	gtcaggaaccctggttgaaa	This study
gapdh-q_for	tgcgttcgtctctgtagatgt	Kratz et al., 2006
gapdh-q_rev	gcctgtggagtgacactga	Kratz et al., 2006

4.7 Sequencing

DNA Sequencing was performed by either EMBL Genomics Core Facility or by GATC Biotech.

4.8 Probe synthesis

4.8.1 Linearising DNA for *in vitro* transcription reactions

- Take 10 µg of a plasmid of interest and set up a digest reaction in 100 µl.
- Incubate for several hours or overnight at 37 C and run 5 µl on gel to check for linearity.
- Add 1 µl of Proteinase K (20 mg/mll) and 5 µl of 10 % SDS and incubate at 50 C for 1h. Add 100 µl water.
- Add an equal amount of 25:24:1 (v/v) phenol-chloroform-isoamyl alcohol and vortex.
- Separate the aqueous phase which contains the DNA from the organic phase by centrifugation at 8000 rpm for 1 min.
- In order to precipitate the DNA, add a 0.1 volume of 3 M sodium acetate, pH 5.5, to the aqueous phase and then 2 volumes of absolute ethanol. Incubate at –20 °C overnight or for shorter periods at –80 °C (20–30 min).
- Recover the precipitated DNA by centrifugation in the microfuge at 10 000 rpm for 15 min. Remove the ethanol with care and dry the pellet in a desiccator or 50 °C oven for 5 minutes.
- Wash with 1 ml of 70% (v/v) ethanol/DEPC. Remove the ethanol solution with care and dry the pellet in a desiccator or 50 °C oven for 5 minutes.
- Resuspend dried DNA in 20 µl of DEPC-treated water and store at –20 °C.

4.8.2 *In vitro* transcription reactions

In vitro transcription reactions for mMessage mMachine SP6 (Ambion, cat# AM1340) and DIG RNA Labeling Kit (Cat # 11175025910)) were performed according to manufacturers' instructions.

4.8.3 Purification of RNA from *in vitro* reactions

After transcription, the DNA template is digested by the addition of 2 µl RNAse free DNAse (Roche 776785) for 15 min at 37°C.

- Add 30 µl DEPC H_2O and 30 µl LiCl precipitation solution (7.5 M)
- Chill for 2 hours at -20 ^{o}C

- Centrifuge at 4°C for 30 min at 10,000 g
- Add 1 ml of 70% Ethanol/DEPC H_2O to the pellet
- Centrifuge at 4 °C for 5 minutes
- Remove the supernatant, shortly air dry and resuspend in 30 µl DEPC H_2O

4.9 Histochemical methods

4.9.1 *In situ* RNA hybridisation

RNA *in situ* hybridisations were performed according to Jowett (2001). Probes were made using Roche DIG RNA Labeling Kit (Cat # 11175025910). Antisense probes were made to detect expression of the following genes: *ptc1*, *pea3* (Norton et al., 2005), *cyclin D1* (Shkumatava and Neumann, 2005), *pcna*, *mcm5*, *ra1*, *bcl2*, *bcl2l*, *mcl1a*, *mcl1b, p53, mdm2, bax1, puma*. cyclinG1 probe was prepared from pCMV-SPORT6.1-cyclinG1 (RZPD Clone ID IMAGp998A0314862Q1) plasmid, which was digested with EcoRI and transcribed with T7 polymerase.Cloning of plasmids for making probes is described in the section on cloning. Templates for making anti-sense probes were prepared either by linearizing plasmids with restriction enzyme digests or by PCR with primers containing phage promoters.

4.9.2 Cryosectioning procedure

- Fix dechorionated embryos in 4% PFA/PBS for 1h at RT or O/N at 4°C
- Wash with PBS
- Incubate 2 hours at RT (O/N – a few days at 4°C) in 20% sucrose/PBS
- Remove embryos from sucrose and place in plastic moulds (Polysciences)
- Take off sucrose as well as possible
- Cover embryos with Tissue-Tek (Plano, cat# 4383)
- Align embryos in required position (ventral to the mold bottom) under the microscope
- Place molds on dry ice or into -80 °C freezer so that Tissue-tek hardens (about 20min)
- Detach blocks by pressing hard with the thumb against the mold bottom

- place blocks on holders
- place a holder in the cryostat and start to cut
- try to find the plane containing embryos by trimming 30-50µm sections
- cut embryos in 12µm sections
- transfer sections in a line to slide (super frost slides, Roth), 5-7 sections per line are optimal
- leave to dry at RT at least 1h

4.9.3 Antibody staining on cryosections

4.9.3.1 Standard antibody staining protocol

- Rehydrate cryosections in PBS with 0.1 % Tween-20 (PBST) for 1 hour
- Block for 1 hour with blocking solution (4 % normal goat serum in PBST).
- Incubate with desired primary antibody for several hours at RT or overnight at 4 ^{o}C
- Wash slides 3 times for 10 min in PBST
- Incubate for 2 hours with a fluorescently-labeled secondary antibody in blocking solution (1:400)
- Wash slides 3 times for 10 min in PBST
- Embed the slides in moviol and let dry before microscopy

The following antibodies were used in this thesis:

Anti- zpr1 - Developmental Studies Hybridoma Bank, 1:100

Anti-zpr3 - Developmental Studies Hybridoma Bank, 1:100

Anti-zn5 - Developmental Studies Hybridoma Bank, 1:50

Anti-parvalbumine – Chemicon (MAB1572), 1:200

Anti-GAD67 – Chemicon (AB5862P), 1:100

Anti-glutamine synthetase – BD Biosciences (cat# 610517), 1:500

Anti-PKCα – Santa Cruz Biotechnology (sc-208), 1:100

Anti-GFP (mouse) – Molecular Probes, Invitrogen (A11120), 1:200

Anti-GFP (rabbit) – Molecular Probes, Invitrogen (A11122), 1:200

Anti-BrdU (mouse) – Roche (cat# 1-299-964), 1:100

Anti-pH3-S10 (rabbit) – Abcam (ab5176-100), 1:400

Anti-Digoxigenin-Alkaline Phosphatase – Roche (cat# 11093274910), 1:2000

Anti-activeCaspase3 – BD Pharmingen (cat# 557035), 1:200

4.9.3.2 BrdU staining protocol

- Rehydrate cryosections in PBST for 1 hour
- Treat with 4N HCl for 20 min
- Wash slides 3 times for 5 min in PBST
- Block for 1 hour with blocking solution
- Incubate with the mouse anti-BrdU antibody diluted in blocking solution (1:100) (Roche, cat# 1 170 376) overnight
- Wash slides 3 times for 10 min in PBST
- Incubate for 2 hours with the anti-mouse Alexa Fluor 488 antibody (Invitrogen, cat# A11001) diluted in blocking solution (1:400)
- Wash slides 3 times for 10 min in PBST
- Embed the slides in moviol and let dry before microscopy

4.9.4 Apoptosis stainings

4.9.4.1 TUNEL assay on whole-mount embryos

Whole-mount TUNEL staining was performed as described in Berghmanns et al., (2005).

- Fix embryos overnight in 4% paraformaldehyde and dehydrated in PBS/methanol series; 50%, 70%, 95%, and 100% (5 minutes each at room temperature (RT))
- Embryos were incubated in 100% acetone at –20ºC (10 min) and rinsed three times in PBS containing 0.1% Tween-20 (PBST) (5 minutes each)
- Embryos were permeabilized by incubation in fresh 0.1% sodium citrate in PBST (15 minutes, RT), followed by three rinses in PBST (5 minutes each)
- Embryos were assayed by TUNEL by using the In Situ Cell Death Detection Kit, TMR Red (Roche).

4.9.4.2 TUNEL assay on cryosections

- Wash cryosections with PBST for 30 min
- Permeabilise by incubating slides for 2 min in ice-cold 0.1 % Sodium Citrate with 0.1 % Triton X-100
- Wash cryosections with PBST 2 times for 5 min
- Incubate with TUNEL reaction mix diluted twice with TUNEL dilution buffer (cat # 1966006001) for 1 hour
- Wash cryosections with PBST 2 times for 5 min

4.9.4.3 ApopTag *In Situ* Apoptosis Detection Kit

The protocol uses the ApopTag kit from Chemicon (cat# S7100).

- Fix embryos for 2 h at RT or overnight at 4 ^{o}C in 4 % PFA/PBST
- Wash in PBST and transfer to methanol for 30 min at -20 ^{o}C
- Rehydrate embryos in a graded methanol:PBST series (75 % MeOH, 50 % MeOH, 25 % MeOH) for 5 min each
- Wash once for 5 min in PBST (Washing volume is 0.5 ml)
- Digest embryos in proteinase K solution in PBST (10 /ul) at RT. 24 hpf embryos should be digested 2 minutes, embryos of all other stages should get 10 minutes for each additional day of development
- Rinse 2 times in PBST
- Postfix in PFA/PBST for 20 min at RT
- Wash 5 times for 5 min in PBST
- Postfix for 10 min at -20 ^{o}C with pre-chilled EtOH : acetic acid in ratio 2 : 1
- Wash 3 times for 5 min in PBST
- Remove very carefully all the liquid from embryos (use vacuum pump with 10 ul tip attached), add 37 ul of **Equilibration buffer** and incubate for 1 h at room temperature
- Remove very carefully the previous buffer. Add 25 ul of **Reaction buffer** and 8 ul of the **TdT enzyme**

- Incubate overnight at 37 ^{o}C
- Wash with 250 ul of **Stop/Wash Buffer** for 3 hours at 37 ^{o}C
- Wash 3 times for 5 min with PBST
- Block with 2 mg/ml BSA, 5 % goat serum in PBST for 1 h at RT
- Remove the liquid as before and add 500 ul of anti-Dig-AP Fab 1:2000 in blocking solution (Roche)
- Wash 4 times for 30 min in PBST
- Wash 3 times for 5 min with 50 % Staining Buffer and develop staining with NBT-BCIP solution (1:100) in 50 % Staining Buffer
- Wash with PBST and store in 4 % PFA/PBST at 4 ^{o}C

4.9.4.3 Acridine Orange apoptosis staining

Dechorionated embryos were incubated with 2 μg/ml of Acridine Orage (AO) in E3 embryo medium for 30 minutes. The traces of AO were removed by 5 changes of the embryo medium. Embryos were then imaged using a fluorescent microscope.

4.10 Chemical inhibitors and treatment procedures

FGF signaling inhibitor SU5402 (Calbiochem, cat # 572630) was dissolved in DMSO at 8 mM. Treatment was performed with a 10 μM solution of SU5402 or a corresponding control DMSO solution in E3 embryo medium. Cyclopamine (Toronto Research Chemicals, cat# C988400) was dissolved in ethanol at 20 mM. Treatment was performed with 100 μM solution of cyclopamine or control ethanol solution in E3 embryo medium. Roscovitine was purchased from Sigma (cat # R7772), resuspended in DMSO at 12.5 mM and used for treatments at 1:250 dilution in E3 medium.

4.11 Bead implantation

Bead implantation was performed as described before (Norton et al., 2005). Recombinant human Fgf4 protein (R&D Systems, cat# 235-F4-025) was dissolved at a concentration 250 ng/μl in PBS with 0.1% bovine serum albumin and mixed in proportion 1:1 with the mix of heparin-acrylamide beads (cat# H5263) filtered through a 70 μm Cell strainer (BD Falcon, cat# 352350).

4.12 Fluorescence Activated Cell Sorting methods methods

4.10.1 EGFP/Propidium Iodide cell cycle analysis protocol

The following protocol is suitable for quantifying cell cycle distribution of EGFP-positive cells. It was provided by Marcel Souren and modified on the basis of a published flow cytometry protocol (Schmid and Sakamoto, 2001), which allows imaging of both Propidium Iodide and EGFP.

- Decapitate 40-50 embryos for each condition
- Transfer to a very small petri dish and remove as much liquid as possible
- Add 3 ml of Trypsin solution (Sigma, cat# T3924)
- Either triturate using an extended Pasteur pipette or 1 ml tip (for the latter it is important to press the tip down to the bottom of the dish)
- Check for complete dissociation visually or under a microscope
- Add 4 ml of TM-1% PEG with 10 % goat serum
- Transfer the solution to a 15 ml Falcon tube
- Centrifuge for 5 min at 1200 g at 4 ^{o}C
- Remove supernatant with the vacuum pump and add 4 ml of TM-1% PEG with 10 % goat serum and centrifuge for 5 min at 1200 g at RT
- Remove supernatant and resuspend cells in 2 ml of cold PBS
- Put a cell strainer on a FACS tube and pipet cell suspension through it
- Add 2 ml µl of 2 % Paraformaldehyde in PBS and incubate for 1 hour at 4 ^{o}C
- Centrifuge for 5 min at 1200 g at 4 ^{o}C and wash once in 5 ml of PBS
- Add 1 ml of 70 % ethanol at -20 ^{o}C drop-wise while mixing the cell suspension on slow vortex regime and incubate overnight
- Centrifuge for 5 min at 1200 g at 4 ^{o}C and wash twice in 3 ml of PBS
- Resuspend in 1 ml of PI buffer

Materials

- TM-1% PEG: 100 mM NaCl, 5 mM KCl, 5 mM Hepes, 1 % (w/v) PEG 20000 pH 7.0
- PBS
- Normal goat serum

- PI buffer: 980 µl PBS + 10 µl propidium iodide + 10 µl RNAse A)

4.13 Confocal microscopy, image processing and analysis

Microscopy was performed using Leica SP2 confocal microscope, images were processed using ImageJ software. Additional image adjustments were made using Adobe Photoshop CS2 and panels of images assembled using Adobe illustrator CS2. For counting nuclei, Cell Counter plugin of ImageJ was employed.

5 PUBLICATIONS

Prykhozhij SV, Neumann CJ.
Distinct roles of Shh and Fgf signaling in regulating cell proliferation during zebrafish pectoral fin development.
BMC Dev Biol. 2008 Sep 23;8:91.

Fischer S, Prykhozhij S, Rau MJ, Neumann CJ.
Mutation of zebrafish caf-1b results in S phase arrest, defective differentiation, and p53-mediated apoptosis during organogenesis.
Cell Cycle. 2007 Dec 1;6(23):2962-9.

Vanoosthuyse V, Prykhozhij S, Hardwick KG.
Shugoshin 2 regulates localization of the chromosomal passenger proteins in fission yeast mitosis.
Mol Biol Cell. 2007 May;18(5):1657-69. Epub 2007 Feb 14.

6 REFERENCES

1. Y Abe, Oda-Sato, E., Tobiume, K., Kawauchi, K., Taya, Y., Okamoto, K., Oren, M., Tanaka, N.: **Hedgehog signaling overrides p53-mediated tumor suppression by activating Mdm2**. *Proc Natl Acad Sci USA* 2008, **105**:4838-4843.
2. M Agathocleous, Locker M, Harris WA, Perron M: **A general role of hedgehog in the regulation of proliferation.** *Cell Cycle* 2007 **6**:156-159.
3. SC Ahlgren, Bronner-Fraser M: **Inhibition of sonic hedgehog signaling in vivo results in craniofacial neural crest cell death.** *Curr Biol* 1999, **9**:1304-1314.
4. BL Allen, Tenzen T, McMahon AP: **The Hedgehog-binding proteins Gas1 and Cdo cooperate to positively regulate Shh signaling during mouse development.** *Genes Dev* 2007, **21**:1244-57.
5. A Baonza, M Freeman: **Control of cell proliferation in the Drosophila eye by Notch signaling**. *Dev Cell* 2005, **8**:529-39.
6. PA Beachy, Karhadkar SS, Berman DM: **Tissue repair and stem cell renewal in carcinogenesis.** *Nature* 2004, **432**:324-31.
7. K Beckett, Franch-Marro X, Vincent JP: **Glypican-mediated endocytosis of Hedgehog has opposite effects in flies and mice.** *Trends Cell Biol* 2008, **18**:360-3.
8. A Beham, Marin MC, Fernandez A, Herrmann J, Brisbay S, Tari AM, Lopez-Berestein G, Lozano G, Sarkiss M, McDonnell TJ: **Bcl-2 inhibits p53 nuclear import following DNA damage.** *Oncogene* 1997, **15**:2767-72.
9. S Berghmans, Murphey, R.D., Wienholds, E., Neuberg, D., Kutok, J.L., Fletcher, C.D., Morris, J.P., Liu, T.X., Schulte-Merker, S., Kanki, J.P., Plasterk, R., Zon, L.I., Look, A.T.: **tp53 mutant zebrafish develop malignant peripheral nerve sheath tumors**. *Proc Natl Acad Sci USA* 2005, **102**:407-412.
10. DM Berman, Karhadkar, S.S., Maitra, A., Montes De Oca, R., Gerstenblith, M.R., Briggs, K., Parker, A.R., Shimada, Y., Eshleman, J.R., Watkins, D.N., Beachy, P.A.: **Widespread requirement for Hedgehog ligand stimulation in growth of digestive tract tumours.** *Nature* 2003, **425**:846-851.
11. RL Bigelow, NS Chari, AB Unden, KB Spurgers, S Lee, DR Roop, R Toftgard, TJ McDonnell: **Transcriptional regulation of bcl-2 mediated by the sonic hedgehog signaling pathway through gli-1**. *J Biol Chem* 2004, **279**:1197-205.
12. J Bilotta, Saszik S: **The zebrafish as a model visual system.** *Int J Dev Neurosci* 2001, **19**:621-9.
13. AG Borycki, B Brunk, S Tajbakhsh, M Buckingham, C Chiang, CP Emerson, Jr.: **Sonic hedgehog controls epaxial muscle determination through Myf5 activation**. *Development* 1999, **126**:4053-63.
14. J Briscoe, Ericson J: **Specification of neuronal fates in the ventral neural tube.** *Curr Opin Neurobiol* 2001, **11**:43-9.
15. J Britto, D Tannahill, R Keynes: **A critical role for sonic hedgehog signaling in the early expansion of the developing brain**. *Nat Neurosci* 2002, **5**:103-10.
16. L Brown, Boswell S, Raj L, Lee SW: **Transcriptional targets of p53 that regulate cellular proliferation.** *Crit Rev Eukaryot Gene Expr* 2007, **17**:73-85.

17. J Brugarolas: **Radiation-induced cell cycle arrest compromised by p21 deficiency.** . *Nature* 1995, **377**:552-557.
18. JA Buglino, Resh MD: **Hhat is a palmitoylacyltransferase with specificity for N-palmitoylation of Sonic Hedgehog.** *J Biol Chem* 2008, **283**:22076-88.
19. TR Bürglin: **The Hedgehog protein family.** *Genome Biology* 2008, **9**:241.
20. R Burke, Basler, K.: **Dpp receptors are autonomously required for cell proliferation in the entire developing Drosophila wing**. *Development* 1996, **122**:2261-2269.
21. R Burke, Nellen D, Bellotto M, Hafen E, Senti KA, Dickson BJ, Basler K.: **Dispatched, a novel sterol-sensing domain protein dedicated to the release of cholesterol-modified hedgehog from signaling cells.** *Cell* 1999, **99**:803-815.
22. A Callejo, Torroja C, Quijada L, Guerrero I: **Hedgehog lipid modifications are required for Hedgehog stabilization in the extracellular matrix.** *Development* 2006, **133**:471-483.
23. J Capdevila, JC Izpisua Belmonte: **Patterning mechanisms controlling vertebrate limb development**. *Annu Rev Cell Dev Biol* 2001, **17**:87-132.
24. MI Capurro, Xu P, Shi W, Li F, Jia A, Filmus J: **Glypican-3 inhibits Hedgehog signaling during development by competing with patched for Hedgehog binding.** *Dev Cell* 2008, **14**:700-711.
25. J Cayuso, Ulloa F, Cox B, Briscoe J, Martí E: **The Sonic hedgehog pathway independently controls the patterning, proliferation and survival of neuroepithelial cells by regulating Gli activity.** *Development* 2006, **133**:517-528.
26. Z Chamoun, Mann RK, Nellen D, von Kessler DP, Bellotto M, Beachy PA, Basler K: **Skinny hedgehog, an acyltransferase required for palmitoylation and activity of the hedgehog signal.** *Science* 2001, **293**:2080-2084.
27. DT Chang, López, A., von Kessler, D.P., Chiang, C., Simandl, B.K., Zhao, R., Seldin, M.F., Fallon, J.F., Beachy, P.A.: **Products, genetic linkage and limb patterning activity of a murine hedgehog gene**. *Development* 1994, **120**:3339-3353.
28. MV Chao: **Dependence receptors: what is the mechanism?** *Sci STKE* 2003, **2003**:PE38.
29. JB Charrier, Lapointe F, Le Douarin NM, Teillet MA: **Anti-apoptotic role of Sonic hedgehog protein at the early stages of nervous system organogenesis.** *Development* 2001, **128**:4011-4020.
30. J Chen, H Ruan, SM Ng, C Gao, HM Soo, W Wu, Z Zhang, Z Wen, DP Lane, J Peng: **Loss of function of def selectively up-regulates Delta113p53 expression to arrest expansion growth of digestive organs in zebrafish**. *Genes Dev* 2005, **19**:2900-11.
31. JK Chen, J Taipale, MK Cooper, PA Beachy: **Inhibition of Hedgehog signaling by direct binding of cyclopamine to Smoothened**. *Genes Dev* 2002, **16**:2743-8.
32. MH Chen, Li YJ, Kawakami T, Xu SM, Chuang PT: **Palmitoylation is required for the production of a soluble multimeric Hedgehog protein complex and long-range signaling in vertebrates.** *Genes Dev* 2004, **18**:641-659.

33. W Chen, Ren XR, Nelson CD, Barak LS, Chen JK, Beachy PA, de Sauvage F, Lefkowitz RJ: **Activity-dependent internalization of smoothened mediated by beta-arrestin 2 and GRK2.** *Science* 2004, **306**:2257-60.
34. Y Chen, Struhl G: **Dual roles for patched in sequestering and transducing Hedgehog.** *Cell* 1996, **87**:553-63.
35. JE Chipuk, Green DR: **How do BCL-2 proteins induce mitochondrial outer membrane permeabilization?** *Trends Cell Biol* 2008, **18**:157-64.
36. V Clement, Sanchez P, de Tribolet N, Radovanovic I, Ruiz i Altaba A: **HEDGEHOG-GLI1 signaling regulates human glioma growth, cancer stem cell self-renewal, and tumorigenicity.** *Curr Biol* 2007, **17**:165-72.
37. LK Cole, Ross LS: **Apoptosis in the developing zebrafish embryo.** *Dev Biol* 2001, **240**:123-42.
38. JP Concordet, Lewis, K.E., Moore, J.W., Goodrich, L.V., Johnson, R.L., Scott, M.P., Ingham, P.W.: **Spatial regulation of a zebrafish patched homologue reflects the roles of sonic hedgehog and protein kinase A in neural tube and somite patterning.** *Development* 1996, **122**:2835-2846.
39. N Dahmane, Ruiz i Altaba A: **Sonic hedgehog regulates the growth and patterning of the cerebellum.** *Development* 1999, **126**:3089-100.
40. N Dahmane, Sánchez P, Gitton Y, Palma V, Sun T, Beyna M, Weiner H, Ruiz i Altaba A: **The Sonic Hedgehog-Gli pathway regulates dorsal brain growth and tumorigenesis.** *Development* 2001, **128**:5201-12.
41. C Dierks, J Grbic, K Zirlik, R Beigi, NP Englund, GR Guo, H Veelken, M Engelhardt, R Mertelsmann, JF Kelleher, et al: **Essential role of stromally induced hedgehog signaling in B-cell malignancies**. *Nat Med* 2007, **13**:944-51.
42. AT Dudley, Ros, M.A., Tabin, C.J.: **A re-examination of proximodistal patterning during vertebrate limb development**. *Nature* 2002, **418**:539-544.
43. M Duman-Scheel, Weng, L., Xin, S., Du, W.: **Hedgehog regulates cell growth and proliferation by inducing Cyclin D and Cyclin E.** *Nature* 2002 **417**:299-304.
44. JK Eberhart, Swartz ME, Crump JG, Kimmel CB: **Early Hedgehog signaling from neural to oral epithelium organizes anterior craniofacial development.** *Development* 2006, **133**:1069-1077.
45. SC Ekker, Ungar AR, Greenstein P, von Kessler DP, Porter JA, Moon RT, Beachy PA: **Patterning activities of vertebrate hedgehog proteins in the developing eye and brain.** *Curr Biol* 1995, **5**:944-955.
46. M Evangelista, Lim TY, Lee J, Parker L, Ashique A, Peterson AS, Ye W, Davis DP, de Sauvage FJ: **Kinome siRNA screen identifies regulators of ciliogenesis and hedgehog signal transduction.** *Sci Signal* 2008, **1**:ra7.
47. JF Fallon, López, A., Ros, M.A., Savage, M.P., Olwin, B.B., Simandl, B.K.: **FGF-2: apical ectodermal ridge growth signal for chick limb development**. *Science* 1994, **264**:104-107.
48. H Fan, PA Khavari: **Sonic hedgehog opposes epithelial cell cycle arrest**. *J Cell Biol* 1999, **147**:71-6.

49. B Feldman, Poueymirou, W., Papaioannou, V.E., DeChiara, T.M., Goldfarb, M.: **Requirement of FGF-4 for postimplantation mouse development.** *Science* 1995, **267**:246-249.
50. J Filmus, Capurro M, Rast J.: **Glypicans.** *Genome Biol* 2008, **9**:224.
51. LC Firth, NE Baker: **Extracellular signals responsible for spatially regulated proliferation in the differentiating Drosophila eye**. *Dev Cell* 2005, **8**:541-51.
52. S Fischer, Prykhozhij S, Rau MJ, Neumann CJ.: **Mutation of zebrafish caf-1b results in S phase arrest, defective differentiation, and p53-mediated apoptosis during organogenesis.** *Cell Cycle* 2007, **6**:2962-2969.
53. A Fortin, Cregan SP, MacLaurin JG, Kushwaha N, Hickman ES, Thompson CS, Hakim A, Albert PR, Cecconi F, Helin K, Park DS, Slack RS: **APAF1 is a key transcriptional target for p53 in the regulation of neuronal cell death.** *J Cell Biol* 2001, **155**:207-16.
54. BA Froesch, Aimé-Sempé C, Leber B, Andrews D, Reed JC: **Inhibition of p53 transcriptional activity by Bcl-2 requires its membrane-anchoring domain.** *J Biol Chem* 1999, **274**:6469-75.
55. S Georgia, R Soliz, M Li, P Zhang, A Bhushan: **p57 and Hes1 coordinate cell cycle exit with self-renewal of pancreatic progenitors**. *Dev Biol* 2006, **298**:22-31.
56. M Gering, Patient R: **Hedgehog signaling is required for adult blood stem cell formation in zebrafish embryos.** *Dev Cell* 2005, **8**:389-400.
57. PS Gill, Rosenblum, N.D.: **Control of murine kidney development by sonic hedgehog and its GLI effectors**. *Cell Cycle* 2006, **5**:1426-1430.
58. B Glise, Miller CA, Crozatier M, Halbisen MA, Wise S, Olson DJ, Vincent A, Blair SS: **Shifted, the Drosophila ortholog of Wnt inhibitory factor-1, controls the distribution and movement of Hedgehog.** *Dev Cell* 2005, **8**:255-66.
59. N Gorfinkiel, Sierra J, Callejo A, Ibañez C, Guerrero I: **The Drosophila ortholog of the human Wnt inhibitor factor Shifted controls the diffusion of lipid-modified Hedgehog.** *Dev Cell* 2005, **8**:241-53.
60. I Guerrero, Ruiz i Altaba, A.: **Longing for Ligand: Hedgehog, Patched, and Cell Death**. *Science* 2003, **301**:774-776.
61. I Guerrero, Chiang C: **A conserved mechanism of Hedgehog gradient formation by lipid modifications.** *Trends Cell Biol* 2007, **17**:1-5.
62. L He, He X, Lowe SW, Hannon GJ: **microRNAs join the p53 network--another piece in the tumour-suppression puzzle.** *Nat Rev Cancer* 2007, **7**:819-22.
63. MJ Hendzel, Wei Y, Mancini MA, Van Hooser A, Ranalli T, Brinkley BR, Bazett-Jones DP, Allis CD: **Mitosis-specific phosphorylation of histone H3 initiates primarily within pericentromeric heterochromatin during G2 and spreads in an ordered fashion coincident with mitotic chromosome condensation.** *Chromosoma* 1997, **106**:348-60.
64. M Hu, Easter SS: **Retinal neurogenesis: the formation of the initial central patch of postmitotic cells.** *Dev Biol* 1999, **207**:309-21.

65. JP Incardona, Gaffield, W., Kapur, R. P., Roelink, H. : **The teratogenic Veratrum alkaloid cyclopamine inhibits Sonic hedgehog signal transduction**. *Development* 1998, **125**:3553-3562.
66. JP Incardona, Lee JH, Robertson CP, Enga K, Kapur RP, Roelink H: **Receptor-mediated endocytosis of soluble and membrane-tethered Sonic hedgehog by Patched-1.** *Proc Natl Acad Sci U S A* 2000, **97**:12044-9.
67. PW Ingham, Kim HR: **Hedgehog signalling and the specification of muscle cell identity in the zebrafish embryo.** *Exp Cell Res* 2005, **306**:336-42.
68. PW Ingham, AP McMahon: **Hedgehog signaling in animal development: paradigms and principles**. *Genes Dev* 2001, **15**:3059-87.
69. J Jeong, J Mao, T Tenzen, AH Kottmann, AP McMahon: **Hedgehog signaling in the neural crest cells regulates the patterning and growth of facial primordia**. *Genes Dev* 2004, **18**:937-51.
70. J Jia, M Lin, L Zhang, JP York, P Zhang: **The Notch signaling pathway controls the size of the ocular lens by directly suppressing p57Kip2 expression**. *Mol Cell Biol* 2007, **27**:7236-47.
71. J Jiang: **Regulation of Hh/Gli signaling by dual ubiquitin pathways.** *Cell Cycle* 2006, **21**:2457-63.
72. J Jiang, Hui CC: **Hedgehog signaling in development and cancer.** *Dev Cell* 2008, **15**:801-812.
73. RG Jones, Plas DR, Kubek S, Buzzai M, Mu J, Xu Y, Birnbaum MJ, Thompson CB: **AMP-activated protein kinase induces a p53-dependent metabolic checkpoint.** *Mol Cell Biol* 2005, **18**:283-93.
74. T Jowett: **Double in situ hybridization techniques in zebrafish**. *Methods* 2001, **23**:345-358.
75. VL Katanaev, GP Solis, G Hausmann, S Buestorf, N Katanayeva, Y Schrock, CA Stuermer, K Basler: **Reggie-1/flotillin-2 promotes secretion of the long-range signalling forms of Wingless and Hedgehog in Drosophila**. *EMBO J* 2008, **27**:509-21.
76. Y Katoh, M Katoh: **Integrative genomic analyses on GLI2: mechanism of Hedgehog priming through basal GLI2 expression, and interaction map of stem cell signaling network with P53**. *Int J Oncol* 2008, **33**:881-6.
77. T Kawakami, Kawcak T, Li YJ, Zhang W, Hu Y, Chuang PT.: **Mouse dispatched mutants fail to distribute hedgehog proteins and are defective in hedgehog signaling.** *Development* 2002, **129**:5753-5765.
78. AM Kenney, DH Rowitch: **Sonic hedgehog promotes G(1) cyclin expression and sustained cell cycle progression in mammalian neuronal precursors**. *Mol Cell Biol* 2000, **20**:9055-67.
79. S Kern, Pietenpol J, Thiagalingam S, Seymour A, Kinzler K, Vogelstein B.: **Oncogenic forms of p53 inhibit p53 regulated gene expression.** *Science* 1992, **256**:827-830.
80. FO Kok, E Oster, L Mentzer, JC Hsieh, CA Henry, HI Sirotkin: **The role of the SPT6 chromatin remodeling factor in zebrafish embryogenesis**. *Dev Biol* 2007, **307**:214-26.
81. MJ Koudijs, den Broeder, M.J., Keijser, A., Wienholds, E., Houwing, S., van Rooijen, E.M., Geisler, R., van Eeden, F.J.: **The zebrafish mutants dre, uki,**

and lep encode negative regulators of the hedgehog signaling pathway. *PLoS Genetics* 2005, **1**.

82. A Kramer, Liashkovich I, Oberleithner H, Ludwig S, Mazur I, Shahin V: **Apoptosis leads to a degradation of vital components of active nuclear transport and a dissociation of the nuclear lamina.** *Proc Natl Acad Sci U S A* 2008, **105**:11236-41.
83. E Kratz, PM Eimon, K Mukhyala, H Stern, J Zha, A Strasser, R Hart, A Ashkenazi: **Functional characterization of the Bcl-2 gene family in the zebrafish**. *Cell Death Differ* 2006, **13**:1631-40.
84. KM Kwan, Fujimoto E, Grabher C, Mangum BD, Hardy ME, Campbell DS, Parant JM, Yost HJ, Kanki JP, Chien CB.: **The Tol2kit: a multisite gateway-based construction kit for Tol2 transposon transgenesis constructs.** *Dev Dyn* 2007, **236**:3088-3099.
85. DM Langenau, C Jette, S Berghmans, T Palomero, JP Kanki, JL Kutok, AT Look: **Suppression of apoptosis by bcl-2 overexpression in lymphoid cells of transgenic zebrafish**. *Blood* 2005, **105**:3278-85.
86. U Langheinrich, E Hennen, G Stott, G Vacun: **Zebrafish as a model organism for the identification and characterization of drugs and genes affecting p53 signaling**. *Curr Biol* 2002, **12**:2023-8.
87. E Laufer, Nelson, C.E., Johnson, R.L., Morgan, B.A., Tabin, C.: **Sonic hedgehog and Fgf-4 act through a signaling cascade and feedback loop to integrate growth and patterning of the developing limb bud.** *Cell* 1994, **79**:993-1003.
88. JD Lee, Kraus P, Gaiano N, Nery S, Kohtz J, Fishell G, Loomis CA, Treisman JE: **An acylatable residue of Hedgehog is differentially required in Drosophila and mouse limb development.** *Dev Biol* 2001, **233**:122-36.
89. KC Lee, Goh WL, Xu M, Kua N, Lunny D, Wong JS, Coomber D, Vojtesek B, Lane EB, Lane DP.: **Detection of the p53 response in zebrafish embryos using new monoclonal antibodies.** *Oncogene* 2008, **27**:629-640.
90. Y Lee, Kawagoe R, Sasai K, Li Y, Russell HR, Curran T, McKinnon PJ: **Loss of suppressor-of-fused function promotes tumorigenesis.** *Oncogene* 2007, **26**:6442-7.
91. MA Lefers, Wang QT, Holmgren RA: **Genetic dissection of the Drosophila Cubitus interruptus signaling complex.** *Dev Biol* 2001, **236**:411-20.
92. K Lefort, A Mandinova, P Ostano, V Kolev, V Calpini, I Kolfschoten, V Devgan, J Lieb, W Raffoul, D Hohl, et al: **Notch1 is a p53 target gene involved in human keratinocyte tumor suppression through negative regulation of ROCK1/2 and MRCKalpha kinases**. *Genes Dev* 2007, **21**:562-77.
93. T Lin, C Chao, S Saito, SJ Mazur, ME Murphy, E Appella, Y Xu: **p53 induces differentiation of mouse embryonic stem cells by suppressing Nanog expression**. *Nat Cell Biol* 2005, **7**:165-71.
94. X Lin: **Functions of heparan sulfate proteoglycans in cell signaling during development.** *Development* 2004, **131**:6009-6021.
95. RK Lindemann: **Stroma-initiated hedgehog signaling takes center stage in B-cell lymphoma**. *Cancer Res* 2008, **68**:961-4.

96. FJ Livesey, Cepko CL: **Vertebrate neural cell-fate determination: lessons from the retina.** *Nat Rev Neurosci* 2001, **2**:109-18.
97. M Locker, M Agathocleous, MA Amato, K Parain, WA Harris, M Perron: **Hedgehog signaling and the retina: insights into the mechanisms controlling the proliferative properties of neural precursors**. *Genes Dev* 2006, **20**:3036-48.
98. F Long, Zhang, X.M., Karp, S., Yang, Y., McMahon, A.P.: **Genetic manipulation of hedgehog signaling in the endochondral skeleton reveals a direct role in the regulation of chondrocyte proliferation**. *Development* 2001, **128**:5099-5108.
99. A Lopez-Martinez, DT Chang, C Chiang, JA Porter, MA Ros, BK Simandl, PA Beachy, JF Fallon: **Limb-patterning activity and restricted posterior localization of the amino-terminal product of Sonic hedgehog cleavage**. *Curr Biol* 1995, **5**:791-6.
100. SW Lowe, Cepero E, Evan G: **Intrinsic tumour suppression.** *Nature* 2004, **432**:307-15.
101. L Lum, Beachy, P.A.: **The Hedgehog Response Network: Sensors, Switches, and Routers**. *Science* 2004, **304**:1755-1759.
102. Y Ma, Erkner A, Gong R, Yao S, Taipale J, Basler K, Beachy PA.: **Hedgehog-mediated patterning of the mammalian embryo requires transporter-like function of dispatched.** *Cell* 2002, **111**:63-75.
103. R Macdonald, Barth KA, Xu Q, Holder N, Mikkola I, Wilson SW: **Midline signalling is required for Pax gene regulation and patterning of the eyes.** *Development* 1995, **121**:3267-3278.
104. R Machold, Hayashi S, Rutlin M, Muzumdar MD, Nery S, Corbin JG, Gritli-Linde A, Dellovade T, Porter JA, Rubin LL, Dudek H, McMahon AP, Fishell G: **Sonic hedgehog is required for progenitor cell maintenance in telencephalic stem cell niches.** *Neuron* 2003, **39**:937-50.
105. L Mandal, Martinez-Agosto JA, Evans CJ, Hartenstein V, Banerjee U: **A Hedgehog- and Antennapedia-dependent niche maintains Drosophila haematopoietic precursors.** *Nature* 2007, **446**:320-4.
106. JC Marine, Jochemsen, AG.: **Mdmx and Mdm2 Brothers in arms?** *Cell Cycle* 2004, **3**:900-904.
107. GR Martin: **The roles of FGFs in the early development of vertebrate limbs**. *Genes Dev* 1998, **12**:1571-86.
108. C Martín-Castellanos, Edgar, B.A.: **A characterization of the effects of Dpp signaling on cell growth and proliferation in the Drosophila wing**. *Development* 2002, **129**:1003-1013.
109. JR Martinez-Morales, Del Bene F, Nica G, Hammerschmidt M, Bovolenta P, Wittbrodt J: **Differentiation of the vertebrate retina is coordinated by an FGF signaling center.** *Dev Cell* 2005, **8**:565-74.
110. I Masai, Stemple DL, Okamoto H, Wilson SW: **Midline signals regulate retinal neurogenesis in zebrafish.** *Neuron* 2000, **27**:251-63.
111. I Masai, Yamaguchi M, Tonou-Fujimori N, Komori A, Okamoto H: **The hedgehog-PKA pathway regulates two distinct steps of the differentiation**

of retinal ganglion cells: the cell-cycle exit of retinoblasts and their neuronal maturation. *Development* 2005, **132**:1539-53.
112. S Matoba, Kang JG, Patino WD, Wragg A, Boehm M, Gavrilova O, Hurley PJ, Bunz F, Hwang PM: **p53 regulates mitochondrial respiration.** *Science* 2006, **312**:1650-3.
113. ND Meeker, Hutchinson SA, Ho L, Trede NS: **Method for isolation of PCR-ready genomic DNA from zebrafish tissues.** *Biotechniques* 2007, **43**:610-14.
114. AR Meloni, Fralish GB, Kelly P, Salahpour A, Chen JK, Wechsler-Reya RJ, Lefkowitz RJ, Caron MG: **Smoothened signal transduction is promoted by G protein-coupled receptor kinase 2.** *Mol Cell Biol* 2006, **26**:7550-60.
115. E Michalak, A Villunger, M Erlacher, A Strasser: **Death squads enlisted by the tumour suppressor p53**. *Biochem Biophys Res Commun* 2005, **331**:786-98.
116. M Mohammadi, McMahon, G., Sun, L., Tang, C., Hirth, P., Yeh, B.K., Hubbard, S.R., Schlessinger, J.: **Structures of the tyrosine kinase domain of fibroblast growth factor receptor in complex with inhibitors** *Science* 1997, **276**:955-960.
117. E Moroni, P Dell'Era, M Rusnati, M Presta: **Fibroblast growth factors and their receptors in hematopoiesis and hematological tumors**. *J Hematother Stem Cell Res* 2002, **11**:19-32.
118. A Moshiri, Reh TA: **Persistent progenitors at the retinal margin of ptc+/- mice.** *J Neurosci* 2004, **24**:229-37.
119. A Moshiri, McGuire CR, Reh TA: **Sonic hedgehog regulates proliferation of the retinal ciliary marginal zone in posthatch chicks.** *Dev Dyn* 2005, **233**:66-75.
120. F Murray-Zmijewski, Slee EA, Lu X: **A complex barcode underlies the heterogeneous response of p53 to stress.** *Nat Rev Mol Cell Biol* 2008, **9**:702-12.
121. K Nakano, KH Vousden: **PUMA, a novel proapoptotic gene, is induced by p53**. *Mol Cell* 2001, **7**:683-94.
122. A Nasevicius, Ekker SC: **Effective targeted gene 'knockdown' in zebrafish.** *Nat Genet* 2000, **26**:216-20.
123. CJ Neumann, Grandel, H., Gaffield, W., Schulte-Merker, S., Nüsslein-Volhard, C.: **Transient establishment of anteroposterior polarity in the zebrafish pectoral fin bud in the absence of sonic hedgehog activity**. *Development* 1999, **126**:4817 - 4826.
124. CJ Neumann, Nuesslein-Volhard C: **Patterning of the zebrafish retina by a wave of sonic hedgehog activity.** *Science* 2000, **289**:2137-9.
125. CJ Neumann: **Hedgehogs as negative regulators of the cell cycle**. *Cell Cycle* 2005, **4**:1139-1140.
126. L Niswander, Tickle, C., Vogel, A., Booth, I., Martin, G.R.: **FGF-4 replaces the apical ectodermal ridge and directs outgrowth and patterning of the limb**. *Cell* 1993, **75**:579-587.
127. L Niswander, Jeffrey, S., Martin, G.R., Tickle, C.: **A positive feedback loop coordinates growth and patterning in the vertebrate limb**. *Nature* 1994 **371**:609-612.

128. L Niswander: **Interplay between the molecular signals that control vertebrate limb development**. *Int J Dev Biol* 2002, **46**:877-81.
129. WH Norton, Ledin, J., Grandel, H., Neumann, C.J.: **HSPG synthesis by zebrafish Ext2 and Extl3 is required for Fgf10 signalling during limb development**. *Development* 2005, **132**:4963-4973.
130. C Nüsslein-Volhard, Wieschaus E: **Mutations affecting segment number and polarity in Drosophila.** . *Nature* 1980, **287**:795-801.
131. E Oda, Ohki R, Murasawa H, Nemoto J, Shibue T, Yamashita T, Tokino T, Taniguchi T, Tanaka N: **Noxa, a BH3-only member of the bcl-2 family and candidate mediator of p53-induced apoptosis.** . *Science* 2000, **288**:1053-1058.
132. N Ohbayashi, M Shibayama, Y Kurotaki, M Imanishi, T Fujimori, N Itoh, S Takada: **FGF18 is required for normal cell proliferation and differentiation during osteogenesis and chondrogenesis**. *Genes Dev* 2002, **16**:870-9.
133. H Ohgaki, Kleihues P: **Genetic pathways to primary and secondary glioblastoma.** *Am J Pathol* 2007, **170**:1445-53.
134. JT Ohlmeyer, Kalderon D: **Hedgehog stimulates maturation of Cubitus interruptus into a labile transcriptional activator.** *Nature* 1998, **396**:749-53.
135. K Ohtani: **Implication of transcription factor E2F in regulation of DNA replication**. *Front Biosci* 1999, **4**:D793-804.
136. S Okamura, H Arakawa, T Tanaka, H Nakanishi, CC Ng, Y Taya, M Monden, Y Nakamura: **p53DINP1, a p53-inducible gene, regulates p53-dependent apoptosis**. *Mol Cell* 2001, **8**:85-94.
137. TG Oliver, LL Grasfeder, AL Carroll, C Kaiser, CL Gillingham, SM Lin, R Wickramasinghe, MP Scott, RJ Wechsler-Reya: **Transcriptional profiling of the Sonic hedgehog response: a critical role for N-myc in proliferation of neuronal precursors**. *Proc Natl Acad Sci U S A* 2003, **100**:7331-6.
138. V Palma, Ruiz i Altaba A: **Hedgehog-GLI signaling regulates the behavior of cells with stem cell properties in the developing neocortex.** *Development* 2004, **131**:337-45.
139. V Palma, Lim DA, Dahmane N, Sánchez P, Brionne TC, Herzberg CD, Gitton Y, Carleton A, Alvarez-Buylla A, Ruiz i Altaba A: **Sonic hedgehog controls stem cell behavior in the postnatal and adult brain.** *Development* 2005, **132**:335-44.
140. Y Pan, Wang C, Wang B: **Phosphorylation of Gli2 by protein kinase A is required for Gli2 processing and degradation and the Sonic Hedgehog-regulated mouse development.** *Dev Biol* 2009, **326**:177-89.
141. D Panáková, Sprong H, Marois E, Thiele C, Eaton S: **Lipoprotein particles are required for Hedgehog and Wingless signalling.** *Nature* 2005, **435**:58-65.
142. HC Park, J Boyce, J Shin, B Appel: **Oligodendrocyte specification in zebrafish requires notch-regulated cyclin-dependent kinase inhibitor function**. *J Neurosci* 2005, **25**:6836-44.
143. J Partanen: **FGF signalling pathways in development of the midbrain and anterior hindbrain**. *J Neurochem* 2007, **101**:1185-93.

144. N Plaster, C Sonntag, CE Busse, M Hammerschmidt: **p53 deficiency rescues apoptosis and differentiation of multiple cell types in zebrafish flathead mutants deficient for zygotic DNA polymerase delta1**. *Cell Death Differ* 2006, **13**:223-35.
145. CJ Powers, SW McLeskey, A Wellstein: **Fibroblast growth factors, their receptors and signaling**. *Endocr Relat Cancer* 2000, **7**:165-97.
146. S Provot, Schipani E: **Molecular mechanisms of endochondral bone development.** *Biochem Biophys Res Commun* 2005, **328**:658-65.
147. S Prykhozhij, Neumann CJ: **Distinct roles of Shh and Fgf signaling in regulating cell proliferation during zebrafish pectoral fin development**. *BMC Dev Biol* 2008.
148. UJ Pyati, Look AT, Hammerschmidt M: **Zebrafish as a powerful vertebrate model system for in vivo studies of cell death.** *Semin Cancer Biol* 2007, **17**:154-165.
149. H Qin, T Yu, T Qing, Y Liu, Y Zhao, J Cai, J Li, Z Song, X Qu, P Zhou, et al: **Regulation of apoptosis and differentiation by p53 in human embryonic stem cells**. *J Biol Chem* 2007, **282**:5842-52.
150. J Reifenberger, Wolter M, Knobbe CB, Köhler B, Schönicke A, Scharwächter C, Kumar K, Blaschke B, Ruzicka T, Reifenberger G: **Somatic mutations in the PTCH, SMOH, SUFUH and TP53 genes in sporadic basal cell carcinomas.** *Br J Dermatol* 2005, **152**:43-51.
151. O Riccio, ME van Gijn, AC Bezdek, L Pellegrinet, JH van Es, U Zimber-Strobl, LJ Strobl, T Honjo, H Clevers, F Radtke: **Loss of intestinal crypt progenitor cells owing to inactivation of both Notch1 and Notch2 is accompanied by derepression of CDK inhibitors p27Kip1 and p57Kip2**. *EMBO Rep* 2008, **9**:377-83.
152. RD Riddle, Johnson, R.L., Laufer, E., Tabin, C.: **Sonic hedgehog mediates the polarizing activity of the ZPA**. *Cell* 1993, **75**:1401-1416.
153. T Riley, Sontag E, Chen P, Levine A: **Transcriptional control of human p53-regulated genes.** *Nat Rev Mol Cell Biol* 2008, **9**:402-12.
154. ML Robinson: **An essential role for FGF receptor signaling in lens development**. *Semin Cell Dev Biol* 2006, **17**:726-40.
155. ME Robu, JD Larson, A Nasevicius, S Beiraghi, C Brenner, SA Farber, SC Ekker: **p53 activation by knockdown technologies**. *PLoS Genet* 2007, **3**:e78.
156. H Roehl, C Nusslein-Volhard: **Zebrafish pea3 and erm are general targets of FGF8 signaling**. *Curr Biol* 2001, **11**:503-7.
157. H Roelink, JA Porter, C Chiang, Y Tanabe, DT Chang, PA Beachy, TM Jessell: **Floor plate and motor neuron induction by different concentrations of the amino-terminal cleavage product of sonic hedgehog autoproteolysis**. *Cell* 1995, **81**:445-55.
158. R Rohatgi, Scott MP: **Patching the gaps in Hedgehog signalling.** *Nat Cell Biol* 2007, **9**:1005-9.
159. S Roy, PW Ingham: **Hedgehogs tryst with the cell cycle**. *J Cell Sci* 2002, **115**:4393-7.

160. LL Rubin, de Sauvage FJ: **Targeting the Hedgehog pathway in cancer.** *Nat Rev Drug Discov* 2006, **5**:1026-33.
161. A Ruiz i Altaba, , Nguyên V, Palma V: **The emergent design of the neural tube: prepattern, SHH morphogen and GLI code.** *Curr Opin Genet Dev* 2003, **13**:513-21.
162. A Ruiz i Altaba, Mas C, Stecca B: **The Gli code: an information nexus regulating cell fate, stemness and cancer.** *Trends Cell Biol* 2007, **17**:438-47.
163. A Ruiz i Altaba, P Sanchez, N Dahmane: **Gli and hedgehog in cancer: tumours, embryos and stem cells**. *Nat Rev Cancer* 2002, **2**:361-72.
164. JJ Ryan, Prochownik E, Gottlieb CA, Apel IJ, Merino R, Nuñez G, Clarke MF: **c-myc and bcl-2 modulate p53 function by altering p53 subcellular trafficking during the cell cycle.** *Proc Natl Acad Sci U S A* 1994, **91**:5878-82.
165. S Ryu, Driever, W.: **Minichromosome maintenance proteins as markers for proliferation zones during embryogenesis.** *Cell Cycle* 2006, **5**:1140-1142.
166. JW Saunders, Jr., MT Gasseling: **Trans-filter propagation of apical ectoderm maintenance factor in the chick embrvo wing bud**. *Dev Biol* 1963, **7**:64-78.
167. JK Sax, P Fei, ME Murphy, E Bernhard, SJ Korsmeyer, WS El-Deiry: **BID regulation by p53 contributes to chemosensitivity**. *Nat Cell Biol* 2002, **4**:842-9.
168. HE Schauerte, van Eeden FJ, Fricke C, Odenthal J, Strähle U, Haffter P: **Sonic hedgehog is not required for the induction of medial floor plate cells in the zebrafish**. *Development* 1998, **125**:2983-2993.
169. I Schmid, KM Sakamoto: **Analysis of DNA content and green fluorescent protein expression**. *Curr Protoc Cytom* 2001, **Chapter 7**:Unit 7 16.
170. P Secchiero, E Melloni, MG di Iasio, M Tiribelli, E Rimondi, F Corallini, V Gattei, G Zauli: **Nutlin-3 upregulates the expression of Notch1 in both myeloid and lymphoid leukemic cells, as part of a negative feed-back anti-apoptotic mechanism**. *Blood* 2009.
171. M Selvakumaran, Lin HK, Miyashita T, Wang HG, Krajewski S, Reed JC, Hoffman B, Liebermann D: **Immediate early up-regulation of bax expression by p53 but not TGF beta 1: a paradigm for distinct apoptotic pathways.** *Oncogene* 1994, **9**:1791-8.
172. JL Shepard, HM Stern, KL Pfaff, JF Amatruda: **Analysis of the cell cycle in zebrafish embryos**. *Methods Cell Biol* 2004, **76**:109-25.
173. A Shkumatava, Fischer S, Müller F, Strahle U, Neumann CJ.: **Sonic hedgehog, secreted by amacrine cells, acts as a short-range signal to direct differentiation and lamination in the zebrafish retina.** *Development* 2004, **131**:3849-3858.
174. A Shkumatava, CJ Neumann: **Shh directs cell-cycle exit by activating p57Kip2 in the zebrafish retina**. *EMBO Rep* 2005, **6**:563-9.
175. JA Stadler, Shkumatava A, Neumann CJ: **The role of hedgehog signaling in the development of the zebrafish visual system.** *Dev Neurosci* 2004, **26**:346-51.
176. B Stecca, A Ruiz i Altaba: **A GLI1-p53 inhibitory loop controls neural stem cell and tumour cell numbers**. *EMBO J* 2009, **28**:663-76.

177. DL Stenkamp, Frey RA, Mallory DE, Shupe EE.: **Embryonic retinal gene expression in sonic-you mutant zebrafish.** *Dev Dyn* 2002, **225**:344-50.
178. DL Stenkamp, Frey RA: **Extraretinal and retinal hedgehog signaling sequentially regulate retinal differentiation in zebrafish.** *Dev Biol* 2003, **258**:349-63.
179. DL Stenkamp: **Neurogenesis in the fish retina.** *Int Rev Cytol* 2007, **259**:173-224.
180. X Sun, Mariani, F.V., Martin, G.R. : **Functions of FGF signalling from the apical ectodermal ridge in limb development.** *Nature* 2002, **418**:501-508.
181. J Svärd, Heby-Henricson K, Persson-Lek M, Rozell B, Lauth M, Bergström A, Ericson J, Toftgård R, Teglund S.: **Genetic elimination of Suppressor of fused reveals an essential repressor function in the mammalian Hedgehog signaling pathway.** *Dev Cell* 2006, **10**:187-197.
182. T Tabata, S Eaton, TB Kornberg: **The Drosophila hedgehog gene is expressed specifically in posterior compartment cells and is a target of engrailed regulation**. *Genes Dev* 1992, **6**:2635-45.
183. MD Taylor, L Liu, C Raffel, CC Hui, TG Mainprize, X Zhang, R Agatep, S Chiappa, L Gao, A Lowrance, et al: **Mutations in SUFU predispose to medulloblastoma**. *Nat Genet* 2002, **31**:306-10.
184. T Tenzen, Allen BL, Cole F, Kang JS, Krauss RS, McMahon AP: **The cell surface membrane proteins Cdo and Boc are components and targets of the Hedgehog signaling pathway and feedback network in mice.** *Dev Cell* 2006, **10**:647-56.
185. SP Thayer, di Magliano, M.P., Heiser, P.W., Nielsen, C.M., Roberts, D.J., Lauwers, G.Y., Qi, Y.P., Gysin, S., Fernández-del Castillo, C., Yajnik, V., Antoniu, B., McMahon, M., Warshaw, A.L., Hebrok, M.: **Hedgehog is an early and late mediator of pancreatic cancer tumorigenesis.** . *Nature* 2003, **425**:851-856.
186. C Thibert, Teillet MA, Lapointe F, Mazelin L, Le Douarin NM, Mehlen P: **Inhibition of neuroepithelial patched-induced apoptosis by sonic hedgehog.** *Science* 2003, **301**:843-846.
187. C Tickle: **The early history of the polarizing region: from classical embryology to molecular biology**. *Int J Dev Biol* 2002, **46**:847-52.
188. F Toledo, GM Wahl: **Regulating the p53 pathway: in vitro hypotheses, in vivo veritas**. *Nat Rev Cancer* 2006, **6**:909-23.
189. M Towers, Mahood R, Yin Y, Tickle C: **Integration of growth and specification in chick wing digit-patterning.** *Nature* 2008, **452**:882-886.
190. F Ulloa, Briscoe J: **Morphogens and the control of cell proliferation and patterning in the spinal cord.** *Cell Cycle* 2007, **6**:2640-2649.
191. AR Ungar, Moon RT.: **Inhibition of protein kinase A phenocopies ectopic expression of hedgehog in the CNS of wild-type and cyclops mutant embryos.** *Dev Biol* 1996, **178**:186-91.
192. T Uziel, Zindy F, Xie S, Lee Y, Forget A, Magdaleno S, Rehg JE, Calabrese C, Solecki D, Eberhart CG, Sherr SE, Plimmer S, Clifford SC, Hatten ME, McKinnon PJ, Gilbertson RJ, Curran T, Sherr CJ, Roussel MF: **The tumor**

suppressors Ink4c and p53 collaborate independently with Patched to suppress medulloblastoma formation. *Genes Dev* 2005, **19**:2656-67.
193. GR van den Brink, Bleuming SA, Hardwick JC, Schepman BL, Offerhaus GJ, Keller JJ, Nielsen C, Gaffield W, van Deventer SJ, Roberts DJ, Peppelenbosch MP: **Indian Hedgehog is an antagonist of Wnt signaling in colonic epithelial cell differentiation.** *Nat Genet* 2004, **36**:277-82.
194. M Varjosalo, Li SP, Taipale J: **Divergence of hedgehog signal transduction mechanism between Drosophila and mammals.** *Dev Cell* 2006, **10**:177-86.
195. M Varjosalo, Taipale J.: **Hedgehog: functions and mechanisms**. *Genes Dev* 2008, **22**:2454-2472.
196. M Varjosalo, Björklund M, Cheng F, Syvänen H, Kivioja T, Kilpinen S, Sun Z, Kallioniemi O, Stunnenberg HG, He WW, Ojala P, Taipale J: **Application of active and kinase-deficient kinome collection for identification of kinases regulating hedgehog signaling.** *Cell* 2008, **133**:537-48.
197. N Wada, Javidan Y, Nelson S, Carney TJ, Kelsh RN, Schilling TF: **Hedgehog signaling is required for cranial neural crest morphogenesis and chondrogenesis at the midline in the zebrafish skull.** *Development* 2005, **132**:3977-3988.
198. B Wang, Fallon JF, Beachy PA: **Hedgehog-regulated processing of Gli3 produces an anterior/posterior repressor gradient in the developing vertebrate limb.** *Cell* 2000, **100**:423-34.
199. Y Wang, Dakubo GD, Thurig S, Mazerolle CJ, Wallace VA: **Retinal ganglion cell-derived sonic hedgehog locally controls proliferation and the timing of RGC development in the embryonic mouse retina.** *Development* 2005, **132**:5103-13.
200. YP Wang, Dakubo G, Howley P, Campsall KD, Mazarolle CJ, Shiga SA, Lewis PM, McMahon AP, Wallace VA: **Development of normal retinal organization depends on Sonic hedgehog signaling from ganglion cells.** *Nat Neurosci* 2002, **5**:831-2.
201. RJ Wechsler-Reya, Scott, M.P.: **Control of neuronal precursor proliferation in the cerebellum by Sonic Hedgehog**. *Neuron* 1999, **22**:103-114.
202. M Westerfield: **The Zebrafish Book. A Guide for the Laboratory Use of Zebrafish (Danio rerio)**, 4th edn. Eugene: Univ. of Oregon Press; 1995.
203. C Wetmore, Eberhart DE, Curran T: **The normal patched allele is expressed in medulloblastomas from mice with heterozygous germ-line mutation of patched.** *Cancer Res* 2000, **60**:2239-46.
204. C Wolff, Roy S, Ingham PW: **Multiple muscle cell identities induced by distinct levels and timing of hedgehog activity in the zebrafish embryo.** *Curr Biol* 2003, **13**:1169-81.
205. LL Wong, DH Rapaport: **Defining retinal progenitor cell competence in Xenopus laevis by clonal analysis**. *Development* 2009, **136**:1707-15.
206. SY Wong, Reiter JF: **The primary cilium at the crossroads of mammalian hedgehog signaling.** *Curr Top Dev Biol* 2008, **85**:225-60.
207. M Yamaguchi, Fujimori-Tonou N, Yoshimura Y, Kishi T, Okamoto H, Masai I.: **Mutation of DNA primase causes extensive apoptosis of retinal neurons**

through the activation of DNA damage checkpoint and tumor suppressor p53. *Development* 2008, **135**:1247-1257.
208. S Yao, Lum L, Beachy P: **The ihog cell-surface proteins bind Hedgehog and mediate pathway activation.** *Cell* 2006, **125**:343-57.
209. KS Yee, Vousden KH: **Complicating the complexity of p53.** *Carcinogenesis* 2005 **26**:1317-22.
210. JW Yoon, Y Kita, DJ Frank, RR Majewski, BA Konicek, MA Nobrega, H Jacob, D Walterhouse, P Iannaccone: **Gene expression profiling leads to identification of GLI1-binding elements in target genes and a role for multiple downstream pathways in GLI1-induced cell transformation**. *J Biol Chem* 2002, **277**:5548-55.
211. X Zeng, Goetz JA, Suber LM, Scott WJ Jr, Schreiner CM, Robbins DJ: **A freely diffusible form of Sonic hedgehog mediates long-range signalling.** *Nature* 2001, **411**:716-720.
212. W Zhang, Kang JS, Cole F, Yi MJ, Krauss RS: **Cdo functions at multiple points in the Sonic Hedgehog pathway, and Cdo-deficient mice accurately model human holoprosencephaly.** *Dev Cell* 2006, **10**:657-65.
213. WW Zhang, S Labrecque, E Azoulay, R Dudley, G Matlashewski: **Development of a p53 responsive GFP reporter; identification of live cells with p53 activity**. *J Biotechnol* 2001, **84**:79-86.
214. XM Zhang, Yang XJ: **Regulation of retinal ganglion cell production by Sonic hedgehog.** *Development* 2001, **128**:943-57.
215. XM Zhang, Yang XJ: **Temporal and spatial effects of Sonic hedgehog signaling in chick eye morphogenesis.** *Dev Biol* 2001, **233**:271-90.
216. Y Zhao, Tong C, Jiang J.: **Hedgehog regulates smoothened activity by inducing a conformational switch**. *Nature* 2007, **450**:252-259.
217. AJ Zhu, MP Scott: **Incredible journey: how do developmental signals travel through tissue?** *Genes Dev* 2004, **18**:2985-97.
218. J Zhu, E Nakamura, MT Nguyen, X Bao, H Akiyama, S Mackem: **Uncoupling Sonic hedgehog control of pattern and expansion of the developing limb bud**. *Dev Cell* 2008, **14**:624-32.

7 Appendix

7.1 Abbreviations

AER	apical ectodermal ridge
AP	Alkaline phosphatase
BAC	bacterial artificial chromosome
bHLH	basic helix-loop-helix
bp	base pairs
BSA	bovine serum albumin
BrdU	5-bromodeoxyuridine
°C	degree Celsius
CDK	Cyclin-dependent kinase
cDNA	complementary DNA
Ci	Cubitus interruptus
CiA	Cubitus interruptus activator form
CiR	Cubitus interruptus repressive form
CKI	Casein kinase I
CNS	Central nervous system
C-terminus	Carboxy-terminus of a peptide
Da	Dalton
DAPI	4',6-Diamidin-2'-phenylindol-dihydrochlorid
DMSO	Dimethylsulfoxide
DNA	Deoxyribonucleic acid
dNTP	deoxy-A/C/G/T-trisphosphate
Dpp	Decapentaplegic
EGFP	Enhanced green fluorescent protein
EtOH	Ethanol
FACS	Fluorescence-activated cell sorting
Fgf (FgfR)	Fibroblast growth factor (receptor)
GCP	Granular cell precursor
GPC3	Glypican3
GS	Glutamine synthetase
h	hour(s)
H2BmRFP1	Histone2B red fluorescent protein 1
Hh	Hedgehog
hpf	hours post fertilization
IFT	Intraflagellar transport
IPL	Inner plexiform layer
ISH	In situ hybridisation
kB	kilo bases
M	mol/l
MO	Morpholino oligonucleotide

mRNA	messenger RNA
nls	nuclear localisation signal
N-terminus	Amino-terminus (of a peptide)
O/N	Overnight
ONL	Puter nuclear layer
PBS	Phosphate-buffered saline
PCR	Polymerase chain reaction
PFA	Paraformaldehyde
pH3	phospho-serine10 Histone3
PG13	13 copies of an optimal p53 binding site
PI	Propidium Iodide
PKA	Protein kinase A
PKC	Protein kinase C
Ptc	Patched
PTU	1-phenyl-2-thiourea
qPCR	quantitative PCR
RBF	Drosophila retinoblastoma
Rb	Retinoblastoma
RGC	Retinal ganglion cells
RNA	Ribonucleic acid
RPE	Retinal pigmented epithelium
RT	Room temperature
Shh	Sonic hedgehog
Smo	Smoothened
TE	Tris/EDTA
TGFβ	Transforming growth factor β
TLF	Tupfel long fin
TUNEL	TdT-mediated dUTP-biotin nick end labeling
ISH	In situ hybridization
ZPA	Zone of polarising activity

Curriculum Vitae

Name **Sergey Prykhozhij**

Born **16th March 1983 in Kishenev, Moldova**

Nationality **Belarusian**

A. University Education and Research

European Molecular Biology Laboratory and University of Heidelberg

09/2008 – up to now *Heidelberg, Germany*	EMBL Heidelberg, research work in the laboratory of Dr. Francesca Peri *Characterising responses of microglia and macrophages to increased apoptosis in the zebrafish brain.*
2005 – 09/2008 *Heidelberg, Germany*	EMBL Heidelberg, PhD work in the laboratory of Dr. Carl Neumann *The role of Sonic Hedgehog in zebrafish fin bud proliferation and as a survival factor in zebrafish*

University of Edinburgh

2003 – 2005 *Edinburgh, United Kingdom*	University of Edinburgh, Bachelor of Science (Honours) in Molecular Biology (First Class Honours Degree, 76 %). Focus on genetics, genomics, molecular and structural biology with strong practical and research components. *Summer research project on mouse embryonic stem cell differentiation into neurons in the lab of Prof. Austin Smith* *Honours project "Characterisation of the Dam kinetochore complex in fission yeast Schizosaccharomyces pombe."* *Summer research project on purification of kinetochore complexes from metaphase-arrested fission yeast Schizosaccharomyces pombe cells.*

Belarusian State University

2000 – 2003 *Minsk, Belarus*	Belarusian State University, Faculty of Biology, Biotechnology group (marks: 4.99 out of 5). General studies of biology, mathematics and natural sciences, humanitarian subjects with later focus on molecular biology, genetics and biochemistry. *Research work on the role of Interleukin-8 in inflammation and sepsis in the lab of Dr. Nikolai Voitenok*

B. Conference attendance

- Poster presentation at Zebrafish Genetics and Development Conference "Identifying pathways involved in apoptosis in *sonic-you* mutant and p57Kip2 morphant" in Amsterdam, 2007
- A selected talk "Analysis of apoptotic pathways in zebrafish Sonic hedgehog mutant and p57Kip2 morphant" at the Horizons PhD symposium in Göttingen 2007

C. Awards

1997 - 5th place in Brest region Chemistry Olympiad

1998, 2000 - First diploma in Belarus Republican Biology Olympiad

2000 - Bronze medal at the International Biology Olympiad (IBO) held in Antalia, Turkey in July 9th –16th, 2000.

2003 - Darwin Trust Scholarship to study at the University of Edinburgh toward Honours BSc degree in Molecular Biology

2005 - Amersham Prize for the Top Molecular Biology student of 2005 at the University of Edinburgh

2005 – EMBL Pre-doctoral Fellowship

D. Publications

Prykhozhij SV, Neumann CJ.
Distinct roles of Shh and Fgf signaling in regulating cell proliferation during zebrafish pectoral fin development.
BMC Dev Biol. 2008 Sep 23;8:91.

Fischer S, **Prykhozhij** S, Rau MJ, Neumann CJ.
Mutation of zebrafish caf-1b results in S phase arrest, defective differentiation, and p53-mediated apoptosis during organogenesis.
Cell Cycle. 2007 Dec 1;6(23):2962-9.

Vanoosthuyse V, **Prykhozhij S**, Hardwick KG.
Shugoshin 2 regulates localization of the chromosomal passenger proteins in fission yeast mitosis.
Mol Biol Cell. 2007 May;18(5):1657-69. Epub 2007 Feb 14.